Understanding the biomolecular interactions involved in dimerisation of the *Saccharomyces cerevisiae* eukaryotic translation initiation factor 5A

A thesis submitted in fulfilment of the requirements for the degree of

Masters of Science (Microbiology)

at

Rhodes University

By

Jane Charlton

January 2012

Abstract

Translation initiation factor 5A (IF5A) is an essential, highly conserved protein found within all eukaryotic (eIF5A) and archaeal (aIF5A) cells. The IF5A protein is unique in that it contains the amino acid hypusine; a two-step post translational modification of a single, conserved lysine residue. Although hypusination of eIF5A is vital for eukaryotic cell viability, the primary role of the protein and its hypusine side chain remain a mystery. eIF5A, initially identified as a translation initiation factor, is not required for global protein synthesis leading to the prevailing proposal that eIF5A is purely involved in the translation of a select subset of mRNAs. Recently a number of mutational studies have focused on the conserved, hypusine-containing loop region of eIF5A where specific residues have been found to be essential for activity without affecting hypusination. It has been postulated that eIF5A exists as a dimer (40 kDa) under native conditions and that these residues may be at the interface of dimerisation. The aim of this research was therefore to conduct a mutational analysis of the loop region in support of this hypothesis. A functional analysis of the *Saccharomyces cerevisiae* eIF5A mutant proteins K48D, G50A, H52A and K56A revealed that these substitutions impaired growth to varying degrees *in vivo* with G50A and K48D mutant proteins displaying the most convincing defects. Gel filtration profiles gave unexpected results determining eIF5A mutant and wild type proteins to have a native molecular weight of 30 to 31 kDa, suggesting that the eIF5A oligomeric state may be transitory and subject to certain conditions. The inconclusive results obtained from using gel filtration studies led to an investigation into the feasibility of producing native, hypusinated peptides for future structural studies using nuclear magnetic resonance. Hypusinated and unhypusinated eIF5A were successfully separated into their domains making this a possibility. Finally, this study proposes a role for eIF5A in eukaryotic IRES-driven translation initiation.

Acknowledgements

My sincere thanks to the following people:

- My supervisor Professor Rosemary Dorrington for your guidance, support and advice
- My co-supervisor Dr. Petra Gentz for all the help, support and encouragement
- Val Hodgson for working tirelessly to ensure the smooth running of lab 417
- My friends, Peta and the members of Lab 417
- The Medical Research Council of South Africa for project funding
- The National Research Foundation of South Africa for personal funding

Table of Contents

List of Figures

List of Tables

List of Abbreviations

eIF5A related abbreviations:

aIF5A	archaeal translation initiation factor 5A
DHS	deoxyhypusine synthase
DOHH	deoxyhypusine hydroxylase
EF-P	elongation factor P
eIF5A	eukaryotic translation initiation factor 5A
eIF5A-1/eIF5Aa	primary isoform of eIF5A
eIF5A-2/eIF5Ab	secondary isoform of eIF5A
$eIF5A_{Thrombin}$	eukaryotic translation initiation factor 5A with a thrombin cleavage site inserted within the flexible linker region
Hpu	hypusine
IF5A	translation initiation factor 5A

General abbreviations:

6xHis	His-tag consisting of 6xhistidine/hexahistidine
ADH-GAPDH	*Saccharomyces cerevisiae* alcohol dehydrogenase-2 glyceraldehyde-3-phosphate dehydrogenase hybrid promoter
ADP	adenosine diphosphate
Amp	ampicillin
ATP	adenosine triphosphate
BSA	bovine serum albumin
$CaCl_2$	calcium chloride
ddH_2O	double distilled water
$dddH_2O$	triple distilled water
DMSO	dimethyl sulfoxide
DNA	deoxyribonucleic acid
DTT	dithiothreitol
EDTA	ethylenediaminetetra acetic acid
G1	gap 1 or growth 1 phase

G1/S	transition in the cell cycle between gap 1 or growth 1 phase (G1) and DNA synthesis phase (S)
G2/M	transition in the cell cycle between gap 2 or growth 2 phase (G1) and mitosis (M)
GC7	*N*1-guanyl-1,7-diaminoheptane
HEAT-repeat	huntingtin, elongation factor 3E a subunit of protein phosphatase 2A, and the target of rapamycin repeat
IRES	internal ribosome entry site
ITAFS	internal ribosome entry site trans-acting factors
kDa	kilo Dalton
L11	ribosomal protein L11
LA	Luria-Bertani agar
LB	Luria-Bertani broth
mRNA	messenger ribonucleic acid
NaCl	sodium chloride
NAD/H	nicotinamide adenine dinucleotide
NH_2	amine functional group
nm	nanometer
NMD	nonsense mediated decay
NMR	nuclear magnetic resonance
Nos2	nitric oxide synthase 2
NRS	nuclear retention signal
OD_{600nm}	optical density at 600 nm
ORF	open reading frame
P-loop	phosphate-binding loop
p53	tumour protein 53
PABP	poly(A)-binding protein
PCD	programmed cell death
PCR	polymerase chain reaction
PKC/WSC	protein kinase C / cell wall and stress response component
PTC	peptidyl transferase centre
RNA	ribonucleic acid

rRNA	ribosomal ribonucleic acid
RNase	ribonuclease
rpm	revolutions per minute
SDS	sodium dodecyl sulphate
SDS-PAGE	sodium dodecyl sulphate polyacrylamide gel electrophoresis
SMM	selective minimal medium
TBS	tris-buffered saline
TCA	trichloroacetic acid
TCS	thrombin cleavage site
Tris	tris (hydroxymethyl) aminomethane
Tris-HCl	tris (hydroxymethyl) aminomethane hydrochloride
TS	temperature sensitive
tRNA	transfer ribonucleic acid
UTR	untranslated region
YNB	yeast nitrogen base
YPD	yeast extract, peptone and dextrose medium
XPO1	gene encoding exportin 1 receptor (yeast CRM1 homologue)

Chapter 1: Literature Review

Chapter 1: Literature Review

1.1 Introduction

Translation initiation factor 5A (IF5A) is a ubiquitous, highly conserved protein found primarily in the cytoplasm of all eukaryotic (eIF5A) and archaeal cells (aIF5A) (Gordon *et al.*, 1987; Bartig *et al.*, 1992). IF5A is the only protein known to contain the amino acid hypusine; which is produced via the two step post-translational modification of a single, conserved lysine residue (Park *et al.*, 1982; Murphey & Gerner, 1987; Bartig *et al*., 1990). The formation of hypusine, known as hypusination, is an essential process and inhibition results in cell cycle arrest in all eukaryotic and archaeal cells (Park *et al.*, 1993; Jansson *et al.*, 2000). The biological activity of IF5A is therefore hypusine dependent.

To date, very little is known about aIF5A's function, while the function of its eukaryotic homologue eIF5A is much better studied. eIF5A was initially identified in 1976 when it was isolated alongside other initiation factors from the ribosomes of rabbit reticulocytes (Kemper *et al.*, 1976). The protein was classified as a translation initiation factor based on its *in vitro* stimulation of methionyl-puromycin biosynthesis (Benne *et al.,* 1978), a model assay for the formation of the first peptide bond during mRNA translation. Since its discovery, eIF5A has been implicated in a number of cellular processes determining cell growth and viability and plays a role in everything from viral replication to cancer and diabetes (discussed in detail below). However, after over three decades of extensive research, the central role of this highly conserved protein and the vital role of hypusine remains unknown.

1.2 The isoforms of IF5A

There are usually two or more eIF5A-encoding genes present in haploid eukaryotic genomes. In the yeast, *Saccharomyces cerevisiae*, the two eIF5A genes, *TIF51A* (or *HYP2*) and *TIF51B* (or *ANB1*), are differentially expressed and their expression is

regulated by oxygen. *TIF51A* encodes eIF5Aa, which is expressed under aerobic conditions and *TIF51B* expresses eIF5Ab under anaerobic conditions (Schnier *et al.,* 1991). eIF5Aa and eIF5Ab share 90 % amino acid sequence identity and are functionally interchangeable (Schwelberger *et al*., 1993). In amphibians, birds and fish the two *EIF5A* genes appear to be co-expressed (Jenkins *et al.*, 2001) whereas in mammalian cells the *EIF5A1* gene is predominantly expressed. Human *EIF5A2* mRNA has been found in the testis and brain suggesting tissue specific expression of the secondary eIF5A isoform in mammalian cells (Jenkins *et al.*, 2001). *EIF5A2* expression has also been detected in certain human cancer cell lines posing the question of an alternate function of the eIF5A2 protein (Clement *et al.*, 2003).

In contrast to animals, the plant eIF5A genes are more numerous with at least four isoforms prevailing (Pay *et al.,* 1991; Ma *et al*., 2010). It has been suggested that their expression is tissue specific and may be regulated by different stages of plant development and environmental stress (Ma *et al*., 2010). In the archaea only a single aIF5A gene has been identified, the expression of which in a yeast eIF5A deficient strain, results in neither a hypusinated protein nor a rescued growth phenotype (Magdolen *et al*., 1994). Slime mould, alfalfa and human eIF5A1 can substitute for the yeast eIF5Aa *in vivo* and thus yeast provides a good model experimental system (Schwelberger *et al.,* 1993; Magdolen *et al*., 1994), highlighting the functional conservation of the primary eIF5A isoform across the eukaryotes.

1.3 General functions of eIF5A

1.3.1 Protein synthesis

As mentioned above, eIF5A was initially identified as a translation initiation factor due to its *in vitro* stimulation of methionyl-puromycin synthesis (Park, 1989). However, it was subsequently shown that eIF5A is not a general translation factor since the absence of a functional protein results in a reduction of total protein synthesis by approximately 30 % in yeast cells (Kang & Hershey, 1994). It has therefore been suggested that eIF5A is a translation factor for a select subset of mRNAs, i.e. those involved in DNA replication and cell cycle progression (Park *et al*., 1993; Shi *et al*., 1996). Recent reports show that eIF5A binds structural components of the 80S

ribosome as well as elongation factor 2 (eEF2) (Zanelli *et al.*, 2006; Jao & Chen, 2006; Ma *et al*., 2010) suggesting that eIF5A may be involved in translation elongation rather than initiation in eukaryotic cells. Valentini *et al*. (2002) suggest an indirect role of eIF5A in translation through the regulation of ribosome synthesis. This they claim is supported by results such as the displacement of the large ribosomal subunit protein L11 in yeast eIF5A mutant strains (Stage-Zimmermann *et al.,* 2000); the connection of eIF5A to PKC/WSC signalling (Valentini *et al.*, 2002); the binding of eIF5A to the 80S ribosome (Zanelli *et al.*, 2006) and the decrease in protein synthesis by 30 % (Kang & Hershey, 1994).

1.3.2 Cell cycle regulation

Hypusinated eIF5A is required for both cell growth (Schnier *et al.*, 1991; Park *et al*., 1993) and cell proliferation where depletion causes cellular arrest at the G1/S boundary in mammalian cells (Park *et al*., 1993). eIF5A is therefore required for the progression of the cell cycle from the G1 to the S phase. Since S phase is the start of DNA replication it was speculated that eIF5A is involved in the translation of proteins involved in DNA replication (Kang & Hershey, 1994). Hanauske-Abel *et al*. (1995) showed that several mRNA species disappeared and reappeared at the polysomes during inhibition and activation of hypusination, respectively. The products of two of these mRNA species were identified as methionine adenosyltransferase and cytochrome-c oxidase subunit 1, both enzymes required for cellular proliferation (Hanauske-Abel *et al*., 1995). Another possibility is that eIF5A is indirectly involved in cell cycle regulation through the regulation of p53 expression. In response to DNA damage p53 expression is increased, resulting in irreversible growth arrest at the G1/S boundary as well as reversible arrest at the G2/M boundary (Agarwal *et al.,* 1995). eIF5A in complex with syntenin has been shown to regulate p53 expression in COS-7 cells (Li *et al.*, 2004). Overexpression of hypusinated eIF5A results in the up-regulation of p53 expression whilst silencing of eIF5A using small interfering RNAs (siRNAs) reduces p53 protein levels thus revealing a new function of eIF5A as the regulator of p53 (Li *et al.*, 2004).

The involvement in the regulation of apoptosis was reported when eIF5A was shown to be upregulated in human lamina cribrosa (LC) cells after inducing apoptosis (Taylor

et al., 2004). Furthermore, LC cells were protected from apoptosis in response to the silencing of eIF5A using siRNAs (Taylor *et al*., 2004). Also of interest is the translocation of presumably unhypusinated eIF5A from the cytoplasm to the nucleus in response to apoptotic cell death and it has therefore been suggested that unhypusinated eIF5A signals pro-apoptotic functions within the nucleus (Taylor *et al*., 2007). In certain human cancer cell lines, including ovarian and colorectal, overexpression of eIF5A-2 has been found suggesting a distinct role of the less abundant eIF5A isoform. eIF5A-2 overexpression has also been observed in local invasions of non-small-cell lung cancer (NSCLC) and may provide a diagnostic marker for patients with stage I NSCLC (He *et al.,* 2011).

1.3.3 Expression of viral proteins

Additional roles of eIF5A in human immunodeficiency virus type 1 (HIV-1) and human T-cell leukemia virus type I (HTLV-1) replication have been identified. eIF5A has been shown to be a cellular partner of the HIV-1 Regulator of Virion (Rev) protein (Ruhl *et al.,* 1993). Rev is a nucleocytoplasmic shuttling protein which transports viral mRNA transcripts from the nucleus to the cytoplasm by binding to the Rev response element (RRE), a function which requires active (hypusinated) eIF5A (Bevec & Hauber, 1997). eIF5A is required by HTLV-1 in the same way, binding to the regulator protein (Rex) of HTLV-1 and together they appear to shuttle viral transcripts containing the Rex response element (RxRE) (Katahira *et al.*, 1995). Curiously both Rev and Rex proteins are mediated by leucine-rich nuclear export signals (NES) and require the exportin 1 (Xpo1) receptor for nucleocytoplasmic shuttling (Elfgang *et al*., 1999) (figure 1.1). In general all leucine-rich NES-containing proteins require Xpo1 as a nuclear export receptor whereas only a few leucine-rich NES-containing proteins are proposed to require eIF5A (Elfgang *et al*., 1999). eIF5A therefore provides an alternate means of inhibiting nuclear translocation of viral transcripts (figure 1.1). Since binding of eIF5A to HIV-1 Rev and (probably) Rex is hypusine dependent (Ruhl *et al.,* 1993), hypusination presents a convenient alternate drug target in the fight against HIV as well as HTLV. The role of eIF5A in the dengue virus lifecycle is also currently under investigation. eIF5A is overexpressed in dengue 2 infected *Aedes albopictus* derived cells and therefore is proposed to prevent the death response in virus-infected mosquito cells (Shih *et al.*, 2010).

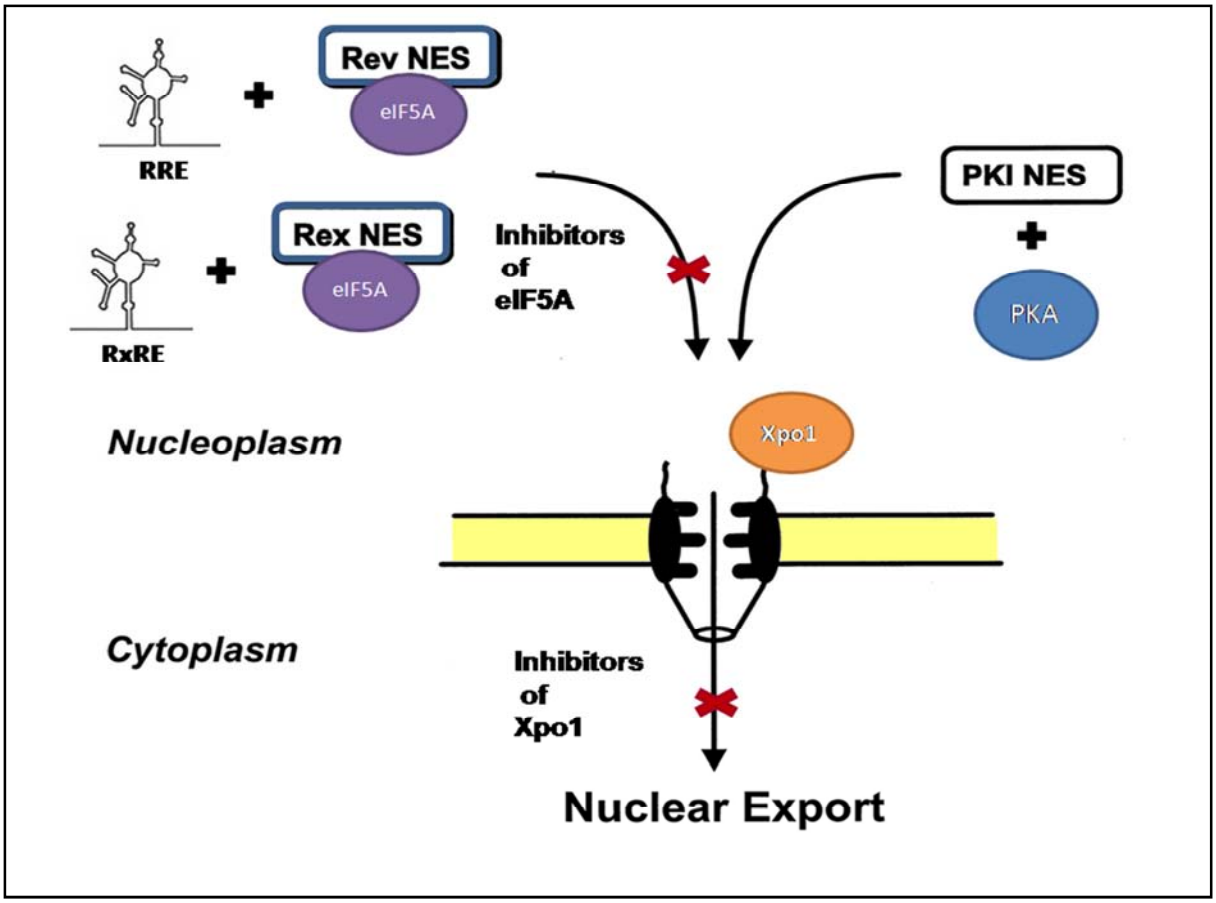

Figure 1.1: eIF5A is involved in nuclear export of Rev and Rex providing an alternate drug target in HIV and HTLV. Nuclear export of Rev and Rex via the exportin 1 (Xpo1) receptor requires active eIF5A and is mediated by leucine-rich nuclear localisation signals (NES). Cellular proteins such as protein kinase inhibitor (PKI), which translocates protein kinase A (PKA) (catalytic domain), contain NESs but do not require eIF5A for export. Therefore eIF5A dependent translocation of Rev/Rex provides another level of inhibition in HIV/HTLV production. Figure adapted from Elfgang *et al.* (1999).

1.3.4 Other functions

eIF5A has been implicated in a number of cellular functions such as cell wall integrity (Valentini *et al.*, 2002), actin polarisation (Zanelli & Valentini, 2005), stem cell differentiation (Luchessi *et al.*, 2009; Dihazi *et al*., 2011), embryonic development (Nishimura *et al*., 2011), neuronal development within the brain, aging (Luchessi *et al.*, 2008), stress granule assembly (Li *et al.,* 2010) and reactive oxygen species (ROS) generation (Tan *et al*., 2010). Moreover eIF5A has been shown to be involved in mRNA turnover (Zuk & Jacobson, 1998), mRNA stabilisation (Schrader *et al.,* 2006) and RNA cleavage (Wagner & Klug, 2007) suggesting that the protein is somehow

involved in RNA metabolism. eIF5A has also been identified as a “critical regulator” of the inflammatory response of pancreatic islets in mice (Maier, Ogihara *et al.*, 2010). The link between eIF5A and cytokine signalling is therefore under investigation and may not only aid in the understanding of the onset of diabetes but also provide a “druggable” target (Maier, Tersey *et al.*, 2010). Such a diverse number of functions supports the hypothesis that eIF5A is required for the translation of a select subset of mRNAs resulting in the indirect involvement of eIF5A with such a broad range of functions. Nevertheless it has not yet been determined whether eIF5A plays a direct or indirect role in the above functions or how they are interlinked.

1.4 IF5A Structure

1.4.1 General structure

The crystal structure of *Leishmania mexicana* eIF5A, solved by Bosch and Hol (2004) shows the general monomeric structure of unhypusinated IF5A (figure 1.2). The protein consists of two antiparallel β-sheet domains each with hydrophobic cores joined by a flexible linker; a basic N-terminal domain, and an acidic C-terminal domain. The C-terminal domain of IF5A has what has been classified as an oligomer-binding (OB) fold, common to nucleic acid binding proteins and is most similar to the cold shock protein CspA from *E. coli* (Kim *et al.*, 1998, Peat *et al*., 1998). Furthermore, the eukaryotic protein has a single α-helix in its C-terminal domain which is missing in archaeal homologues (Kim *et al.*, 1998, Peat *et al*., 1998). The N-terminal domain of IF5A contains a SH3-like barrel (Wagner & Klug, 2007) which is also found in several ribosomal proteins such as L2, L24 and L26 (Garrett *et al.*, 2000).

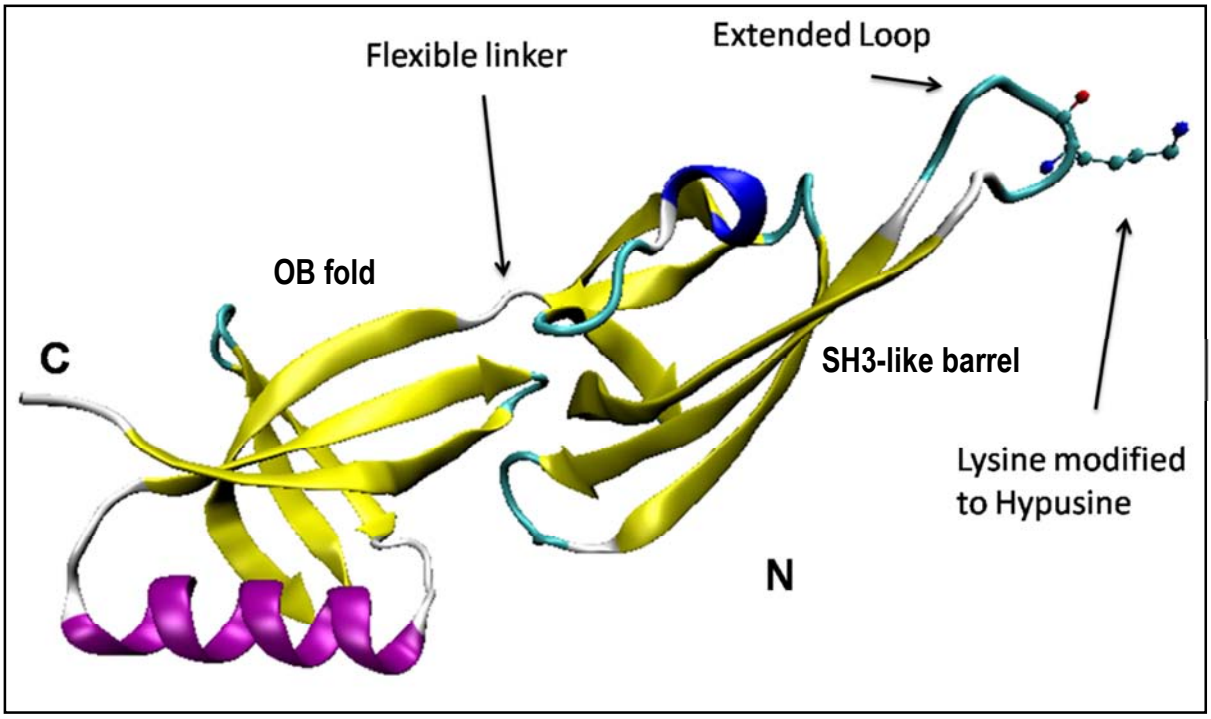

Figure 1.2: General monomeric structure of unhypusinated IF5A. The extended loop region, the site of hypusination and the two β-sheet domains separated by a flexible linker region are highlighted. The α-helix (purple) is missing in archaeal homologues. The respective oligomer-binding (OB) fold and SH3-like barrel conformations of the C and N-terminal domains are also indicated. The model of *Leishmania mexicana* eIF5A (PDB code 1XTDa) was visualised using Visual Molecular Dynamics (VMD) (Humphrey *et al.,* 1996).

The N-terminal domain of eIF5A houses the conserved extended loop region in which the hypusinated lysine residue is situated (figure 1.2). The loop consists of 12 highly conserved amino acid residues and is fully solvent exposed (Park *et al*., 1993). This sequence of amino acids is conserved throughout all eukaryote and archaeal proteins (figure 1.3) and therefore suggests its involvement in an important cellular function conserved throughout evolution. Recently a number of functional studies have been carried out on residues within the conserved loop through site-directed mutagenesis. Many of the single amino acid substitutions resulted in a severe impairment of hypusination. Interestingly the mutants K56A and G53A in yeast eIF5Aa (Dias *et al.,* 2008) and K47D and G49A in human eIF5A1 (Cano *et al.*, 2008) produced stable, but inactive mutant proteins that still acted as effective substrates for hypusination. This data suggests the involvement of residues in the hypusine containing loop in some function other than that of providing the unique substrate specificity for the hypusine modifying enzymes, deoxyhypusine synthase (DHS) and deoxyhypusine hydroxylase

(DOHH). Putative functions include sequence specific RNA binding; anchoring of eIF5A to its downstream effectors or simply in the correct orientation of the extended loop and or hypusine side chain (Cano *et al.*, 2008).

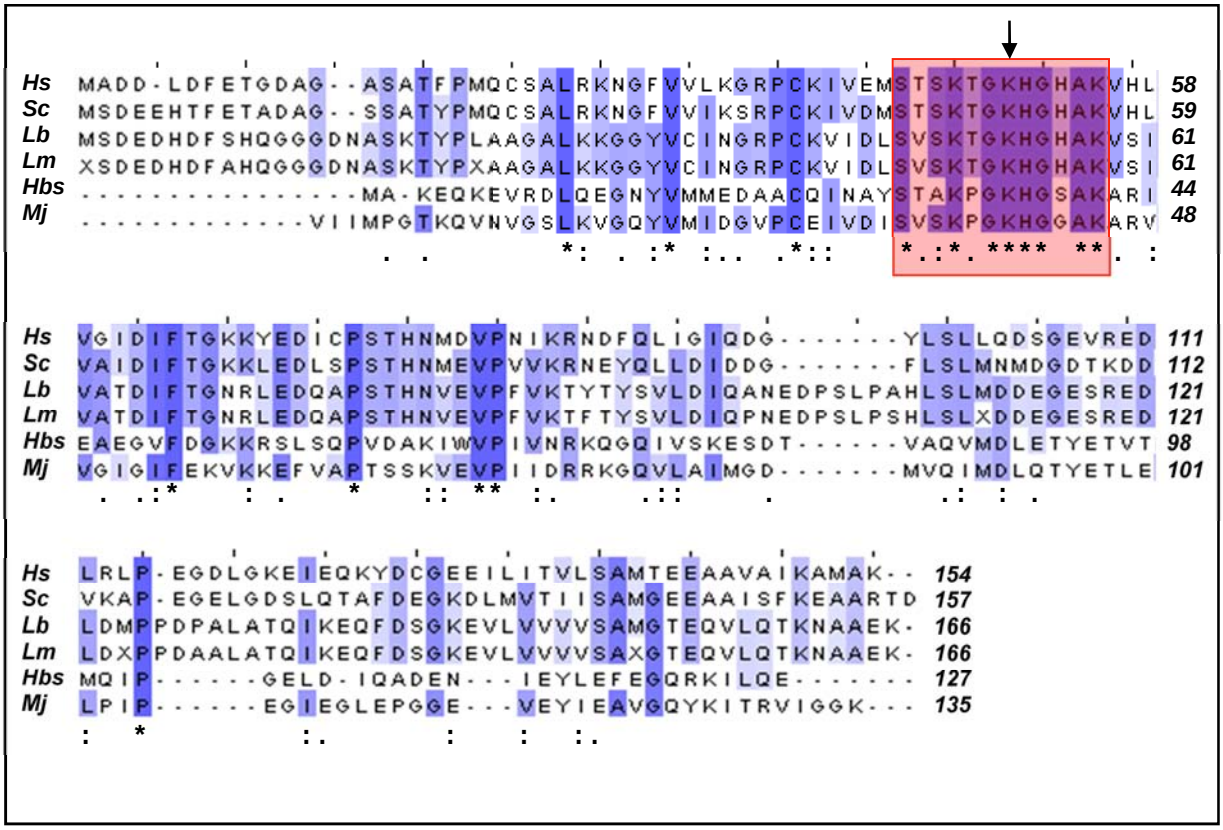

Figure 1.3: Alignment of the amino acid sequence of IF5A proteins from representative species of the eukarya and archaea. The highly conserved extended loop region is highlighted (red) with the site of hypusination indicated (downward arrow). The species names are as follows: *Homo sapiens* (Hs, accession number AAH80196), *Saccharomyces cerevisiae* (Sc, accession number P23301), *Leishmania braziliensis* (Lb, accession number XP_001565566), *Leishmania mexicana* (Lm, accession number 1XTD_A), *Halobacterium salinarum* (Hbs, accession number CAP14283) and *Methanococcus jannaschii* (Mj, accession number 1EIF). The alignment image was generated using ClustalW (Chenna *et al*., 2003) with the level of amino acid conservation coloured blue.

The 10 N-terminal residues of yeast eIF5A are not essential for activity (Dias *et al.,* 2008). This was supported by Cano *et al.* (2008) who showed that those human eIF5A mutants with truncations of 6 or 13 residues from the N-terminus or 5 residues from the C-terminus supported growth whereas any further truncations abolished activity. A structurally important feature required for eIF5A function is the α-helix, which is not present in archaeal homologues (Cano *et al.*, 2008). Also of interest was the finding by

Cano *et al.* (2008) that mutant human eIF5A with a K47R substitution supported normal growth in yeast cells, whereas K47A resulted in slow growth and K47D resulted in no growth. In a recent study the same lysine residue was shown to be the site of acetylation in unhypusinated human eIF5A protein (Lee *et al.*, 2010). This result suggested that active, hypusinated eIF5A is un-acetylated whilst the inactive precursor is acetylated at K47. This result is significant since acetylation of proteins is known to affect nucleic acid binding interactions as well as protein-protein interactions and protein stability (Kouzarides, 2000). Indeed this specific lysine residue is highly conserved across the three domains of life (Ganoza *et al.,* 2002) and therefore it would not be unreasonable to suggest that deacetylation occurs during hypusine biosynthesis and acts as a mechanism of distinguishing between the active and non-active forms of eIF5A.

1.4.2 Evolution and conservation of eIF5A homologues

eIF5A is one of a few translation factors conserved throughout all three domains of life and thought to be common to some ancient ancestor (Kyrpides & Woese, 1998). eIF5A is present in both the eukarya and archaea (aIF5A) whereas in the eubacteria the evolutionary homologue elongation factor P (EF-P) is found (figure 1.4). On average eIF5A shares 32 % amino acid sequence identity with its archaeal counterpart aIF5A and 20 % identity with the prokaryotic homologue EF-P, whereas aIF5A and EF-P share on average a slightly higher 26 % identity (Kyrpides & Woese, 1998). All three homologues share a degree of amino acid conservation, the highest being within the vicinity of the extended loop region (Kyrpides & Woese, 1998). eIF5A, hypusine, DHS and DOHH are present in eukaryote cells whereas only eIF5A, hypusine and DHS have been detected in archaeal proteomes (Park, 2006). The presence of deoxyhypusine and hypusine has been reported in archaeal species (Bartig *et al*., 1992), but it is unclear how hypusine can be produced without the presence of DOHH. In the eubacteria hypusination is thought to be non-existent. However, EF-P does undergo some modification of its corresponding lysine residue and this may even involve modification by spermidine (Aoki *et al.*, 2008). DHS-like genes have even been found in some bacterial species although phylogenetic analysis suggests an archaeal origin, most likely via horizontal gene transfer (Brochier *et al.*, 2004). Another key difference between EF-P and its evolved homologues is that

EF-P has a third domain not present in either eIF5A or aIF5A (figure 1.4). This domain has been reported to be similar to numerous ribosomal proteins (Ganoza, 2002) and therefore its function might have been replaced by such a protein in eukaryotic and archaeal cells.

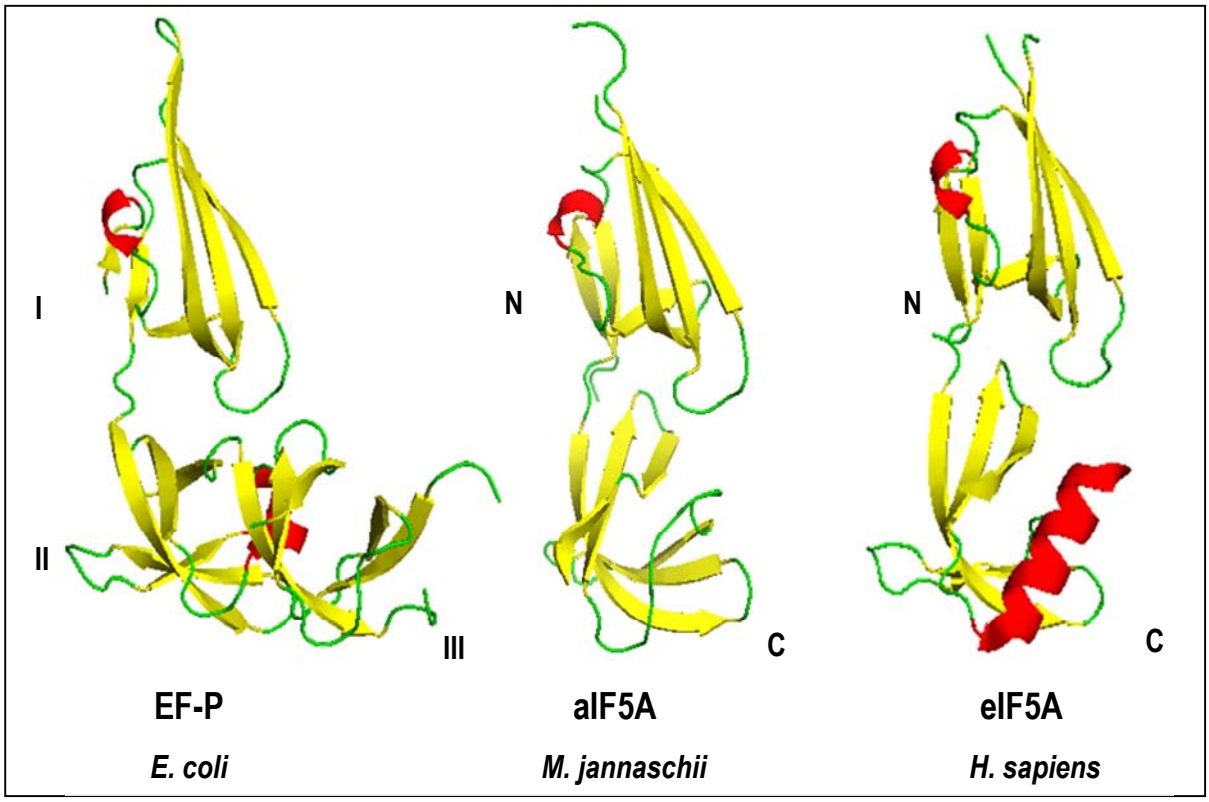

Figure 1.4: The evolution of eIF5A. From left to right elongation factor P (EF-P), archaeal translation initiation factor 5A (aIF5A) and eukaryotic translation factor 5A (eIF5A) from *E. coli, M. jannaschii* and *H. sapiens* (PDB codes: 1UEB, 1EIF and 3CPF) respectively. Structures were visualised using PyMOL (DeLano, 2002). I, II and III indicate the three EF-P domains whereas C and N indicate the C and N-terminal domains of both aIF5A and eIF5A.

1.4.3 RNA binding

Due to the general structure and charge distribution of eIF5A it has been postulated that the protein is bimodular; binding both RNA and protein at two different surfaces (Liu *et al*., 1997). The Systematic Evolution of Ligands by Exponential Enrichment (SELEX) method was therefore used by Xu and Chen (2001) to show that hypusinated human eIF5A binds to RNA carrying the consensus sequence AAAUGUCACAC. In the same study it was shown that RNA binding was both sequence specific and hypusine dependent (Xu & Chen, 2001). In follow up study eIF5A-binding mRNAs,

achieved from affinity co-purification, were identified and shown to encode proteins (amongst unidentifiable products) such as ribosomal L35a, plasminogen activation inhibitor (PAI-1) mRNA-binding protein, NADH dehydrogenase subunit 1 and ADP ribose pyrophosphatase (Xu *et al.*, 2004). Furthermore, all of the mRNA species that bound to eIF5A were shown to have the ability to form extensive stem-loop structures. Taken together this data supports the theory that eIF5A is involved in the translation of a select subset of mRNA. However, in a recent study eIF5A was shown to bind mRNA in a hypusine dependent but non sequence specific manner (Ma *et al.*, 2010). This suggests that the hypusinated loop region of eIF5A has a high affinity for the phosphate backbone of RNA and more work will need to be done to identify eIF5A mRNA binding partners *in vivo*.

Since eIF5A binds to translating 80S ribosomal complexes (Zanelli *et al.*, 2006; Jao & Chen, 2006; Ma *et al*., 2010), its direct involvement with tRNA, mRNA or rRNA is inherently implied. An alternate hypothesis that is yet to be excluded holds that eIF5A may bind the rRNA or tRNA of the 80S after the formation of the ribosomal complex. Support for this hypothesis is derived from the finding that the prokaryotic eIF5A homologue, EF-P binds to both rRNA and tRNA during the correct positioning of initiator tRNA at the peptidyl-transferase centre (PTC) (Blaha *et al.*, 2009). Although it seems that an evolved EF-P function is generally not accepted for eIF5A, it is of interest that a study conducted by Hershey *et al.* (1990) revealed formylated methionyl-tRNA (fmet-tRNA) to be approximately 20 fold less dependent on eIF5A than its eukaryotic counterpart (met-tRNA) in the methionyl-puromycin assay. The proposal is that hypusine replaces the function of the formyl group at the PTC during the formation of the first peptide bond (Hershey *et al.,* 1990; Blaha *et al.*, 2009).

1.5 Hypusine

1.5.1 Hypusination

In eukaryotic cells post-translational modification of lysine to form hypusine is catalysed by two highly specific enzymes, namely deoxyhypusine synthase (DHS) and deoxyhypusine hydroxylase (DOHH) (Murphey & Gerner, 1987). In the first step of the reaction, DHS transfers a 4-aminobutyl moiety from spermidine to the amino group of

lysine to form deoxyhypusine (figure 1.5). Deoxyhypusine is then hydroxylated by DOHH to form hypusine, and consequently active eIF5A (Park *et al*., 1982; Murphey & Gerner, 1987). Both steps of the modification have been shown to be required for eIF5A activity in mammalian cells (Park *et al.,* 1993). Interestingly in yeast the second step is not as critical for activity with deoxyhypusinated proteins still, although not as effectively, supporting growth (Park *et al.,* 2006). In another study the structural stringency of the spermidine moiety was demonstrated by its replacement with an aminopentyl side chain (homodeoxyhypusine) (Park *et al.,* 1991). The substitution rendered eIF5A inactive *in vitro* and highlights the strict structural requirements of the hypusine side chain (Park *et al.,* 1991). The stringent requirement of hypusination for eIF5A function is strong evidence for the involvement of the hypusine side chain in a vital cellular function.

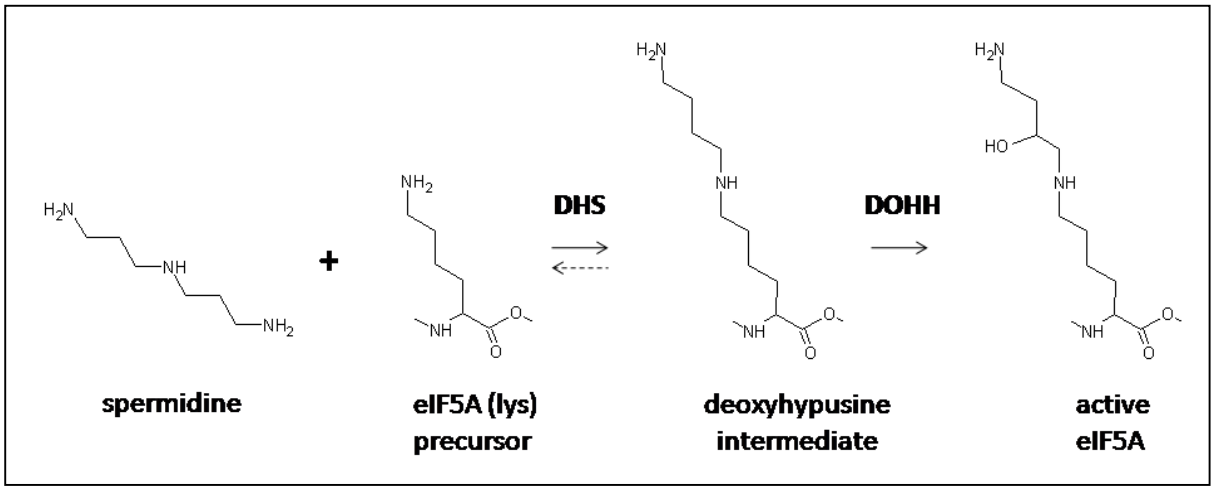

Figure 1.5: Hypusine biosynthesis is a two-step post-translational modification. A 4-aminobutyl moiety is transferred from spermidine to the amino group of lysine by deoxyhypusine synthase (DHS) forming a deoxyhypusine intermediate. The deoxyhypusine residue is then hydroxylated by deoxyhypusine hydroxylase (DOHH) forming hypusine and active eIF5A (Murphey & Gerner, 1987). Figure generated using ACD/ChemSketch 12.01 (Advanced Chemistry Development, Inc.).

1.5.2 The hypusination enzymes

DHS catalyses the first step in the hypusine reaction and is therefore the major target for inhibition studies and drug development (Caraglia *et al*., 2000; Sommer *et al.,* 2004). The enzyme has been extensively studied and the crystal structure of DHS in complex with its cofactor, NAD, has been solved (Umland *et al.*, 2004). DHS exists as

a homotetramer with two catalytic sites formed each by two DHS monomers (figure 1.6, A) (Umland *et al.*, 2004). Each DHS tetramer only binds one eIF5A monomer (Lee *et al*., 1999) and therefore the tetramer conformation is thought to be required for either regulatory means (see below) or stability (Umland *et al.*, 2004). The DHS complex in conjunction with NAD, catalyses a sequence of intricate reactions involving its substrates, spermidine and eIF5A to form the deoxyhypusine-eIF5A intermediate. DHS exhibits absolute specificity towards its protein substrate eIF5A and does not require the presence of spermidine or NAD for this interaction (Lee *et al*., 1999). On the other hand DHS exhibits a narrow specificity towards spermidine allowing a number of spermidine analogs to bind as substrates or inhibitors of DHS (Wolff *et al.*, 2007). Interestingly DHS has also been found to regulate eIF5A activity. DHS can bind to both eIF5A domains and the α-helix of the DHS N-terminal domain can inhibit eIF5A function by binding to the eIF5A N-terminal domain (Thompson *et al*., 2003). This suggests that eIF5A has two independent DHS binding sites and is possibly inhibited by DHS when eIF5A activity is not required.

In contrast less is known about DOHH, which catalyses the final step of hypusine biosynthesis (figure 1.5) and its level of activity is comparable to that of DHS (Park, 2006). The crystal structure of DOHH has yet to be solved although a predicted structure has been proposed (Park *et al.*, 2006). Thus bioinformatic analysis and computational modelling has revealed DOHH as a unique hydroxylase; the enzyme has been classified as a heat-repeat metalloenzyme (Park *et al*., 2006) with Fe(II) being the required metal for DOHH activity (Kim *et al.*, 2006). The protein has four highly conserved His-Glu motifs making up two possible metal co-ordination/chelating sites (figure 1.6, B) (Park *et al*., 2006). Furthermore, the His-Glu motifs are required for substrate binding possibly through ionic interactions with the amino groups of the deoxyhypusine side chain (Kang *et al.,* 2007). DOHH specifically recognises only the deoxyhypusine intermediate and not the precursor (lysine) form of eIF5A (Kang *et al.,* 2007).

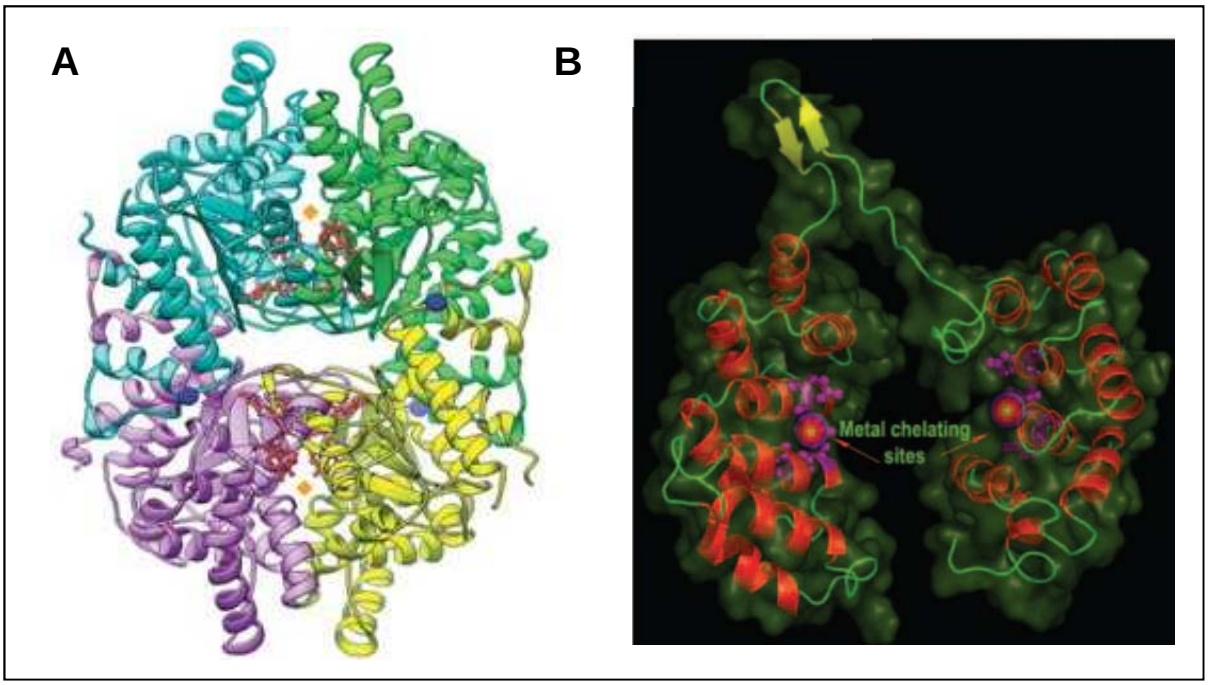

Figure 1.6: The structure of the hypusination enzymes, DHS and DOHH. (A) The DHS-NAD tetramer complex (taken form Park, 2006). The DHS homotetramer has two catalytic sites formed each by two DHS monomers (marked with a ♦). (B) The predicted structure of DOHH (taken from Park *et al*., 2006) showing an approximation of the actual structure. The metal chelating sites (highlighted) are formed by the appropriately positioned His-Glu motifs (purple).

1.5.3 Polyamines

Putrescine, spermine and spermidine, collectively known as polyamines, are important biomolecules as they are required for cell growth and development (Tabor & Tabor, 1985). It was thought that the proliferative effect of polyamines in many cases could be attributed to the role of spermidine in forming active eIF5A (Nishimura *et al*., 2005). However, polyamines have been shown to play an independent role in cell growth and proliferation (Nishimura *et al*., 2005). Polyamines are known to bind nucleic acids and specific sites on tRNA as a result of the high affinity of the NH_2 groups for the phosphate backbone (Frydman *et al*., 1992). It has also been shown that the binding of spermidine as well as spermine to tRNA is required to stabilise tRNA tertiary structure (Prinz *et al.*, 1976; Tropp & Redfield, 1983) by binding sequence-specific regions (Sakai *et al.*, 1975). This supports a role for hypusine in binding specific RNA sequences and the idea that eIF5A is involved in translation of selected mRNAs. It has been shown in yeast that under spermidine limiting conditions an increasing proportion of the molecule is taken up in hypusine biosynthesis (Chattopadhyay *et al*., 2008)

suggesting that hypusination is the primary role of cellular spermidine. Furthermore, near-normal growth and protein synthesis was obtained in cells grown in very low concentrations of spermidine (10^{-8} M). However the proportion of unmodified eIF5A increased substantially (Chattopadhyay *et al*., 2008). This suggests that both spermidine and hypusinated eIF5A exist in excess under normal cellular conditions and emphasises the importance of a complete depletion of hypusinated eIF5A when studying the subsequent effects on protein synthesis or biological function (Chattopadhyay *et al*., 2008).

1.6 Hypusination inhibition studies

Investigation into the structure and function of the eIF5A protein is an important step towards developing functional inhibitors and enabling the identification of potential drug targets. Hypusination is essential for eIF5A activity (Park*,* 1989; Park *et al.,* 1991) and is therefore the main target in the development of inhibitors. The two hypusination enzymes, DHS and DOHH, are highly specific towards their substrates and therefore may be useful drug targets (Park *et al.*, 1993). Over the years DHS has been the main focus of inhibition studies with molecules such as N1-guanyl-diaminoheptane (GC_7), guanylhydrazone (CNI-1493) and siRNAs acting as effective inhibitors of the HIV-1 replication cycle (Hauber *et al.*, 2005). A synthetic guanylhydrazone molecule known as semapimod is a potent inhibitor of DHS that has undergone phase II trials for Crohn's disease and psoriasis due to its respective anti-inflammatory and antiproliferative effects (Hommes *et al.*, 2002).

Only recently has DOHH become the focus of drug development studies. For example Hoque *et al.* (2009) showed that the use of DOHH inhibitors such as the fungicide ciclopirox and the iron chelator deferiprone prevent HIV-1 replication and suggested their use in clinical trials as antiretrovirals. Inhibition of hypusination has also, inadvertently, been the target of a number of commercial products containing known DHS/DOHH inhibitors for example an agricultural fungicide (guazatin), a sheep defleecing agent (mimosine), a topical fungicide (ciclopirox) and an anti-dandruff agent (piroctone) (Reis *et al.*, 1975; Kellner *et al*., 1982; Futterer, 1988). As more information on eIF5A function and structure is uncovered, inhibition of hypusine formation could

advance towards providing a selective means of controlling cellular proliferation in specific cells or under specific conditions.

1.7 Sub-cellular localisation of eIF5A

It might be expected that the subcellular localisation of the different eIF5A variants would shed light on the proteins function. However, subcellular localisation studies on eIF5A have produced varied and contradictory results. In 1999 eIF5A was proposed to be a nucleocytoplasmic shuttling protein by Rosorius *et al.* (1999). They demonstrated that eIF5A interacts with the general export receptor, Xpo1, and localises to both the cytoplasm and the nucleus of mammalian cells accumulating at the face of nuclear pore complexes (NPCs). Rosorius *et al.* (1999) were able to show through a series of microinjection studies that eIF5A is exported from the nucleus to the cytoplasm. A more recent study in support of these observations established that murine eIF5A is preferentially localised within the nucleus and suggests that the N-terminal extension of eIF5A, not present in archaeal homologues, is responsible for signaling the protein for nuclear localisation (Parreiras-e-Silva *et al.*, 2007).

However, other subcellular localisation studies have produced contradictory results. A detailed study by Shi *et al.* (1996) showed eIF5A to be a cytoplasmic protein that was nearly undetectable in the nuclei of mammalian cells. They claimed that 34-58 % of the protein was associated with the endoplasmic reticulum (ER) and 42-65 % was cytosolic. They also showed that the subcellular distribution did not vary greatly in relation to the cell cycle. In agreement with these results two further studies suggested that eIF5A only gains entry into the nucleus by passive diffusion and does not undergo active nucleocytoplasmic shuttling (Lipowsky *et al*., 2000; Jao & Chen, 2002).

Taken together these results could imply that under normal cellular conditions eIF5A is preferentially present in the cytoplasm and only under specific circumstance is the protein shuttled to the nucleus. Indeed this was the case in a study conducted by Taylor *et al*. (2007) where the majority of eIF5A was located in the cytoplasm under normal cell growth but unhypusinated protein was rapidly translocated to the nucleus in response to the onset of programmed cell death or after the addition of actinomycin

D, which inhibits cellular transcription (Taylor *et al.,* 2007). This seems to suggest that unhypusinated eIF5A may act as a signaling protein within the nucleus in programmed cell death inducing apoptosis. An alternate hypothesis is that unhypusinated eIF5A plays an additional role in the nucleocytoplasmic shuttling of mRNA under these adverse cellular conditions. This is supported by the requirement of Rev and Rex proteins on eIF5A for nucleocytoplasmic shuttling upon viral infection (see figure 1.6) (Bevec & Hauber, 1997), the disappearance of specific mRNAs from the polysomes upon inhibition of hypusination (Hanauske-Abel *et al.*, 1995) and the eIF5A dependent translocation of cellular mRNA, such as Nos2 mRNA, via Xpo1 (Maeir, Tersey *et al.*, 2010). It was recently discovered that phosphorylation of an N-terminal serine residue (Ser^2) resulted in accumulation of eIF5A within the nucleus in plant cells (Lebska *et al.*, 2010). This is in accordance with the pre-mentioned observations of Parreiras-e-Silva *et al.* (2007) that the N-terminal 19 residues of eIF5A were necessary for nuclear localisation and thus could be the mechanism by which eIF5A is signaled for nuclear localisation. However, as discussed previously, the N-terminal extension of eIF5A was not required for activity and therefore eIF5A's primary function might reside in the cytoplasm.

1.8 Tertiary structure of IF5A

Approximately one third of existing cellular protein is predicted to be oligomeric (Goodsell & Olson, 2000), which allows for numerous functional advantages over evolutionary monomeric predecessors (Ali & Imperiali, 2005). Under denaturing conditions the monomeric molecular weight of eIF5A is between 16 and 18 kDa. However, under native conditions there seems to be mixed results as to the oligomeric state of eIF5A. In 1995 Klier *et al.* observed an intermediate result using gel filtration (26 kDa) but declared eIF5A (human) a monomer under native conditions. This conclusion was drawn due to a number of experiments: (1) a 100 fold dilution of eIF5A did not affect the gel filtration profile; (2) folding of eIF5A was concentration independent; (3) crosslinking with glutaraldehyde did not yield specific oligomers; (4) in a yeast two hybrid system, using GAL4-DNA-binding-domain:eIF5A and eIF5A:GAL4-activation-domain fusion proteins, no significant β-galactosidase was produced (Schatz in Klier *et al.*, 1995) and (5) refolding of eIF5A together with a

glutathione-S-transferase:eIF5A fusion protein did not result in heteromer formation (Klier *et al.,* 1995). Wagner and Klug (2007) also observed a dimer/monomer intermediate (26-36 kDa) for aIF5A purified from *Halobacterium* NRC-1 cells. However, they showed that the RNA cleavage activity observed with aIF5A was dependent on its oligomeric state as aIF5A was inactive as a monomer.

In contrast to these results Chung *et al.* (1991) observed the formation of dimers, and to a lesser degree higher order polymers under native conditions, and no monomer was detected (Chung *et al.*, 1991). No monomer was observed when Ma *et al.* (2010) analysed pumpkin phloem sap using gel filtration and found eIF5A residing in fractions eluting between 40 and 150 kDa. Gel filtration experiments have shown that hypusinated yeast eIF5A exists as a dimer in solution under native conditions and that dimerisation requires RNA binding. In addition, a substitution of the lysine 51 residue (the site of hypusination in yeast) with an arginine residue results in a mutant protein (K51R) that elutes as a monomer (Gentz *et al.*, 2009). The data led to the proposal that hypusinated eIF5A monomers may associate to form loose dimers which then require RNA binding to form tightly associated functional dimers.

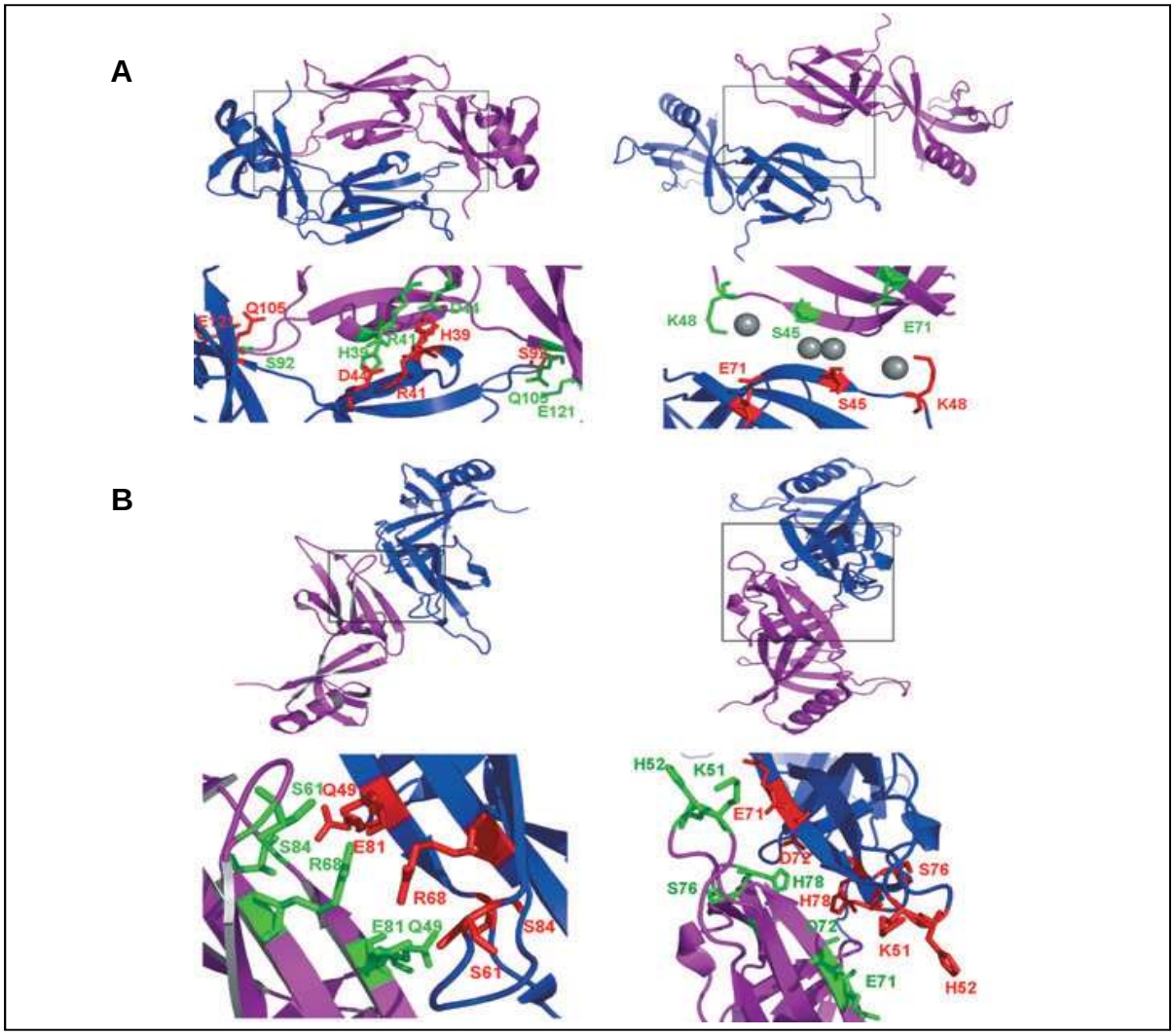

Figure 1.7: Possible eIF5A dimerisation contacts identified from HEX-1 group I and group II interfaces. (A) Left: The Hex-1 protein highlighting residues involved in group I dimerisation. Right: The yeast eIF5A dimer model highlighting the corresponding contacts. (B) Left: The Hex-1 protein highlighting residues involved in group II interactions. Right: The yeast eIF5A dimer model highlighting the corresponding contacts (Adapted from Gentz *et al.*, 2009).

There is significant structural conservation between IF5A and the protein beta-hexosaminidase (HEX-1), a self-assembling protein forming the core of the Woronin body of *Neurospora crassa* (Yuan *et al*., 2003). aIF5A was found to have a structural similarity of 83 % to that of the HEX-1 monomer but an amino acid sequence identity of only 20 % suggesting little functional homology (Yuan *et al*., 2003). Of interest however is the finding that HEX-1 forms a series of three molecular interfaces within the crystal lattice, with group I interactions forming HEX-1 dimers (Yuan *et al*., 2003). Corresponding residues of IF5A may therefore be involved in a similar interaction.

These residues were identified on yeast eIF5A dimer models (figure 1.7) by Gentz *et al.* (2009) for both group I and group II HEX-1 interfaces. The potential for salt-bridges between K48 and E71 (corresponding to group I interactions of HEX-1) and between K51 or Hpu51 and E71 or D72 (corresponding to group II interactions of HEX-1) were identified (Gentz *et al.*, 2009).

1.9 Knowledge gap

eIF5A has been implicated in a host of cellular functions over the years, however the vital and essential role of hypusine is yet to be elucidated. Hypusination is arguably the most conserved and specific protein modification known to date and therefore hypusine and its conserved loop region must be at the forefront of a common and vital cellular function. Recent mutational analyses of eIF5A have identified residues in the hypusine containing loop region involved in some function other than that of providing unique substrate specificity for DHS and DOHH (Cano *et al.*, 2008; Dias *et al.*, 2009). Speculations include the dimerisation of eIF5A (Gentz *et al.,* 2009), sequence specific RNA binding, anchoring of eIF5A to its downstream effectors or simply in the correct orientation of the extended loop and/or hypusine side chain (Cano *et al.*, 2008). There is thus a need to investigate the role that these residues play with regard to this unique protein's structure-function relationship. Current crystallographic data for eIF5A and its homologues has been derived from recombinant protein expressed in *E. coli* which is unhypusinated and in which the extended loop region is invariably disordered. A hypusinated structure would be important in answering some of the questions surrounding eIF5A such as whether hypusination causes conformational changes within the protein, possibly activating it, or whether hypusine is required for dimerisation of eIF5A. Furthermore, an increasing amount of crystallographic studies are focusing on the formation of protein complexes and, as evidence shows, one requires active, hypusinated eIF5A for protein/RNA interactions to occur (Xu & Chen, 2001; Jao & Chen, 2006; Gentz *et al.*, 2009).

1.10 Research hypothesis

Conserved amino acid residues present in the extended loop region containing the hypusinated lysine residue are involved in promoting dimerisation of yeast eIF5A.

1.11 Research objectives

1. To generate appropriate eIF5A mutations and determine the biological activity of mutant proteins
2. To conduct a biochemical characterisation of mutant proteins to determine their oligomeric state
3. To develop a biological system for producing hypusinated eIF5A suitable for structural studies using nuclear magnetic resonance

Chapter 2: Mutational analysis of eIF5A

Chapter 2: Mutational analysis of eIF5A

2.1 Introduction

Site directed mutagenesis (SDM) has been a popular approach in recent years for characterising protein structure and function relationships. Mutational analyses of proteins involve making a random array of mutations through PCR (random mutagenesis) or by targeting specific residues within the protein (oligonucleotide-directed mutagenesis) (Handa *et al*., 2002). In either case the effect of the mutation can be evaluated and key catalytic or structural residues can be identified.

It is well established that hypusine is crucial for eIF5A function (Park, 1989; Park *et al.*, 1991) and a range of mutations made at the site of hypusination (K50A, K50I, K50R and K50D in human eIF5A) result in complete inactivation *in vivo* (Cano *et al.*, 2008). In the last few years mutational analyses of eIF5A using yeast null mutants have revealed other point mutations that result in total inactivation of eIF5A, the majority of which surround the site of hypusination (Cano *et al*., 2008; Dias *et al*., 2008). This is not unexpected since these residues are at the interface of hypusination and probably play a role in the recognition of the loop region by DHS and DOHH. Interestingly, a few of these mutations did not inhibit hypusine formation when expressed in a yeast complementation system: K47D and G49A in human eIF5A (Cano *et al.*, 2008) and K56A (temperature sensitive at 37℃) in yeast eIF5A (Dias *et al.*, 2008). Furthermore, the human H52A mutant was fully hypusinated and resulted in impaired function (Cano *et al*., 2008) whereas the yeast H52A eIF5A was nonviable (Dias *et al*., 2008). Therefore the role these residues play is of interest and speculations have included sequence specific RNA binding; anchoring of eIF5A to its downstream effectors, hypusine side chain orientation (Cano *et al*., 2008) and dimerisation (Gentz *et al.,* 2009).

This chapter describes the characterization of yeast eIF5A mutant proteins carrying substitutions for key residues in the loop region containing the hypusinated K51. The

effect of each mutation on eIF5A function was tested *in vivo*. Next the hypusination state of each protein was determined *in vivo* and finally a biochemical characterisation of purified mutant proteins established the effect of each mutation on eIF5A oligomeric state.

2.2 Materials and Methods

2.2.1 Plasmids, strains and culture conditions

The bacterial strains, yeast strains and plasmid DNA used in this study are summarised in table 2.1 and the composition of the various media can be found in Appendix D. *E. coli* DH5α cultures were grown overnight at 37 ℃ in Luria-Be rtani broth (LB) or on LB agar (LA) plates in the presence of ampicillin (100 µg/mL). Competent *E. coli* DH5α cells were prepared from existing stocks using the calcium chloride method described by Dagert and Ehrlich (1979) and transformed as outlined by Sambrook *et al.* (1989).

PGY10 and INVSc1 yeast cells (table 2.1) were grown in selective minimal medium (SMM) or on SMM agar plates supplemented with the necessary amino acids and appropriate carbon source (0.002 % His, 0.002 % Trp and 2 % galactose or glucose for PGY10 cells and 0.002 % His, 0.002 % Trp, 0.01 % Leu and 2 % glucose for INVSc1 cells) (see Appendix D) and transformed with $URA3^{+}$ plasmid DNA. PGY10 and INVSc1 competent cells were prepared and transformed using the Frozen-EZ Yeast Transformation II^{TM} Kit (Zymo) as per manufacturer's instructions. All yeast transformants were grown at 28 ℃ for three to four days. Colonies were patched onto fresh SMM agar plates and grown for a further two days at 28 ℃. Liquid cultures were grown at 28 ℃ and 200 rpm for 48 - 72 hours whilst those cells exposed to glucose starvation conditions were incubated for 48 - 60 hours. The same conditions applied when using yeast extract, peptone and dextrose (YPD) or yeast extract, peptone and galactose (YPG) complete media (Appendix D) in place of SMM.

Table 2.1: **Genotypes of *S. cerevisiae* and *E. coli* strains and a description of plasmid DNA used in this study**

	Genotype / Description	**Phenotype^{+}**	**Source / Reference**
Strains			
DH5α (*E. coli*)	*supE44*, Δ*lac*U169, (*80lacZ*ΔM15), *hsdR17*, *recA1, endA1, gyrA96, thi-1, relA1*	Amp^{-}	Hanahan, 1983
PGY10 (*S. cerevisiae*)	*MATa his3Δ1 trp1-289 ura3-52 P_{GAL1}TIF51A::LEU2 TIF51B::hisG TIF51A::hisG/ Matα his3Δ1 trp1-289 ura3-52 P_{GAL1}TIF51A::LEU2 TIF51B::hisG TIF51A::hisG*	*Ura^{-}, His^{-},Leu^{+}, Trp^{-}*	Gentz *et al.,* 2009
INVSc1 (*S. cerevisiae*)	*MATa his3Δ leu2 trp1-289 ura3-52/ Matα his3Δ leu2 trp1-289 ura3-52*	*Ura^{-},His^{-},Leu^{-}, Trp^{-}*	Invitrogen
Plasmids			
pPG20	Complementation vector containing the yeast 6xHis-*TIF51A* gene under control of its endogenous promoter	Amp^{R}, *URA3*	Gentz *et al.,* 2009
pPG20 K51R	The pPG20 complementation vector containing the yeast 6x His-*TIF51A* K51R gene	Amp^{R}, *URA3*	Gentz *et al.,* 2009
pYES2	Bacterial and yeast expression vector backbone	Amp^{R}, *URA3*	Invitrogen
pPG39	Expression vector containing the yeast 6xHis-*TIF51A* gene under control of the *ADH-GAPDH* promoter	Amp^{R}, *URA3*	Gentz *et al.,* 2009
pPG39 K51R	The pPG39 expression vector containing the yeast 6xHis-*TIF51A* K51R gene	Amp^{R}, *URA3*	Gentz *et al.,* 2009

2.2.2 Recombinant DNA techniques

2.2.2.1 General techniques

Recombinant DNA techniques were carried out as described by Sambrook *et al.* (1989). Plasmid DNA was propagated in *E. coli* DH5α cells and purified using either the High Pure Plasmid Isolation Kit (Roche) or the QIAprep® Spin Miniprep Kit (Qiagen). All DNA concentrations were measured using the NanoDrop™ 2000 (Thermo Scientific) as recommended by the manufacturer and stored at -20 ℃ until further use. Screening of recombinant plasmid DNA was performed using DNA

obtained using the “EasyPrep” protocol (Berghammer & Auer, 1993). Restriction analysis of DNA was carried out using the appropriate restriction endonucleases as instructed by the manufacturer. All DNA isolates were resolved using agarose gel electrophoresis (AGE) containing 0.8 - 1.0 % agarose and 0.1 mg/mL ethidium bromide. DNA was resolved alongside 1 µg λ DNA digested with *Pst* I (λ/*Pst* I) used as a molecular weight marker and visualised using the UVIprochemi Chemiluminescence and Fluorescence system (UVItec) (referred to from here on out as a gel documentation system).

2.2.2.2 DNA sequencing

Plasmid DNA was sequenced using the ABI Prism® Big Dye™ Terminator 3.1 Cycle Sequencing Kit (Applied Biosciences) as per manufacturer’s instructions, using the sequencing primers listed in Appendix B. Sequencing reactions were analysed at the Rhodes University Sequencing Unit using the ABI Prism 3100 Genetic Analyser (Applied Biosystems). Results were visualised and edited using Chromas 2.23 (Technelysium Pty Ltd.) and analysed using the AlignX component of Vector NTI Advance 11.0 (Invitrogen).

2.2.2.3 Site-directed mutagenesis (SDM)

Mutagenic oligonucleotides for SDM were designed *in silico* using GeneRunner (Hastings Software, Inc) and Vector NTI Advance 11.0 (Invitrogen) (table 2.2). SDM was carried out using QiaPrep pPG20 and pPG39 plasmid DNA (Qiagen) and *Pfu* DNA Polymerase (Promega). The method and the temperature cycling parameters were adapted from the instructions of the manufacturer of the QuikChange™ Site-Directed Mutagenesis Kit (Stratagene) (Appendix E.1). Successful reactions were verified by AGE before and after treatment with 1 µL *Dpn* I (Fermentas) at 37 ℃ for 1 hour. The treated product was then transformed into *E. coli* DH5-α competent cells and the introduction of the correct sequence mutations was determined by restriction analysis of plasmid DNA (table 2.2) followed by DNA sequencing.

Table 2.2: Oligonucleotides used in site directed mutagenesis. The mutations, primer sequences, restriction sites introduced and plasmid names are summarised below. The mutated amino acid is highlighted in bold and nucleotide substitutions are boxed and displayed using lowercase letters. In the case of the K48D mutation a *Sal* I restriction site was removed (-) instead of introduced (+). Only the sense primers are displayed below while the antisense primer sequences and further details can be found in Appendix B.

Mutation	Primer sequence (sense)
K48D	K I V D M S T S **D** T G K H GT AAG ATT GTC GAt ATG TCC ACT TCA **gAc** ACT GGT AAG CAC GG - *Sal* I
G50A	M S T S K T **A** K H G H C ATG TCC ACT TCg AAG ACT **GcT** AAG CAC GGT CAC GC + *Csp* 45I
H52A	S K T G K **A** G H A K V H L CT TCT AAG ACT GGT AAG **gcC** GGc CAC GCT AAA GTC CAT TTG G +*Ngo* MIV
K56A	G K H G H A **A** V H L V A GGT AAG CAC GGT CAC GCT **gcA** GTC CAT TTG GTT GCC + *Pst* I

2.2.3 Heterologous expression of eIF5A and its mutants in the yeast null mutant PGY10

PGY10 yeast competent cells were transformed with the appropriate plasmid DNA and plated onto SMM plates containing 2% galactose. Transformants were each subsequently patched onto a fresh SMM plate containing galactose and incubated at 28 ℃ for two days. Pooled colonies were scraped of f each plate, resuspended in dddH_2O and inoculated to an optical density ($OD_{600\ nm}$) of approximately 0.3 in 50 mL of SMM media. Media was supplemented with either 2 % galactose or 2 % glucose and cultures were incubated at 28 ℃ for three days at 200 rpm. In the same manner patched cells were pooled and inoculated into either YPD or YPG complete medium and grown under the same culture conditions.

2.2.3.1 Functional analyses

Functional assays were carried out using the PGY10 complementation system as described by Gentz *et al.* (2009). Following expression of wild-type and mutant eIF5A, PGY10 cells were harvested by centrifugation at 3345 x *g* for 10 minutes at 4 ℃. The

resulting pellets were then resuspended in $dddH_2O$ and re-inoculated at an approximate $OD_{600\ nm}$ of 5 in 50 mL of fresh SMM containing glucose or galactose (2 %). Following incubation for three days, cultures were harvested as above and the resulting pellets were resuspended in 2 mL $dddH_2O$. Eight-fold serial dilutions of the resuspended cells were then spotted in duplicate onto SMM plates containing either 2 % galactose or 2 % glucose and incubated at 28 ℃ for three to four days. The same method was followed for cells grown in either YPD or YPG medium and serial dilutions were similarly spotted in duplicate onto YPD or YPG agar plates containing 2 % glucose or 2 % galactose respectively. When determining temperature sensitivity of strains harbouring mutant eIF5A constructs, agar plates were incubated at 22 ℃ and 34 ℃ respectively.

2.2.3.2 SDS-PAGE and western analysis

To verify His-eIF5A expression in PGY10 cells five $OD_{600\ nm}$ units (approximately 1 mL) of culture were removed and harvested in a bench top microfuge at 4000 x *g* for 5 minutes. The pellet was resuspended in 50 µL sample buffer (10 % glycerol, 125 mM Tris-Cl pH 6.8, 4 % SDS, 10 % β-mercaptoethanol, 0.01 % bromophenol blue). Cells were then lysed mechanically (by vortexing) with 2/3 (v/v) of acid washed glass beads (425 – 600 µm, Sigma) for 30 second intervals on ice for a total of 10 minutes. For each sample 5 µL of cell-free lysate (approximately 10 µg of total protein) was subjected to discontinuous SDS-PAGE on a 15% bis-acrylamide resolving gel with a 4 % stacking gel as described by Laemmli (1970) and stained with Coomassie Brilliant Blue stain (Appendix E.2).

Following SDS-PAGE, resolved proteins were either visualised by coomassie staining or transferred to Hybond-C Extra nitrocellulose membrane (GE Healthcare) using a Mini Trans-Blot® Electrophoretic Transfer Cell system (Bio-Rad) and western analysis was performed according to Towbin *et al.* (1979) (Appendix E.3). His-eIF5A recombinant proteins were detected with anti-eIF5A polyclonal rabbit antiserum (Gentz, 2008) at a dilution of 1:15000 using the BM Chemiluminescence Western Blotting Kit (Roche) as per manufacturer's instructions. Chemiluminescence was captured during 1 - 5 minute exposures using the UVIprochemi Chemiluminescence and Fluorescence system (UVItec).

2.2.4 Hypusination assays

Recombinant pPG39 wild-type and mutant constructs were transformed into competent yeast INVSc1 cells and plated onto SMM agar containing 2% glucose for three to four days at 28 ℃. Transformants were the n each patched onto a single fresh SMM glucose plate and incubated for two days at 28 ℃. Pooled colonies were then scraped off each plate, resuspended in $dddH_2O$ and inoculated to an optical density ($OD_{600\ nm}$) of approximately 0.3 in 50 mL of SMM containing 2 % glucose. Cultures were incubated at 28 ℃ for three days with shaking at 200 rpm. After harvesting as described in section 2.2.3.1, cells were re-inoculated into 50 mL of fresh SMM containing a final concentration of 0.1% glucose and 5 µCi of [C^{14}]-spermidine trihydochloride (GE Healthcare) and grown for 60 hours with shaking at 28 ºC. Cells transformed with pPG39 were also grown in the presence of the DHS inhibitor, GC_7 (20 µg/mL of culture). Five $OD_{600\ nm}$ units (approximately 1 mL) of culture were harvested and cell-free lysates (see section 2.2.3.2) were subjected to gel electrophoresis followed by autoradiography. This was achieved by resolving 8 µL of lysates by SDS-PAGE, the gel stained and destained as per normal with coomassie and dried on filter paper as described by Smith (1996). EN^{3}HANCE^{TM} Spray (Perkin Elmer) was used as an autoradiography enhancer according to the manufacturer's recommendations. The dried gel was then placed under Amersham HyperFilm^{TM} (GE Healthcare) inside an Amersham Hypercassette^{TM} (GE Healthcare) for two to three weeks at -80 ℃ prior to developing the film.

2.2.5 Heterologous protein expression

INVSc1 yeast competent cells were transformed with the appropriate pPG39 plasmid DNA and plated onto SMM agar containing 2% glucose. Transformants were subsequently patched onto four fresh SMM glucose agar plates and incubated for two days. Patched cells were scraped off each plate, resuspended in $dddH_2O$ and inoculated to an optical density ($OD_{600\ nm}$) of approximately 0.5 in 1 L of SMM broth containing 2 % glucose and incubated at 28 ℃ for t hree days with shaking at 200 rpm.

2.2.5.1 Overexpression of His-eIF5A in yeast INVSc1 cells by glucose starvation

Following the culturing of yeast as explained above, the cells were harvested at 4000 x *g* for 10 minutes at 4 ℃. The resulting pellets were resuspended in $dddH_2O$ and re-inoculated to an approximate $OD_{600\ nm}$ of 5 in 1 L of fresh SMM broth containing 0.1 % glucose. Following further incubation for 60 hours, cultures were harvested at 3345 x *g* for 10 minutes at 4 ℃. The resulting pellets were stored at -80 ℃ until required.

To optimise growth conditions for expression of eIF5A, INVSc1 cells transformed with the pPG39 construct were grown as described above in 200 mL SMM containing 2 % glucose for three days. The cells were harvested by centrifugation and inoculated into YPD broth containing 0.1 or 0.5 % glucose or SMM containing 0.1 or 0.5 %. Cultures were incubated with shaking at 28 ºC at 200 rpm and monitored for a total of 60 hours. The optical density at 600 nm was measured and 5 $OD_{600\ nm}$ units were harvested from each culture every 12 hours. Cell-free extracts were subjected to SDS-PAGE and the level of eIF5A expression detected by western analysis (described in section 2.2.3.2).

2.2.6 Purification of His-eIF5A from INVSc1 cells

INVSc1 pellets were thawed on ice and resuspended in 1 mL / 0.8 $OD_{600\ nm}$ units of lysis buffer (100 mM Tris-Cl, 300 mM NaCl, 40 mM Imidazole, pH 8.0) in the presence of a 1 x proteinase inhibitor cocktail (cOmplete^{TM} EDTA free tablets, Roche). Cells were then lysed mechanically by the method of glass beads using the BioSpec bead beater. 3/4 (v/v) of acid washed glass beads (425 – 600 µm, Sigma) were added to the suspension and cells were agitated on ice for 30 second intervals for a total of 20 minutes. The suspension was then removed and centrifuged at 3345 x *g* for 20 minutes at 4 ℃. The supernatant (clear lysate) was filtered using sterile 0.45 µm Acrodisc Syringe filters (Life Sciences). His-eIF5A was purified by nickel affinity chromatography using a HisTrap^{TM} Chelating HP 5 mL column (GE Healthcare). His-tagged protein was separated as per manufacturer's instructions by FPLC (fast protein liquid chromatography) using the Amersham ÄKTA FPLC UPC-900/P-920 (GE Healthcare) with a linear gradient over 20 column volumes (CV) from His-trap buffer A (pH 8.0, 100 mM Tris-Cl, 300 mM NaCl, 40 mM Imidazole) to His-trap buffer B

(pH 8.0, 100 mM Tris-Cl, 300 mM NaCl, 500 mM Imidazole) as described by Gentz (2008). A flow rate of 2 mL/min and an initial concentration of 8 % His-trap buffer B were used and 1 mL fractions were collected. Fractions were analysed using SDS-PAGE and protein-containing fractions were pooled together and concentrated using Amicon Ultra-15 Centrifuge Filter devices (Millipore) as per manufacturer's instructions. The concentrated protein was then dialysed with gel filtration (GF) buffer (100 mM Tris-Cl, 150 mM NaCl, pH 7.5) and concentrated to a final volume of approximately 500 µl. The concentrated protein was stored in 120 µl aliquots at -80 ℃ for future use. All protein concentrations were calculated using the NanoDrop™ 2000 (Thermo Scientific) by setting the extinction coefficient and molecular weight parameters to those of the eIF5A protein. The extinction coefficient and molecular weight were calculated using ProtParam from the ExPASy Proteomics server (Gasteiger *et al*., 2005). All steps of the purification procedure were analysed using SDS-PAGE to resolve 5 µL of each fraction and 1 µL of final concentrated protein (diluted in appropriate volumes with 2 x sample buffer, Appendix E.2). The homogeneity of purified eIF5A was determined by analysing 1 µL of purified protein by western analysis using either a 1:200 dilution of polyclonal anti-His probe antibody (Santa Cruz Biotechnology) or a 1:15000 dilution of anti-eIF5A antiserum (as described in section 2.2.3.2).

2.2.7 Gel filtration

Gel filtration was performed using the Amersham ÄKTA FPLC system and UNICORN™ software (GE healthcare). An Amersham Tricorn™ 10/30 column (GE Healthcare) was packed manually with Superdex 75 prep grade (GE Healthcare) according to the manufacturer's recommendations. Superdex 75 preparation grade resin was chosen as the column packing material for this study because it has a fractionation range of 3-70 kDa. The column's efficiency was tested and the column was calibrated according to the manufacturers of Superdex 75 prep grade. All samples were injected using a 200 µL injection tube. The column efficiency was tested using a tracer substance (2 % acetone in $dddH_2O$) injected at a flow rate of 0.5 mL/min in a $dddH_20$ mobile phase. The void volume of the packed column was established as 9.19 mL and the V_e of acetone was found to be 22.64 mL (Appendix F, figure A.4).The column was calibrated by injecting 40 µL of each of 2 mg/mL myoglobin (18 000 Da),

carbonic anhydrase (29 000 Da), ovalbumin (44 300 Da), bovine serum albumin (67 000 Da) and β-galactosidase (116 000 Da) proteins (Sigma) at 0.3 mL/min in GF buffer (100 mM Tris-Cl, 100 mM NaCl, pH 8.0). The equation y= -1.6224x + 1.9219, obtained from calibrating the column (Appendix F, figure A.5), was used for calculating the molecular weight of eluted proteins. For analysing samples the column was equilibrated with at least 2 CV of GF buffer at a flow rate of 0.3 mL/min. 120 µl of purified protein was then thawed on ice and immediately injected onto the column. Protein was detected at an absorbance of 280 nm and nucleic acids detected at 254 nm. When not in use the column was stored in 20 % ethanol and washed with 2 CV dddH_20 prior to equilibration with GF buffer. All buffers were filtered and degassed for 30 minutes prior to use.

2.2.8 Enzymatic and chemical treatment of purified His-eIF5A

Wild-type His-purified protein (approximately 0.8 - 1 mg) was subjected to RNase treatment by the addition of RNase A (Roche) to a final concentration of 1 µM. The protein mixture was incubated at 37 ºC for 30 minutes, placed immediately on ice and analysed by gel filtration. In a similar manner dithiothreitol (DTT) was added to wild-type protein (1 µM final concentration) and incubated for 15 minutes at room temperature and then analysed using gel filtration. Wild-type eIF5A was treated with a final concentration of 0.2 M NaOH (30 minutes at 37 ºC) and by boiling (5 minutes at 95 ºC) prior to gel filtration. The concentration dependent aggregation was tested by concentrating protein 3 fold (as outlined in section 2.2.7) prior to gel filtration.

2.2.9 Native PAGE

Approximately 10 µg of purified protein was resolved on a native discontinuous 10 % polyacrylamide gel with a 4 % stacking gel (Appendix E.2) according to Laemmli (1970). Purified protein was diluted 1:1 with a 2 x solution of native sample buffer (10 % glycerol, 125 mM Tris-Cl pH 8.8, 0.01 % bromophenol blue) and electrophoresed at 20 V/cm on ice for approximately 1 hour and 30 minutes.

2.3 Results and Discussion

2.3.1 Functional analysis of eIF5A mutants in the yeast null mutant PGY10

Four mutations were introduced into the *TIF51A* coding sequence, all of which were situated within the loop region which contains the hypusinated K51 residue. These include K48D, G50A, H52A and K56A (figure 2.1).

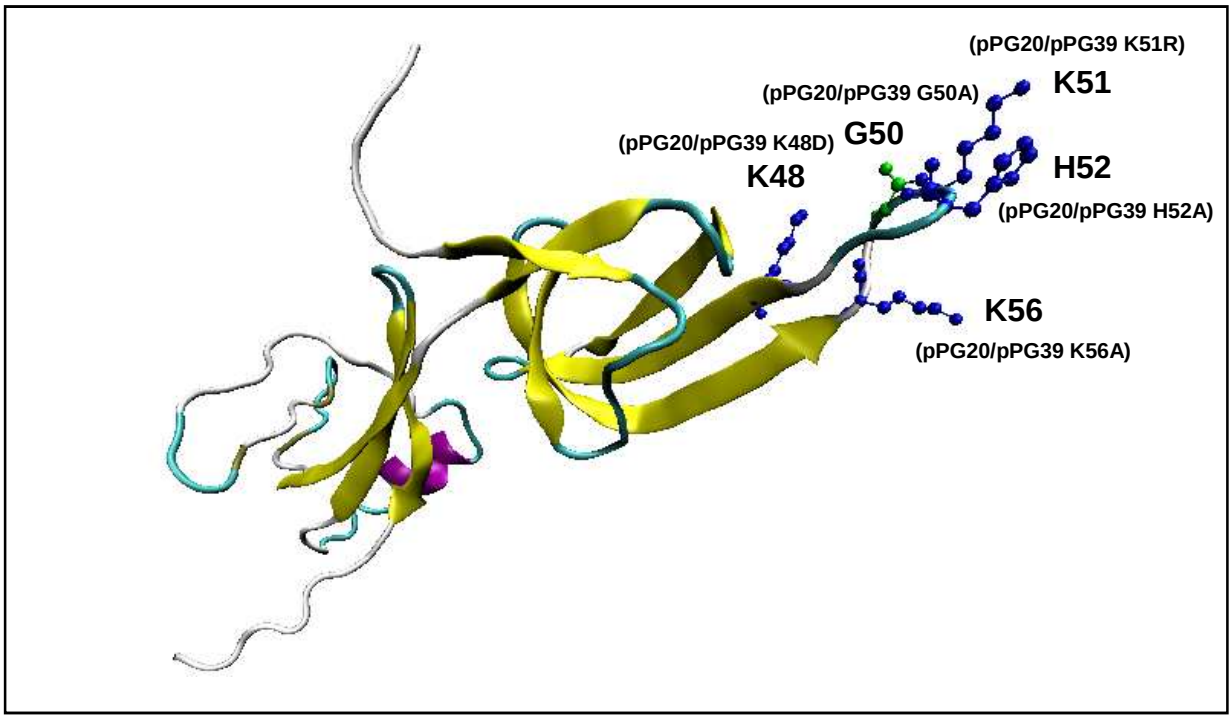

Figure 2.1: **Structural model of yeast eIF5A highlighting relevant amino acid residues.** The model highlights the position of amino acids that were mutated in this study in ball and stick mode (blue). These include K48, G50, H52, and K56. K51, the site of hypusination, is also indicated. The mutant constructs generated in this study as well as the mutant K51R constructs (Gentz *et al*., 2009) are indicated alongside each residue. The model of *S. cerevisiae* eIF5A (PDB code 3ERO) was visualised using Visual Molecular Dynamics (VMD) (Humphrey *et al.,* 1996).

The yeast strain, PGY10, in which the native *TIF51A* and *TIF51B* genes are disrupted (Gentz *et al*., 2009), was used to determine whether the four mutants were still functional *in vivo*. The strain contains a functional copy of *TIF51A* under control of the *GAL1* promoter inserted into the *LEU2* gene on the chromosome. Transcription of native *TIF51A* is therefore induced when cells are grown in medium containing galactose as a carbon source, but is repressed when cells are grown in medium

containing glucose. Mutant genes are expressed under the control of the native eIF5A promoter which is therefore not glucose repressed. First it was important to confirm that the mutant proteins were stably expressed in the PGY10 yeast strain. Cell-free extracts were analysed by SDS-PAGE followed by western analysis to detect eIF5A protein.

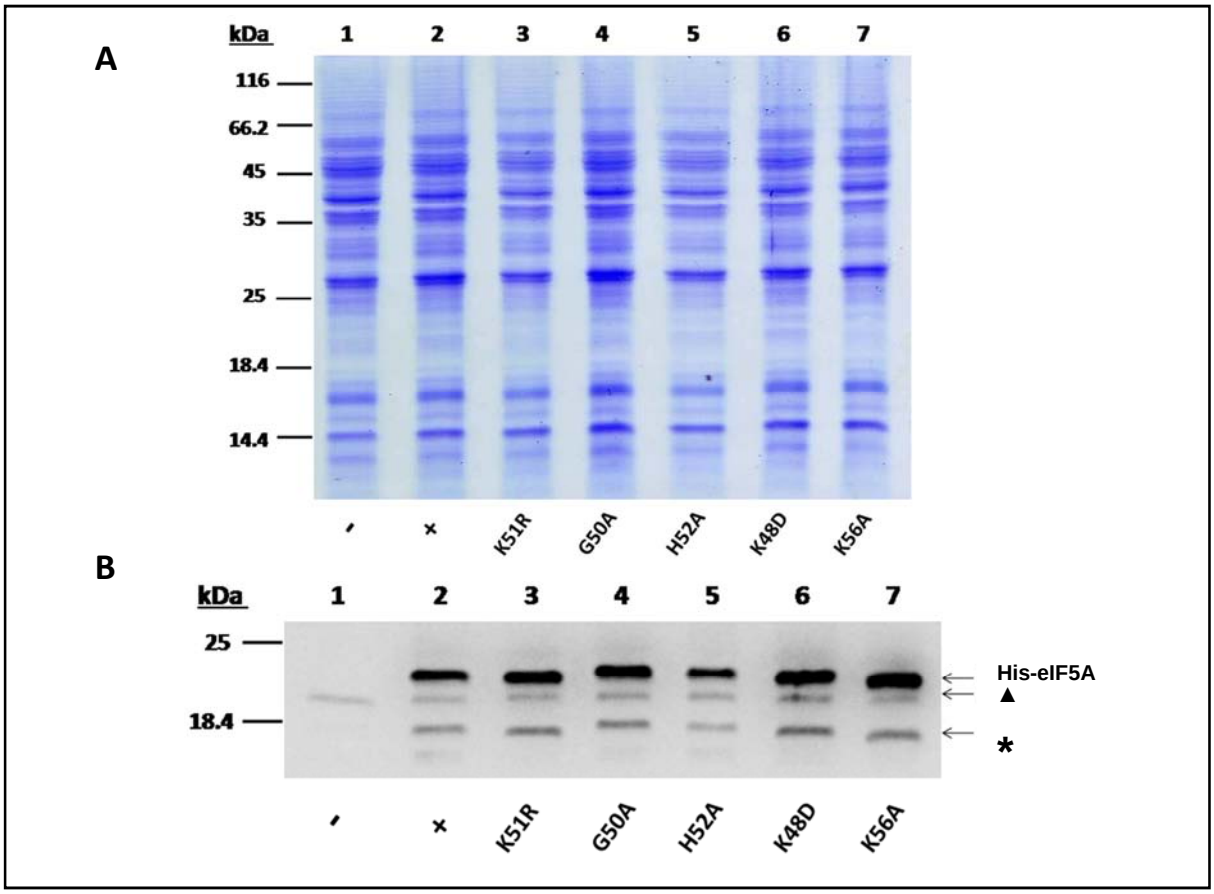

Figure 2.2: Verification of heterologous protein expression by western analysis using anti-eIF5A antibodies against yeast cell lysates. (A) SDS-PAGE gel showing total protein stained with coomassie. (B) Western analysis of yeast cell-free lysates using anti-eIF5A antiserum. Chemiluminescence was captured during a five minute exposure of the membrane using the gel documentation system. Recombinant His-eIF5A is indicated alongside, ▲ indicates endogenous-eIF5A and * indicates a common degradation product. PGY10 cells were transformed with the following plasmid DNA: Lane 1: pYES2 (-), lane 2: pPG20 (wild-type His-eIF5A, +), lane 3: pPG20 K51R (eIF5A K51R), lane 4: pPG20 G50A (eIF5A G50A), lane 5: pPG20 H52A (eIF5A H52A), lane 6: pPG20 K48D (eIF5A K48D), lane 7: pPG20 K56A (eF5A K56A).

Coomassie staining of the SDS-PAGE acrylamide gel showed that approximately similar amounts of cell-free extracts were used from all yeast strains (figure 2.2A). Western analysis showed that all four mutant proteins were expressed at approximately the same levels as the wild-type His-eIF5A protein (figure 2.2B, lanes 2 to 7) and no recombinant eIF5A was detected in cells transformed with the vector, pYES2 (Figure 2.2B, lane 1).

To determine the functionality of mutant proteins, their ability to complement growth in the PGY10 null mutant was tested. The functional complementation of the eIF5A$^-$ phenotype was tested in minimal (SMM) and complete (YPD media) by looking for growth of transformed cells in the presence of glucose. Growth was scored after 3 and 4 days of incubation at 28 ^oC.

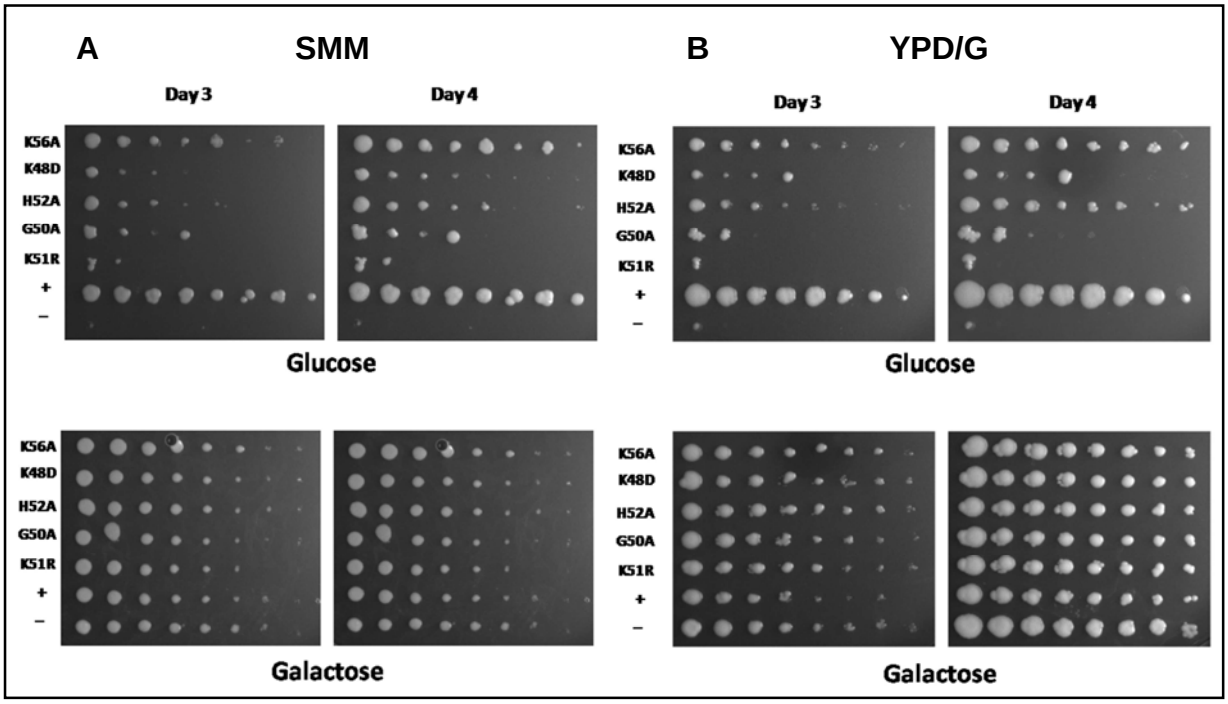

Figure 2.3: Functional analysis of eIF5A mutant proteins. Yeast PGY10 cultures spotted on both glucose (above) and galactose (below) containing SMM (A) or YPD/G complete (B) plates grown at 28 ℃. Cultures were spotted from l eft to right as 8-fold serial, 1:10 dilutions. Cells were transformed with the following plasmid DNA: pYES2 (-), pPG20 (+), pPG20 K51R (K51R), pPG20 G50A (G50A), pPG20 H52A (H52A), pPG20 K48D (K48D), pPG20 K56A (K56A).

In the presence of galactose (figure 2.3, below) growth was observed in all cases due to expression of the endogenous *TIF51A* gene under the control of the *GAL1*

promoter. However, when glucose was used as a carbon source (figure 2.3, above), growth could only be supported by a functional *TIF51A* gene product supplied by exogenous plasmid DNA (figure 2.3, +). No growth was obtained for cells transformed with the vector PYES2 which does not encode any *TIF51A* sequences and thus cannot complement the eIF5A$^-$ phenotype (figure 2.3, -). The eIF5A K51R mutant was not able to complement the null strain and therefore could not support growth (figure 2.3, K51R). The inactivity of K51R is in agreement with the results of Gentz *et al*. (2009), Cano *et al.* (2008) and Dias *et al.* (2008). The wild-type protein (+) complemented growth fully on both SMM and YPD agar with glucose as the sole carbon source. All four mutant proteins constructed in this study appeared to partially complement the eIF5A$^-$ phenotype, supporting weaker growth than the wild-type protein. On SMM agar (figure 2.3A) K56A supported growth the best at 28 ℃ (80 %), then H52A (60 %) followed by K48D (50%) and finally G50A which supported growth the least (40 %). No significant difference was observed when cells were gown in YPD/YPG complete media (figure 2.3B). K56A and H52A supported growth to approximately the same extent (75 %), followed by K48D (40 %) and then G50A (30 %). Therefore there was no difference in the ability to complement the eIF5A$^-$ phenotype when cells were grown on complete medium (YPD) as opposed to SMM.

The observation in this study that the mutant proteins K48D, G50A, H52A and K56A were able to partially complement the eIF5A$^-$ phenotype in PGY10 cells differs from the results of Cano *et al*. (2008) and Dias *et al.* (2008). Human G49A, K47D and K55A mutants were non-functional in yeast cells assayed at 30 ℃ (Cano *et al*., 2008) whilst yeast G50A and H52A mutants assayed at 25 ℃ also exhibited non-viable phenotypes (Dias *et al*., 2008). The yeast K56A mutant was temperature sensitive at 37 ℃ (Dias *et al*., 2008). These discrepancies are most likely due to the different system used by these researchers to assay mutant functionality. Both Cano *et al.* (2008) and Dias *et al*. (2008) used a 5-fluoroorotic acid (5-FOA) containing medium in a negative selection procedure for cells expressing solely mutant eIF5As.

Since temperature sensitivity of the yeast K56A protein has been reported (Dias *et al*., 2008), the temperature sensitivity of all mutant eIF5A proteins was tested in the PGY10 yeast strain. Complementation assays were carried out at both the permissive

(22 ℃) and non-permissive temperatures (34 ℃) usi ng SMM agar plates. If the mutant proteins were temperature sensitive, then one would expect that growth phenotypes would be relieved or rescued at the permissive temperature and more pronounced, if not lethal, at the restrictive temperature.

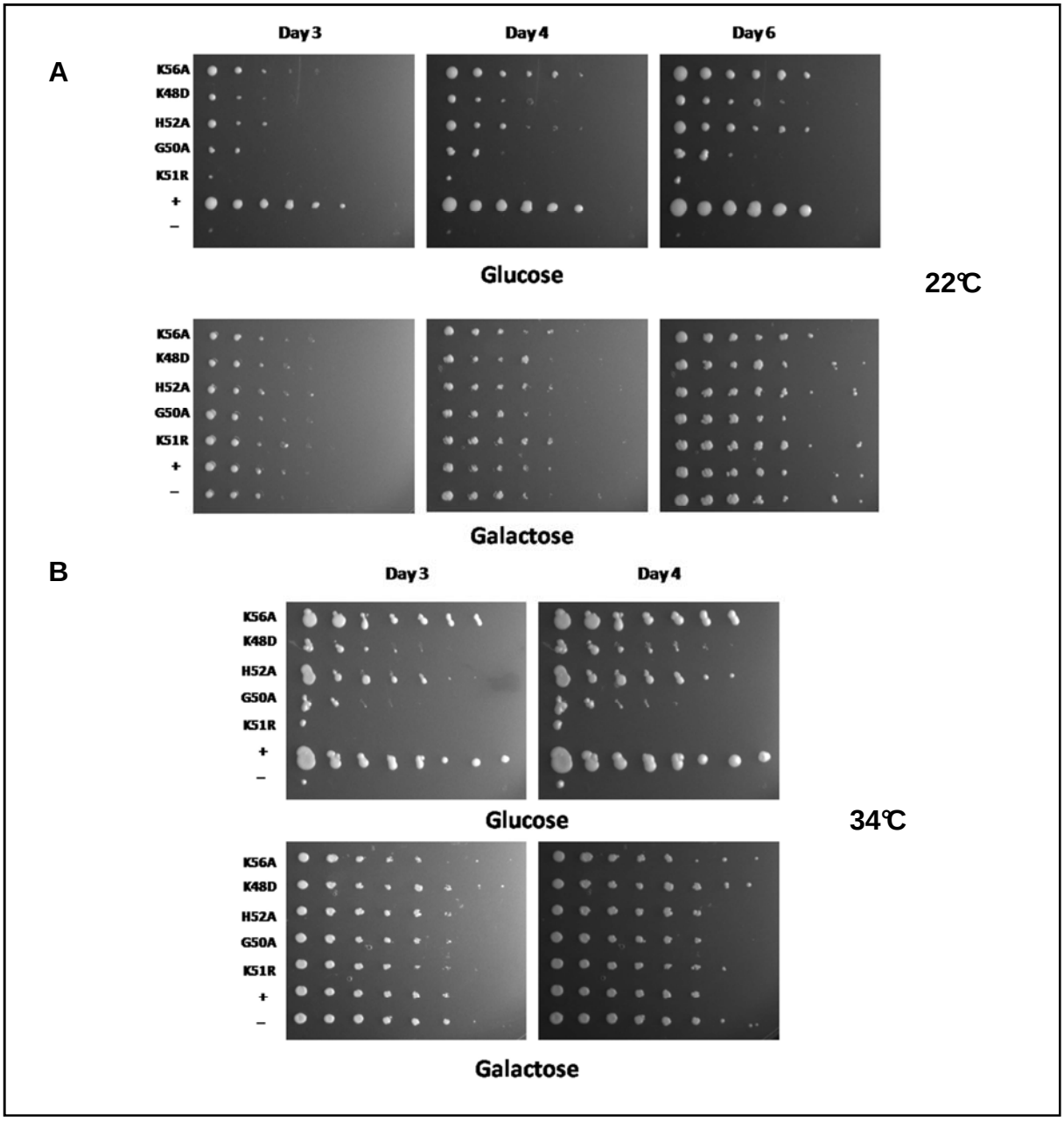

Figure 2.4: **Temperature sensitivity of mutant eIF5A proteins.** Yeast PGY10 cultures spotted on both glucose (above) and galactose (below) containing SMM plates grown at (A) 22 ℃ and (B) 34 ℃. Cultures were spotted from lef t to right as 8-fold serial, 1:10 dilutions. Cells were transformed with the following plasmid DNA: pYES2 (-), pPG20 (+), pPG20 K51R (K51R), pPG20 G50A (G50A), pPG20 H52A (H52A), pPG20 K48D (K48D), pPG20 K56A (K56A).

No significant differences were observed between the degree of complementation at the permissive (figure 2.4A) and restrictive (figure 2.4B) temperatures. Cells grew proportionally slower at 22 ℃ as compared with 34° C but displayed similar growth trends. This suggested that the impaired activity observed for the four mutant proteins was not due to the instability of mutant proteins (i.e. protein folding instability). In contrast temperature sensitivity has been reported for K56A at 37 ℃ (Dias *et al.*, 2008). In this study 34 ℃ was chosen as the restri ctive temperature because *S. cerevisiae* cells are affected by heat stress upwards of 36 ℃ (Miller *et al.,* 1979; Jenkins *et al.*, 1997). Therefore it might be possible that the temperature sensitivity observed by Dias *et al*. (2008) for the K56A mutant could be the result of conditional inactivity under the imposed heat stress and subsequent osmotic pressure induced at 37 ℃.

A recent report by Xu *et al*. (2011) shows that eIF5A is involved in the heat and osmotic stress responses and therefore it could be possible that the mutant proteins are unable to support this stress-related role induced at 37 ℃. This is further supported by the results of Valentini *et al.* (2002) and Dias *et al.* (2008) where the addition of 1 M sorbitol (an osmotic stabiliser) partially suppressed the temperature sensitivity of all yeast *TIF51A* mutant strains at 37 ℃.

2.3.2 Hypusination assays

As all mutant proteins generated supported growth to some extent (see above) it was reasonable to suggest that they may at least be hypusinated to some degree *in vivo*. The next step was therefore to verify the hypusination state of mutant proteins to determine if the partial defects in activity observed can be attributed to varying degrees of hypusination. Transformed yeast cells were therefore grown in the presence of [^{14}C]-labelled spermidine trihydrochloride and cell-free extracts were resolved by gel electrophoresis followed by autoradiography. The expression of wild-type and mutant proteins was confirmed by western analysis.

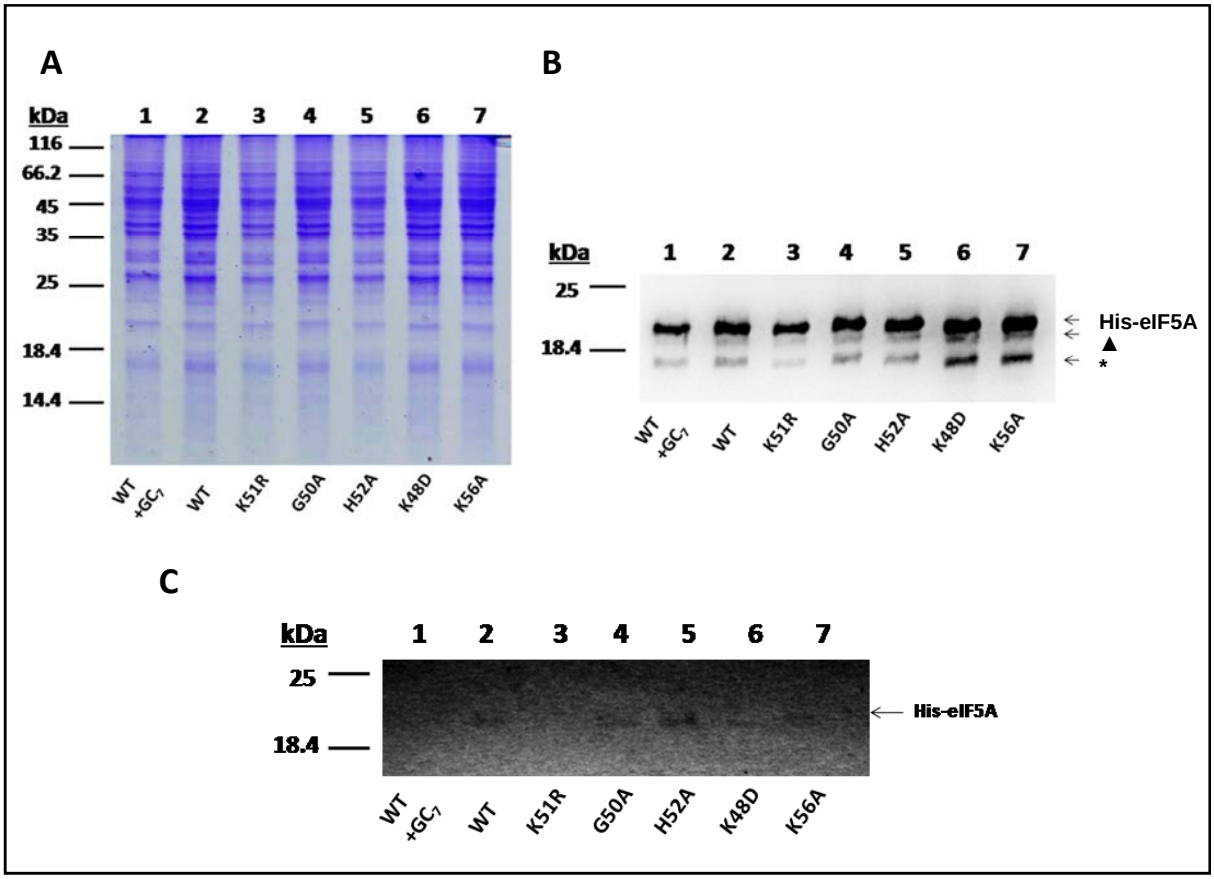

Figure 2.5: *In vivo* hypusination state of His-eIF5A mutant proteins. (A) SDS-PAGE gel showing total protein stained with coomassie. (B) Western analysis of yeast cell-free lysates using anti-eIF5A antiserum. A 1 minute exposure of the membrane was captured using the gel documentation system. Recombinant His-eIF5A is indicated alongside, ▲ indicates endogenous-eIF5A and * indicates a common degradation product. (C) Gel electrophoresis-autoradiographic image of radiolabelled eIF5A. In each case yeast INVSc1 cells were transformed with the following plasmid DNA: lane 1 & 2: pPG39 (WT), lane 3: pPG39 K51R (K51R), lane 4: pPG39 G50A (G50A), lane 5: pPG39 H52A (H52A), lane 6: pPG39 K48D (K48D), lane 7: pPG39 K56A (K56A). Cells transformed with pPG39 were grown with (lane 1, WT + GC_7) or without (lane 2, WT) the presence of 20 µg/mL GC_7.

SDS-PAGE analysis was used as a loading control showing equivalent amounts of total protein (figure 2.5A) and western analysis confirmed consistent expression of wild-type and mutant eIF5A proteins (figure 2.5B). Cells grown in the presence of GC_7 (a potent DHS inhibitor) were used as a negative control (figure 2.5, WT + GC_7). Unfortunately only a very weak signal was detected by autoradiography (possibly due to the enhancing solution used) (figure 2.5C). However the wild-type and mutant proteins, excluding the eIF5A K51R mutant, were hypusinated *in vivo* (figure 2.5C, lanes 2 and 4 to 7), while the presence of the DHS inhibitor resulted in a reduction of hypusination of the wild-type protein (figure 2.5C, lane 1). Based on the amount of

signal detected, there did not appear to be a difference in the rate of hypusination of the mutants versus the wild-type protein, however whether or not the degree of hypusination was affected by the mutations needs to be confirmed with a better signal. Cano *et al.* (2008) reported human G49A, H51A and K47D eIF5A to be fully hypusinated *in vitro* whilst Dias *et al*. (2008) detected only strong radiolabelling for the K56A mutant *in vivo*. Since it has been shown that very little active eIF5A is required for normal cell growth (Chattopadhyay *et al*., 2008), it is debatable that variations in hypusination efficiency could be responsible for the growth phenotypes observed in this study. It may be that these residues play some other important role in eIF5A function.

2.3.3 Biochemical analysis

2.3.3.1 Optimisation of growth conditions for *ADH-GAPDH* derived overexpression of eIF5A

In order to obtain sufficient native protein for biochemical analysis via gel filtration, His-eIF5A was overexpressed in yeast INVSc1 cells under control of the hybrid *ADH-GAPDH* promoter. Although recombinant protein expression in yeast cells is not as effective as the bacterial expression system, the *ADH-GAPDH* promoter allows for relatively high levels of expression of recombinant protein in low glucose conditions as well as in the presence of ethanol (Gray & Subramanian, 2001). Initially, unexpectedly low amounts of recombinant protein were obtained from yeast INVSc1 cells (2 – 3 mg/L) as compared with approximately 10 mg/L of 6x His-eIF5A obtained in previous studies in the laboratory (Gentz *et al.*, 2009). It was therefore decided to optimise growth conditions to achieve the maximum overexpression of recombinant eIF5A.

The idea was to use complete medium (YPD) instead of SMM for the second phase of expression with the aim of increasing the biomass produced per litre of cells. The intent was to use an appropriate glucose concentration that would also result in maximum expression after 48 hours of growth. Tomasicchio (2007) examined the effect of a range of glucose concentrations (0.1 %, 0.5 %, 1 % and 1.5 %) on the expression of a recombinant virus capsid protein and determined that after 39 hours of growth the glucose was significantly depleted to induce expression of the promoter in SMM containing 0.1 % and 0.5 % glucose. He reported that the $OD_{600\ nm}$ of cells grown

in medium containing 0.5 % glucose was almost double than that containing 0.1 % glucose. Therefore in this study growth profiles and recombinant eIF5A expression were monitored for 60 hours of induction for cells grown in YPD compared with SMM containing either 0.1 % or 0.5 % glucose.

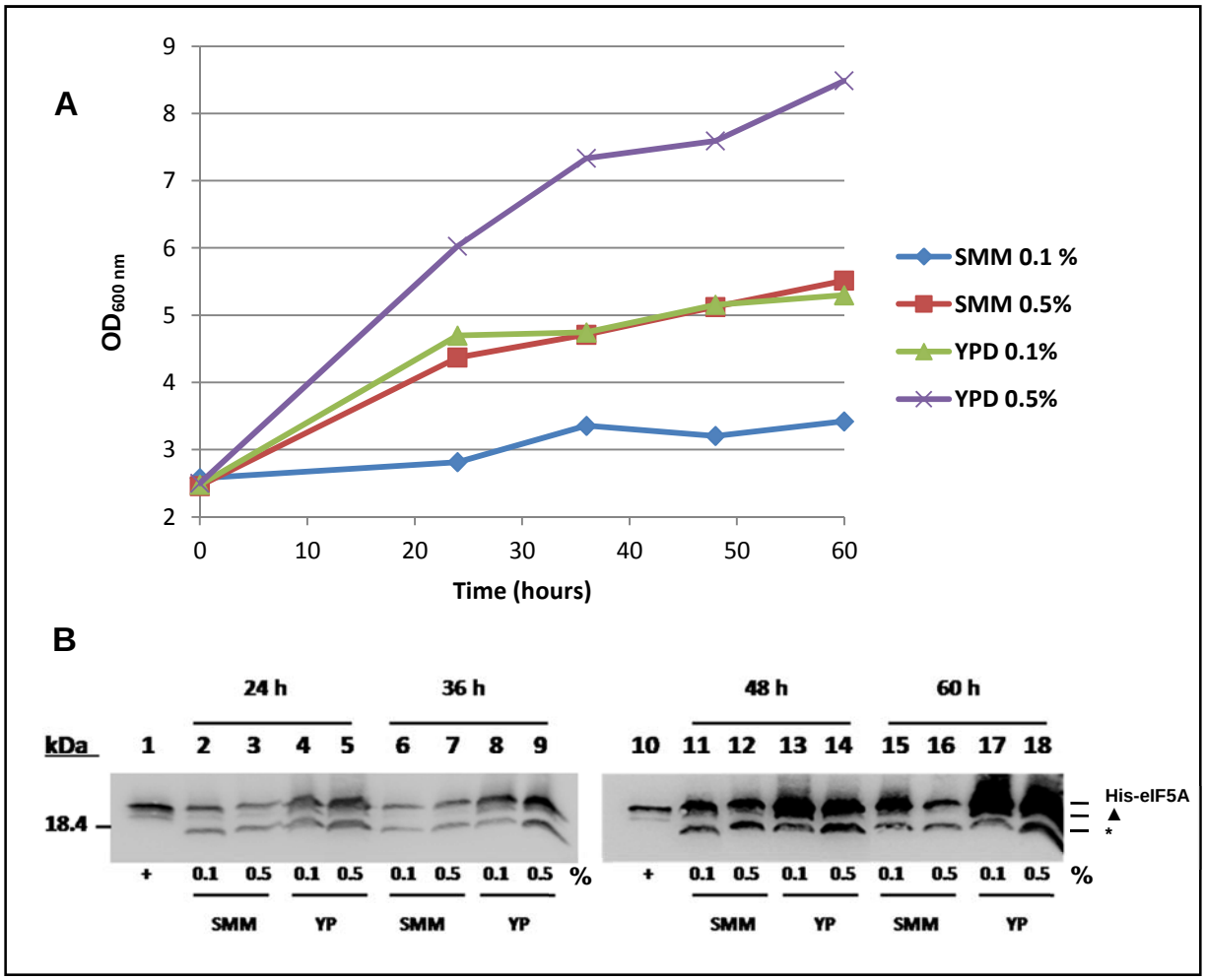

Figure 2.6: Optimisation of growth conditions for *ADH-GAPDH* derived over-expression of eIF5A. (A) Growth profiles of INVSc1 cells grown under differing glucose conditions and media composition. (B) Western analysis of yeast cell-free lysates using anti-eIF5A antiserum and a 5 minute exposure captured with the gel documentation system. Lane 1 and 10: eIF5A purified from *E. coli* used as a positive control (+), lanes 2,6,11,15: SMM 0.1 % glucose, lanes 3,7,12,16: SMM 0.5 % glucose, lanes 4,8,13,17: YPD 0.1 % glucose, lanes 5,9,14,18: YPD 0.5 % glucose. Each reading was recorded every 12 hours during the 24 - 60 hour growth period.

Analysis of the growth data (figure 2.6A) showed that more biomass was produced (1) when using YPD medium instead of SMM for the induction phase of growth and (2) when using 0.5 % glucose instead of 0.1 % glucose as the carbon source. Growth of

cells in YPD medium containing an increased glucose concentration of 0.5 % resulted in more than double the amount of biomass. Western analysis of cell-free extracts showed the induction of eIF5A expression as glucose was depleted over time (figure 2.6B). After 60 hours there was more recombinant His-eIF5A expressed in cells grown in YPD medium than in SMM (figure 2.6B, lanes 15 to 18) with very little difference in recombinant eIF5A expression between 0.1 % and 0.5 % glucose concentrations. This data led to the conclusion that the optimal expression of His-eIF5A was achieved in YPD medium containing 0.5 % glucose.

2.3.3.2 Purification of native His-eIF5A

Unless otherwise stated, His-eIF5A was purified from cells grown using the adapted, optimised protocol described above. Western analysis of cell-free extracts from yeast INVSc1 cells was used on each occasion to verify the expression of wild-type and mutant His-eIF5A under control of the *ADH-GAPDH* promoter prior to the purification of His-tagged protein (figure 2.7).

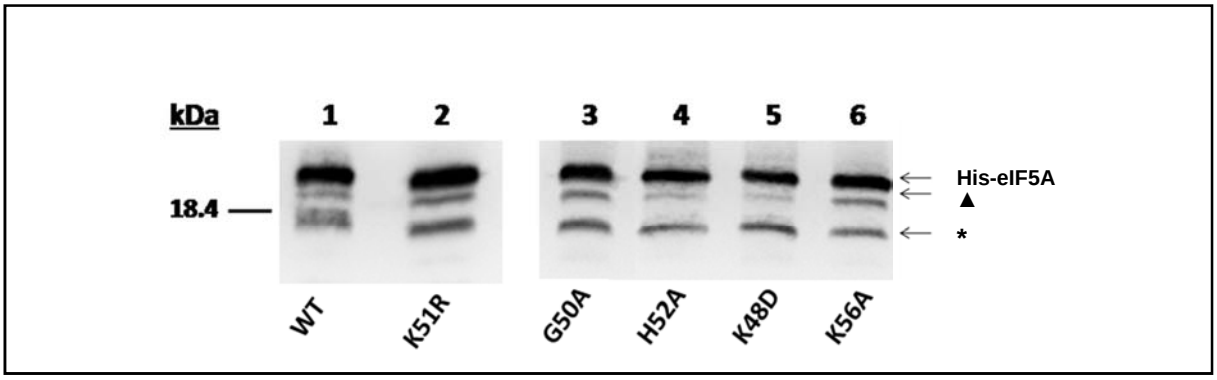

Figure 2.7: Western analysis of cell-free extracts from yeast INVSc1 cells expressing wild-type and mutant His-eIF5A under control of the *ADH-GAPDH* promoter. Western analysis using a 1:15000 dilution of anti-eIF5A antiserum against yeast cell-free lysates. Recombinant His-eIF5A is indicated alongside, ▲ indicates endogenous-eIF5A and * indicates a common degradation product. Chemiluminescence was detected for 1 minute using the gel documentation system. INVSc1 cells were transformed with the following plasmid DNA: Lane 1: pPG39 (WT), lane 2: pPG39 K51R (K51R), lane 3: pPG39 G50A (G50A), lane 4: pPG39 H52A (H52A), lane 5: pPG39 K48D (K48D), lane 6: pPG39 K56A (K56A).

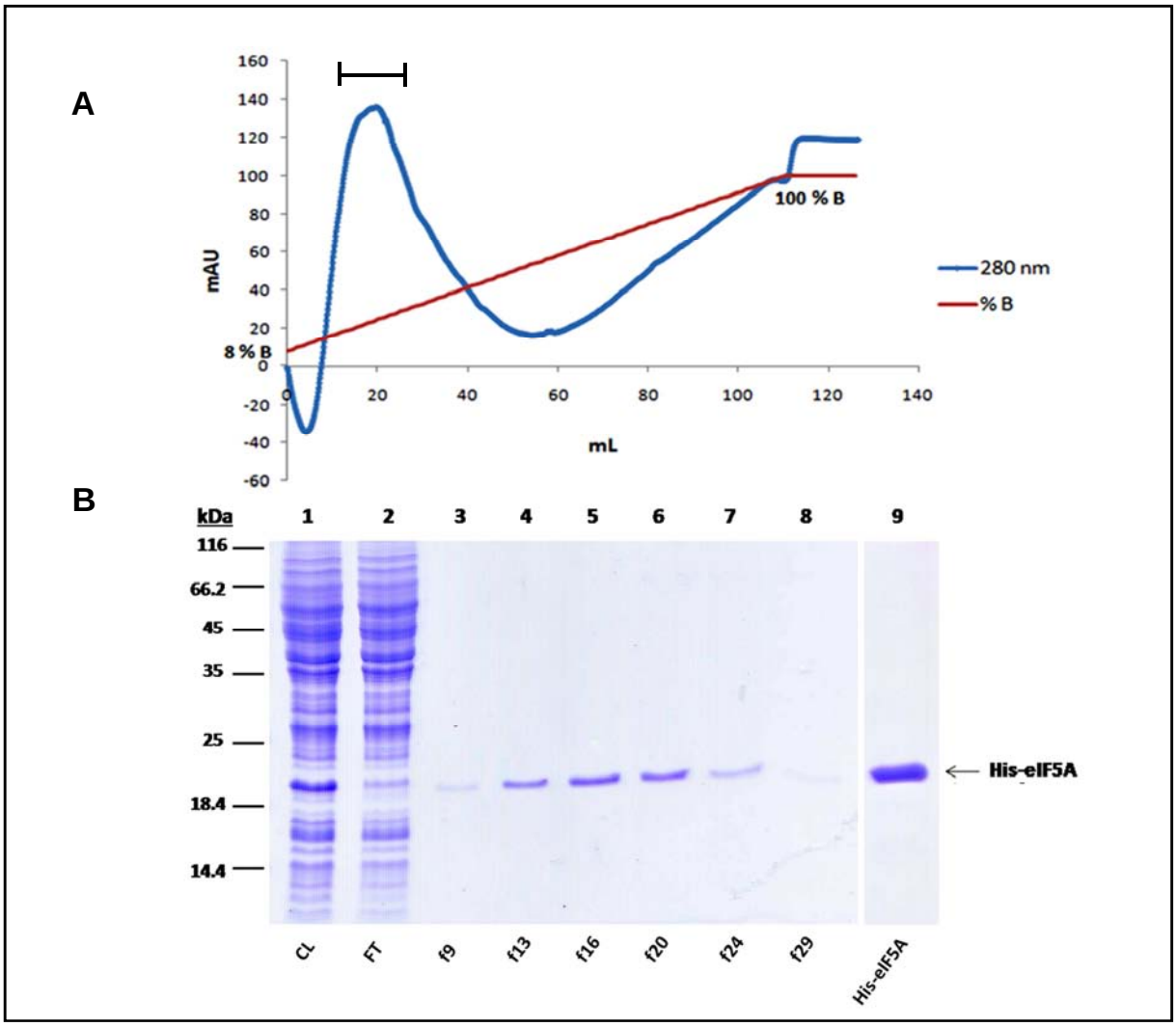

Figure 2.8: **His-eIF5A protein purification by nickel affinity chromatography.** (A) An example of the chromatogram generated during purification of His-eIF5A proteins. Fractions corresponding to the peak at 280 nm (highlighted with a H) were pooled and concentrated. % B (red) represents the linear gradient of His-trap buffer B from 8 to 100 %. (B) SDS-PAGE analysis was used to depict each step of the purification process. Lane 1: clear lysate (CL), lane 2: flow through (FT), lanes 3-8: fraction 9-29 (f9-f29), lane 9: concentrated His-tagged eIF5A protein (His-eIF5A). Each fraction corresponds to 1 mL of elution volume.

His-eIF5A wild-type and mutant protein was purified by nickel affinity chromatography (figure 2.8A) using an initial concentration of 8 % buffer B (see methodology) to obtain a higher purity by avoiding co-elution with contaminating proteins. In each case all steps of the purification procedure were analysed by SDS-PAGE analysis to determine the fractions containing purified His-eIF5A (figure 2.8B). In general all proteins had the same elution profile and fractions 12 - 24 were pooled, dialysed and concentrated to approximately 500 µL. Protein concentrations were calculated with the molecular

weight set to 17.9 kDa and a molar extinction coefficient of 2980 M^{-1} cm^{-1}. As there are no tryptophan and only two tyrosine residues within the yeast *TIF51A* protein, the molar extinction coefficient is low and therefore it was necessary to factor this in when calculating protein concentration based upon absorbance at 280 nm. Final protein concentrations obtained subsequent to nickel affinity chromatography were between 8 - 11 mg of recombinant protein per litre of culture.

2.3.3.3 Homogeneity of native purified His-eIF5A

The homogeneity of wild-type purified protein was tested to determine if endogenous protein is purified with the recombinant His-tagged protein. Nickel affinity-purified wild-type protein was subjected to western analysis (figure 2.9) using anti-eIF5A antibodies to detect endogenous eIF5A.

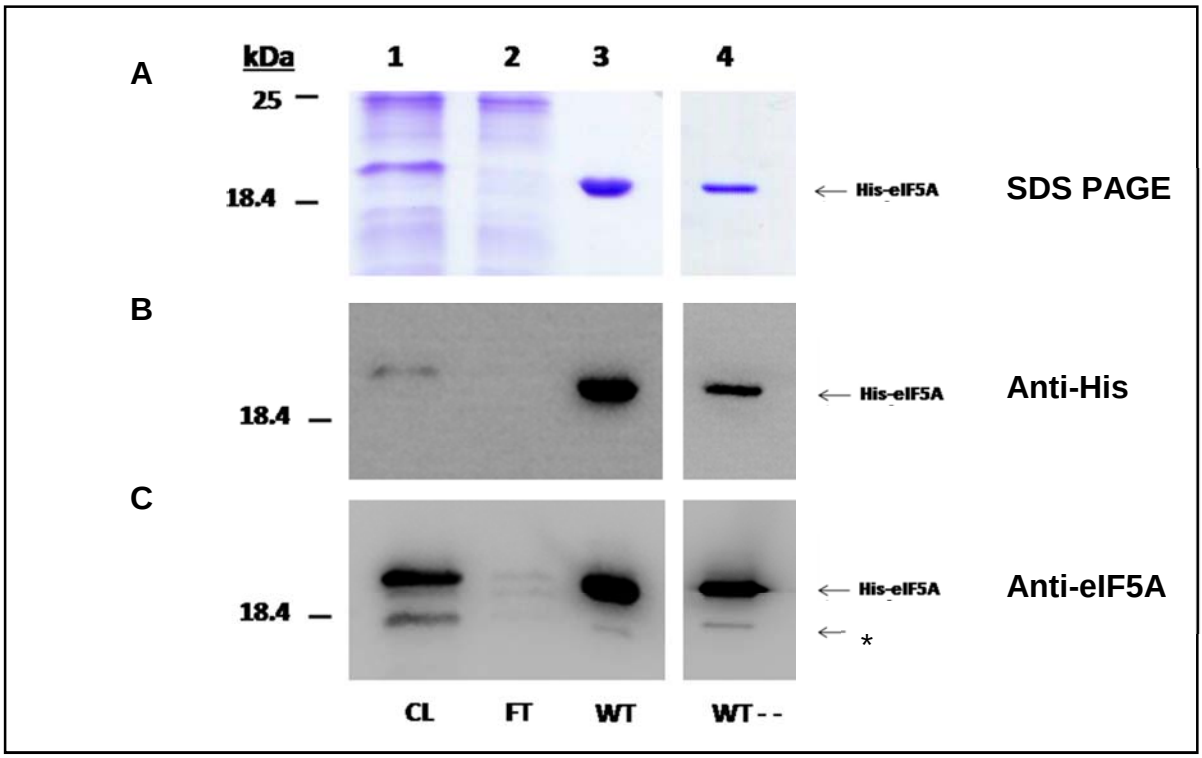

Figure 2.9: Homogeneity of purified His-eIF5A protein. All purified protein was analysed alongside a yeast clear lysate and flow through samples for comparisons sake. (A) SDS-PAGE analysis showing total protein stained with coomassie. His-eIF5A recombinant proteins were probed with a 1:200 dilution of anti-His antibody (B) or a 1:15000 dilution of anti-eIF5A antibody (C) and indirectly detected using the BM Chemiluminescence kit (Roche) and a five minute exposure of membrane captured with the gel documentation system. Lane 1: cleared lysate (CL), lane 2: flow through (FT), lane 3: 6 µg of concentrated eIF5A wild-type protein (WT), lane 4: a 1:3 dilution (2 µg) of concentrated His-tagged eIF5A protein (WT--). * indicates a common degradation product.

Endogenous eIF5A was only detected in the clear lysate and flow through fractions (figure 2.9, below: CL and FT) and not in the purified protein sample (figure 2.9, below: WT and WT--). This alone indicates that eIF5A does not form heterodimers with the endogenous protein. Furthermore, the eIF5A protein is degraded from the N-terminus as degraded protein is not detected by the anti-His antibody (figure 2.9, centre).

2.3.3.4 Oligomeric state of His-eIF5A proteins

Approximately 0.8 - 1 mg of each wild-type and mutant eIF5A protein was analysed by gel filtration. The absorbance of eluted fractions was determined at both 280 and 254 nm to detect the presence of protein and RNA respectively since it has been proposed that RNA was responsible for stabilizing the eIF5A dimer (Gentz *et al*., 2009). Wild-type and K51R proteins were used as controls since previous studies had shown that the hypusinated wild-type protein eluted as a dimer at approximately 40 kDa and the unhypusinated K51R mutant protein eluted as a monomer (17 kDa) (Gentz *et al*., 2009).

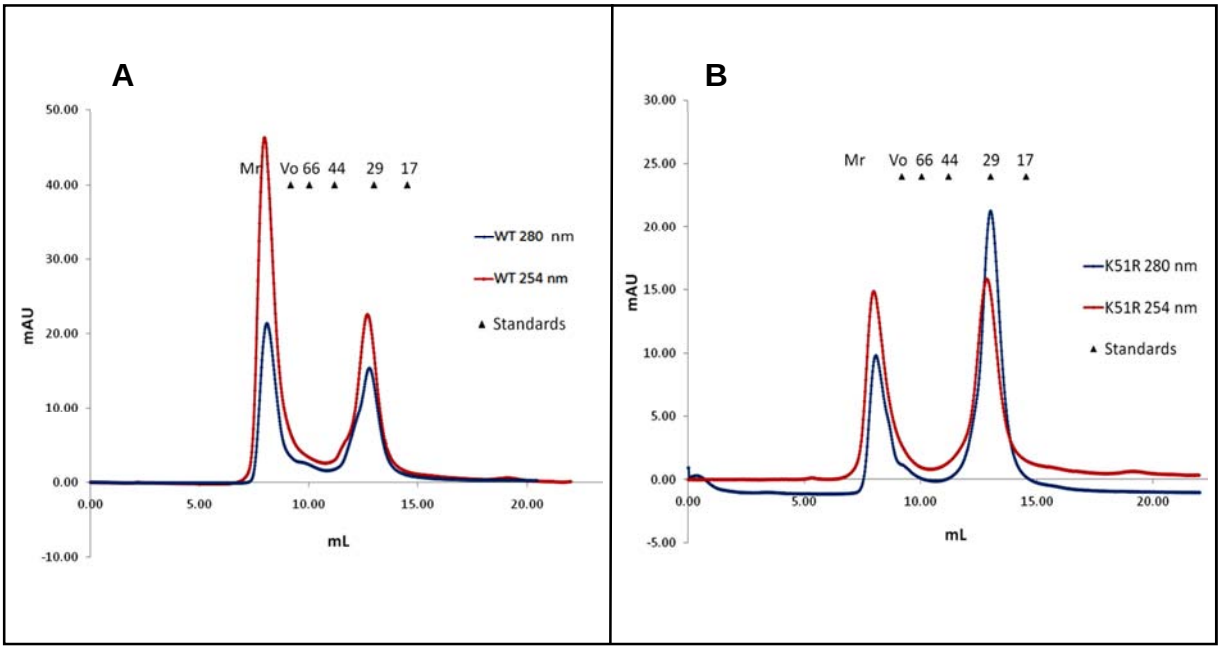

Figure 2.10: **Gel filtration chromatographic characterisation of wild-type and K51R protein controls.** For both wild-type (A) and K51R (B) protein, samples of the same concentration were resolved at both 280 nm (blue) and 254 nm (red) to determine the relative presence of RNA at 254 nm. Molecular weight (Mr) standards are represented by triangles above: myoglobin (17 kDa), carbonic anhydrase (29 kDa), Ovalbumin (44 kDa) and β-galactosidase (V_o).

In contrast to the data obtained by Gentz *et al.* (2009) and Chung *et al.* (1991) this study showed that both wild-type and mutant K51R proteins eluted at an intermediate molecular weight of 30-31 kDa (figure 2.10). This result is similar to the results of Klier *et al.* (1995) and Wagner and Klug (2007) who also obtained a monomer/dimer intermediate result for native human eIF5A and *Halobacterium NRC-1* aIF5A respectively. Secondly, the variation in absorbance at 254 nm between the wild-type and K51R proteins (figure 2.10) was not significant enough to suggest the total absence of RNA for the K51R mutant protein as shown with Gentz *et al.* (2009).

Since the data produced in this study was not in agreement with the results of Gentz *et al*. (2009), the reproducibility of results was tested as well as the robustness of the purification and gel filtration techniques. The purification protocol was examined for the potential introduction of denaturing conditions or contaminating factors that could alter the folding of the protein. The potential of artefacts introduced due to the different (YD) culture medium that cells were grown in was analysed: (1) wild-type and K51R protein purified from cells grown in SMM medium versus complete YPD medium were compared and shown to have no affect on protein elution profiles and (2) the addition of trace elements into the cell culture media did not result in any noticeable differences. Furthermore, data was reproducible on a separate gel filtration system (located in the laboratory of Professor Greg Blatch) eliminating any equipment-related problems. Concentration dependent aggregation was also eliminated by comparing the elution profiles of both concentrated and diluted protein samples. Finally the possibility of introducing cross-linking chemicals with the addition of proteinase inhibitor was eliminated as its addition was determined to have no effect on wild-type eIF5A elution profiles (data not shown).

After eliminating a range of possibilities, mutant proteins were subjected to gel filtration chromatographic analysis and the absorbance of eluted fractions at 280 and 254 nm was recorded (figure 2.11). As observed for the wild-type His-eIF5A, all four mutant proteins (K48D, G50A, H52A and K56A) eluted at a molecular weight of between 30 and 31 kDa. In the case of the H52A mutant, protein peaks at 280 nm (blue) were observed at 43 and 22 kDa possibly indicative of dimer and monomer formations

(figure 2.11D). However, these shoulders were not apparent in the RNA readings at 254 nm (red). Also of interest is that in all four cases the readings at 254 nm, in comparison to those at 280 nm, vary. However, there are no differences in the retention volume of mutant proteins. Therefore, conformational changes within the protein or RNA (if indeed present), due to the mutation made, could be responsible for the variation in absorbance at 254 nm.

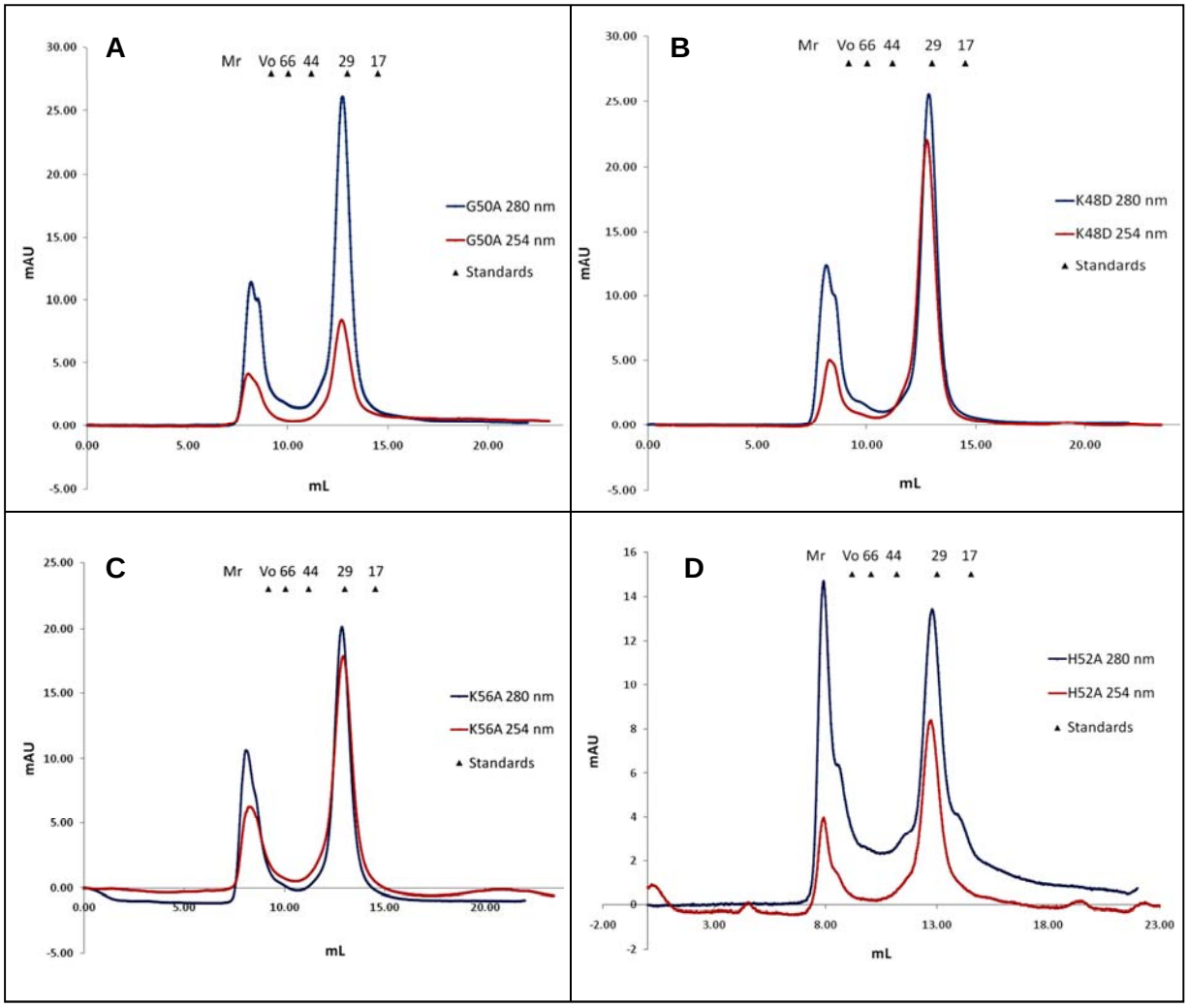

Figure 2.11: Gel filtration chromatographic characterisation of mutant proteins. Approximately 0.8-1 mg of protein was resolved in each case. For each mutant protein samples of the same concentration were resolved at both 280 nm (blue) and 254 nm (red) to determine the relative presence of RNA at 254 nm. Panel A: eIF5A G50A (G50A), panel B: eIF5A K48D (K48D), panel C: eIF5A K56A (K56A), panel D: eIF5A H52A (H52A). Molecular weight (Mr) standards are represented by triangles above each plot: myoglobin (17 kDa), carbonic anhydrase (29 kDa), Ovalbumin (44 kDa) and β-galactosidase (V_o).

The data suggested that the protein was present as either a compact oligomer or an extended monomer possibly bound to RNA, so an attempt was made to generate the monomeric species as observed by Gentz *et al.* (2009). Gentz *et al.* (2009) observed a monomeric species (17 kDa) when wild-type protein was treated with either dithiothreitol (DTT) or RNase A.

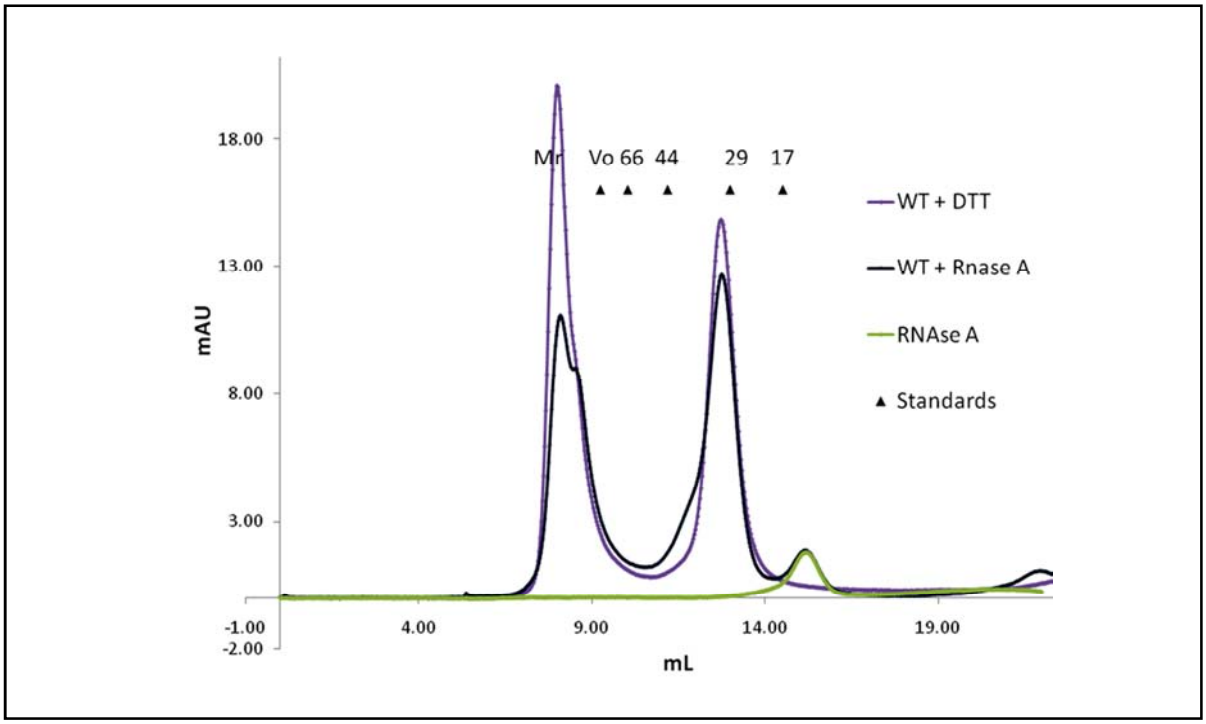

Figure 2.12: RNase A and DTT treatment of wild-type His-eIF5A protein. Approximately 0.8-1 mg of protein was resolved at 280 nm in each case. Wild-type protein was either treated with RNase A (1 µM final concentration) for 30 minutes (WT + RNase A) or DTT (1 µM final concentration) for 15 minutes (WT + DTT). RNase A (1 µM) was resolved independently as a positive control for RNase A (RNase A). Molecular weight (Mr) standards are represented by triangles above: myoglobin (17 kDa), carbonic anhydrase (29 kDa), ovalbumin (44 kDa) and β-galactosidase (V_o).

Treatment of the wild-type His-eIF5A with DTT and RNase A, a ribonuclease that cleaves single-stranded RNA, did not shift the elution profile of the protein to the monomeric species as observed by Gentz *et al*. (2009). Both treated proteins eluted at between 30 and 31 kDa and the peak observed at approximately 15 mL (14.3 kDa) after RNase A treatment (figure 2.12, WT + RNase A) is representative of RNase A as shown by the RNase A control (figure 2.12, RNase A). This data suggests that the 30-31 kDa protein species observed in this study might represent the monomeric species possibly adopting an extended monomer formation. The observation that RNase A did

not shift the protein species to that of a monomer could suggest that there is no, at least single stranded, RNA bound to the protein species. Nevertheless the variation at 254 nm was tested both before and after RNase A treatment and showed no significant difference between the readings at 254 nm confirming the absence of any RNA digestion by RNase A (figure 2.13, WT 254 nm vs. WT + RNase A 254 nm).

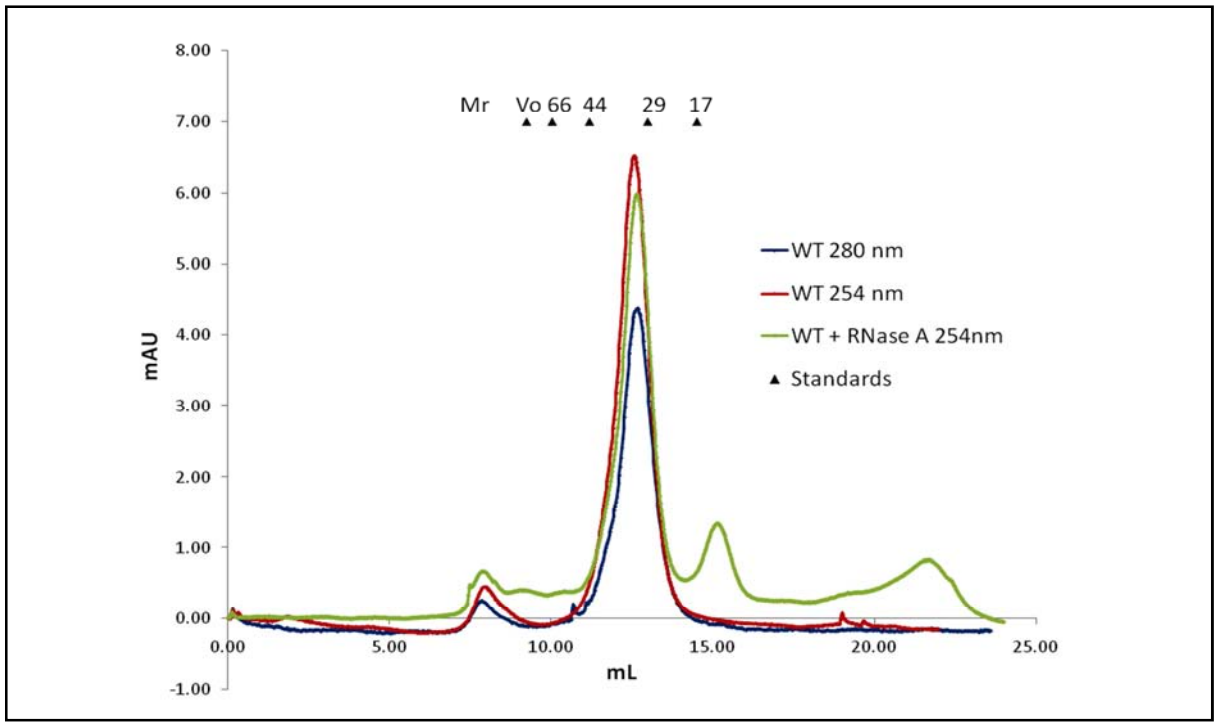

Figure 2.13: Treatment of wild-type protein with RNase A. The same concentration of protein (approximately 0.3 mg) was resolved in each case. Wild-type (WT) protein was resolved at 280 nm (blue) and 254 nm (red) and wild-type protein treated with RNase A (1 µM final concentration) for 30 minutes was resolved at 254 nm (green). Molecular weight (Mr) standards are represented by triangles above: myoglobin (17 kDa), carbonic anhydrase (29 kDa), ovalbumin (44 kDa) and β-galactosidase (V_o).

2.3.3.5 Native PAGE

Native PAGE was used as an alternate method to size exclusion chromatography for determining protein oligomeric state. Native PAGE analysis of His-eIF5A purified proteins confirmed that wild-type and mutant proteins have a molecular weight of approximately 30 kDa (figure 2.14). The K51R mutant as well as the four mutant proteins generated in this study (K48D, G50A, H52A and K56A) are similar in native appearance to that of the wild-type protein. Whether eIF5A protein is eluting in complex with RNA not degradable by RNase A (rRNA or tRNA) or has simply adopted

an extended monomer formation displaying interference at 254 nm requires further investigation.

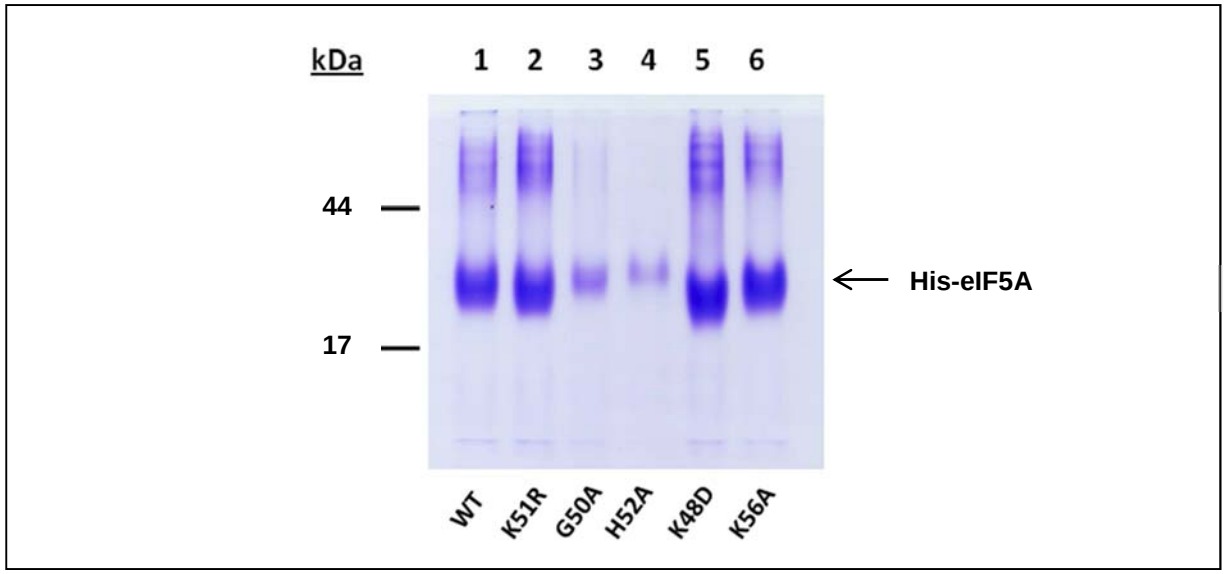

Figure 2.14: **Native PAGE analysis of wild-type and mutant His-eIF5A**. Approximately 10 µg of nickel affinity-purified protein was resolved in each case. Native protein was resolved alongside the standard globular proteins, myoglobin (17 kDa) and ovalbumin (44 kDa), to give an estimation of their molecular weight. Lane 1: wild-type eIF5A (WT), lane 2: eIF5A K51R (K51R), lane 3: eIF5A G50A (G50A), lane 4: eIF5A H52A (H52A), lane 5: eIF5A K48D (K48D), lane 6: eIF5A K56A (K56A).

2.4 Conclusions

The single point mutations G50A, K48D, H52A and K56A were successfully generated in the *TIF51A* gene allowing for subsequent functional and biochemical studies. All mutations generated in this study were in the vicinity of the highly unstructured extended loop region and hence were unlikely to affect the secondary structure of the eIF5A protein. A functional analysis conducted using the yeast null mutant PGY10, revealed that mutant proteins were able to support growth to varying degrees *in vivo* with G50A and K48D mutant proteins displaying the most convincing defects. The non-lethality of mutants alone suggested a level of hypusine biosynthesis was present within the PGY10 cells however to verify this each mutant protein was subjected to *in vivo* hypusination assays which showed that all mutant proteins were hypusinated. However, the extent to which could not be determined conclusively due to an overall

weak signal being detected and will therefore require further investigation. Whether variable degrees of hypusination efficiency could be responsible for the growth defects observed here is questionable since eIF5A is known to exist in excess of which very little is required for normal cell growth (Chattopadhyay *et al*., 2007). Mutant proteins did not exhibit temperature sensitivity at the range of temperatures tested (22 ºC - 34 ºC) suggesting that the results observed by Dias *et al*. (2008) for the K56A protein may be related to the imposed heat stress at 37 ºC.

The K51R mutant protein exhibits a non-viable growth phenotype however in this study the loop mutations generated only resulted in impaired growth. This suggests that the hypusinated lysine residue is critical at some point of interaction and making point mutations in the loop region reduces the efficiency of this interaction. As the loop residues have been postulated to be involved in eIF5A dimerisation, mutant proteins were subjected to a biochemical analysis and their oligomeric state was investigated. Gel filtration profiles determined eIF5A mutant and wild-type proteins to have a native molecular weight of 30 - 31 kDa. This is intermediate between those values obtained by Gentz *et al.* (2009) for both monomer (17 kDa) and dimer species (40 kDa). The inability to reproduce the results generated by Gentz *et al*. (2009) was confusing and as all potential possibilities were eliminated it seems as though eIF5A oligomeric state may be transitory and subject to certain conditions. In general gel filtration was not the most accurate method of determining the oligomeric state of native proteins and there is therefore a need to visit alternate methods of determining eIF5A tertiary structure. The ideal situation would be to obtain the crystal structure of the native, hypusinated eIF5A protein possibly through a technique such as solution NMR spectroscopy.

Chapter 3: An experimental system for producing eIF5A peptides for structural studies

Chapter 3: An experimental system for producing eIF5A peptides for structural studies

3.1 Introduction

The crystal structures of several eIF5A/aIF5A proteins have provided valuable insight into IF5A's general monomeric structure (Kim *et al*., 1998; Yao *et al*., 2003; Bosch & Hol, 2004; Tong *et al*., 2009). This structural data has been obtained using recombinant expressed in *E. coli* which lacks the vital hypusine modification. It is thus unknown whether the presence of hypusine results in conformational changes within the protein or how this residue is involved in interactions with eIF5A binding partners. Recently the foundations have been laid for achieving recombinant hypusine-modified eIF5A for structural studies (Park *et al.,* 2011).

The objective of the research described in this chapter was to develop an experimental system for producing sufficient quantities of native hypusinated yeast eIF5A for structural studies. In particular, the objective was to produce peptides that would be small enough for nuclear magnetic resonance (NMR) studies. This was achieved by engineering a thrombin cleavage site within the flexible linker region between the N-terminal and C-terminal domains of the protein.

3.2 Methods and Materials

3.2.1 Plasmids, strains and culture conditions

Bacterial strains and plasmid constructs used in this study are listed in table 3.1 The *E*. *coli* BL21 (DE3) strain was used for overexpression of recombinant protein (for

culture conditions see section 2.2.1) and expression vectors are depicted in figure 3.1 and details on the construction of pJC6 can be found in Appendix A.2. Yeast PGY10 and INVSc1 strains were cultured as described in section 2.2.1. The yeast expression and complementation vectors, pPG57 and pPG58, containing the yeast His-*TIF51A* gene with a thrombin cleavage site inserted into the flexible linker region of eIF5A (eIF5A$_{Thrombin}$) used in this study, were obtained from Dr PM Gentz (Rhodes University, South Africa).

Table 3.1: Genotypes of yeast and *E. coli* strains and a description of plasmid DNA used in this study

	Genotype / Description	**Phenotype^{+}**	**Source / Reference**
Strain			
INVSc1 (*S. cerevisiae*)	*MATa his3*Δ *leu2 trp1-289 ura3-52 / Matα his3*Δ *leu2 trp1-289 ura3-52*	*Ura^{-},His^{-},Leu^{-}, Trp^{-}*	Invitrogen
BL21 (DE3) (*E. coli*)	F–, *omp*T, *hsd*S$_B$(r$_B$-, m$_B$-), *dcm*, *gal*, λ(DE3)		Studier & Moffatt, 1986; Studier *et al.*, 1990
Plasmid			
pPG57	The pPG39 expression vector containing the yeast 6x His-*TIF51A* gene with a thrombin cleavage site inserted into the flexible linker region of eIF5A (eIF5A$_{Thrombin}$)	Amp^{R}, *URA3*	PM Gentz, unpublished
pPG58	The pPG20 complementation vector containing the yeast 6x His-*TIF51A* gene with a thrombin cleavage site inserted into the flexible linker region of eIF5A (eIF5A$_{Thrombin}$)	Amp^{R}, *URA3*	PM Gentz, unpublished
pT7-7 6xHis	Bacterial expression backbone vector with T7 promoter and 6xHis-tag	Amp^{R}	Cortay *et al*., 1994
pJC6	Bacterial expression vector derived from pT7-7 6xHis containing the yeast *TIF51A* gene with a thrombin cleavage site inserted into the flexible linker region of eIF5A (eIF5A$_{Thrombin}$)	Amp^{R}	This study

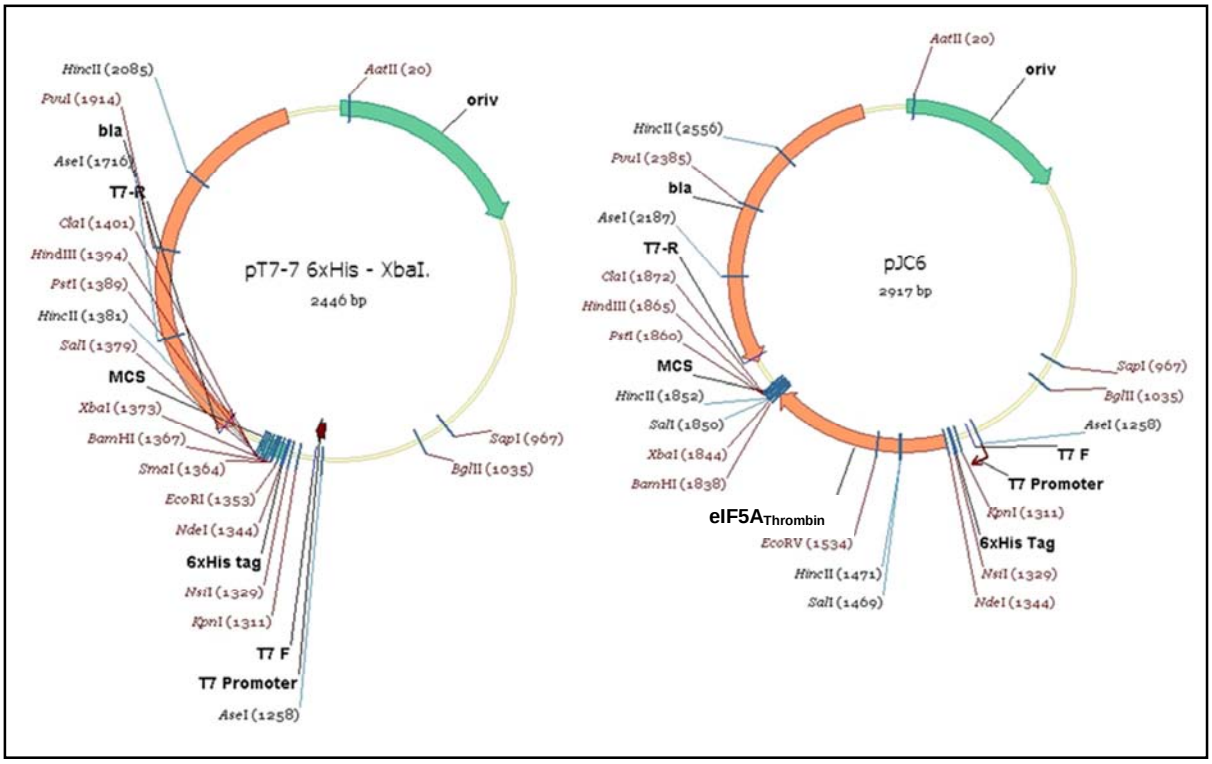

Figure 3.1: Restriction maps of the recombinant bacterial expression vectors used in the overproduction of eIF5A$_{Thrombin}$ in *E. coli* cells. Bla: *β*-lactamase, T7 Promoter: T7 bacteriophage RNA polymerase promoter, MCS: multiple cloning site, eIF5A$_{Thrombin}$: *TIF51A* gene with a thrombin cleavage site included in the linker region. The cloning strategy used to generate pJC6 can be found in Appendix A.2.

3.2.2 Complementation assays

Recombinant constructs pYES2, pPG20 and pPG20 K51R (section 2.2.1, table 2.1), and pPG58 were transformed into competent yeast PGY10 cells as described in section 2.2.1. Complementation assays were carried out as described in section 2.2.3 and agar plates were incubated at 22 ℃, 28 ℃ and 34 ℃ for 4 - 6 days.

3.2.3 Hypusination assays

Recombinant constructs pPG39 (section 2.2.1, table 2.1) and pPG57 were transformed into competent yeast INVSc1 cells. The cultures were grown in the presence of 0.1 µCi of [C^{14}]-spermidine trihydrochloride (GE Healthcare) per mL of culture. Cells transformed with pPG39 (wild-type) were grown with or without the DHS inhibitor, GC_7 (20 µg per mL of culture). Yeast cell-free extracts were then analysed by SDS-PAGE followed by autoradiography as outlined in section 2.2.4. Amplify™ Fluorographic reagent (GE Healthcare) was used according to the manufacturer's

recommendations, as an enhancing solution to visualise [C^{14}]-labelled eIF5A, prior to autoradiography.

3.2.4 Overexpression of eIF5A$_{Thrombin}$ in *E. coli* BL21 (DE3) cells

The recombinant construct, pJC6, carrying the gene for His-tagged eIF5A$_{Thrombin}$ was transformed into *E. coli* BL21 (DE3) cells along with pT7-7 as a negative control. 5 mL of an overnight culture was inoculated into 200 mL of LB broth containing 100 µg/mL ampicillin. Cultures were grown at 37 ℃ and 200 rp m for 3 - 4 hours until an OD_{600nm} of 0.6 - 0.8 was reached. At this point protein expression was induced by the addition of isopropyl β-D-1-thiogalactopyranoside (IPTG) to a final concentration of 1 µM. Cultures were then grown for an additional 3 hours with OD_{600nm} readings being taken hourly and 1 OD_{600nm} unit of culture set aside after each hour. Samples were harvested by centrifugation at 10 000 x *g* for 1 minute in a desktop microfuge whilst the final cell suspension was harvested at 10 000 x *g* at 4 ℃ for 10 minutes. Samples were analysed by SDS-PAGE (Laemmli, 1970) using a 15 % resolving gel with a 4 % stacking gel. *E. coli* cell-free extracts were obtained by resuspending pellets in 100 µL of 1 x sample buffer (10 % glycerol, 125 mM Tris-Cl pH 6.8, 4 % SDS, 10 % β-mercaptoethanol, 0.01 % bromophenol blue) and boiling for 5 minutes.

3.2.5 Overexpression of eIF5A$_{Thrombin}$ in yeast INVSc1 cells

A total of 4 L of INVSc1 cell culture was prepared as by the optimised YPD expression protocol outlined in section 2.2.5 eIF5A$_{Thrombin}$ overexpression was induced by glucose starvation as per the method described in section 2.2.4.1 Expression of eIF5A$_{Thrombin}$ was verified by SDS-PAGE and western analysis (see section 2.2.3.2). eIF5A$_{Thrombin}$ yeast cell lysates were resolved alongside wild-type eIF5A cell lysates for comparisons sake.

3.2.6 Purification of eIF5A$_{Thrombin}$

E. coli cells expressing eIF5A$_{Thrombin}$ (with a His-tagged N-terminal domain) were harvested as described in section 3.2.4 and pellets were resuspended in 5 mL of lysis buffer (100 mM Tris-Cl pH 8.0, 100 mM NaCl, 40 mM imidazole) in the presence of a 1 x proteinase inhibitor cocktail (Complete^{TM} EDTA free tablets, Roche). Lysozyme (50 µg) was added to each sample followed by incubation on ice for 30 minutes. Cells

were subsequently subjected to sonication at 4 ℃ using a hand-held 3 mm probe (Vibra Cell™) at 60 mA for 8 second intervals on ice for a total period of 10 minutes. Cell lysates were then centrifuged at 4 000 x *g* at 4 ℃ for 30 minutes. The supernatant (soluble fraction) was collected and passed through a sterile 0.45 µm syringe filter (Acrodisc®, Pall Life Sciences) and labelled clear lysate.

eIF5A$_{Thrombin}$, with an N-terminal His-tag, was extracted from yeast INVSc1 cells as by the methods described in section 2.2.6. Both yeast and *E. coli* clear lysates were subjected to nickel affinity chromatography (see section 2.2.6) over a 0 - 100 % gradient of buffer B, and eIF5A$_{Thrombin}$-containing fractions were concentrated to a volume of approximately 2 mL using Amicon Ultra-15 Centrifuge Filter devices (Millipore) as per manufacturer's instructions. In both cases His-tagged protein (1 mL) was subjected to gel filtration as previously described in section 2.2.7 using a 1 mL injection tube. eIF5A$_{Thrombin}$-containing fractions were pooled and concentrated down to approximately 300 µL. All protein concentrations were calculated using the NanoDrop™ 2000 (Thermo Scientific) with adjusted molecular weight (18.3 kDa) and extinction coefficient (2980 M^{-1} cm^{-1}) factors. Each step of the purification procedure was analysed by SDS-PAGE as described in section 2.2.6. Purified protein was stored at -80 ºC until further analysis.

3.2.7 Thrombin cleavage

100 µL of purified protein was cleaved using restriction grade human thrombin (Novagen) at a concentration of 1 U per mg protein. Cleavage was performed overnight (16 hours) with agitation in the thrombin cleavage buffer (20 mM Tris-HCl pH 8.4, 150 mM NaCl, 2.5 mM $CaCl_2$). The His-tagged peptide (N-terminal domain) was purified using the His-Spin Protein Miniprep™ (Roche) kit as per manufacturer's instructions allowing for separation of the two eIF5A domains. SDS-PAGE analysis was used to depict each step of the cleavage and subsequent purification procedures by resolving 5 µL of each sample.

3.3 Results and Discussion

The objective of experiments described in this chapter was to develop a system for producing eIF5A peptides that were small enough for solution NMR studies (approximately 10 kDa). eIF5A appears to consist of two domains separated by a flexible linker region. The approach was therefore to devise a strategy to develop an expression system that would facilitate the production of each of the two domains, each of which would then be suitable for NMR studies. In addition, since the aim of NMR studies would be to determine the solution structure of the hypusinated loop region, it was important to ensure that the purified N-terminal domain was hypusinated. The strategy was to introduce a thrombin cleavage site (LeuValProArg↓GlySer) within the flexible linker region of eIF5A ($eIF5A_{Thrombin}$). The flexible linker region of eIF5A potentially provides a convenient separation point of the two domains without affecting the folding of the two domains. The strategy for producing both hypusinated and unhypusinated variants of the eIF5A protein was to express the construct in yeast or *E. coli* cells respectively followed by treatment of recombinant protein with thrombin to produce the His-tagged N-terminal domain of 10.35 kDa and a C-terminal domain of 8.03 kDa. Thrombin has a molecular weight of 37 kDa and therefore separation of the two eIF5A peptides can be easily obtained using nickel affinity chromatography followed by gel filtration.

3.3.1 Functional analysis of $eIF5A_{Thrombin}$

The $eIF5A_{Thrombin}$ protein was subjected to a complementation assay using the PGY10 null mutant as described in the previous chapter. The mutant protein was unable to substitute for wild-type eIF5A in PGY10 cells grown in the presence of glucose, with a phenotype similar to the K51R mutant (Figure 3.2B). Lowering the temperature did not result in expression of a functional protein (Figure 3.2A) as was the case for cells grown at 34 ℃ (Figure 3.2C).

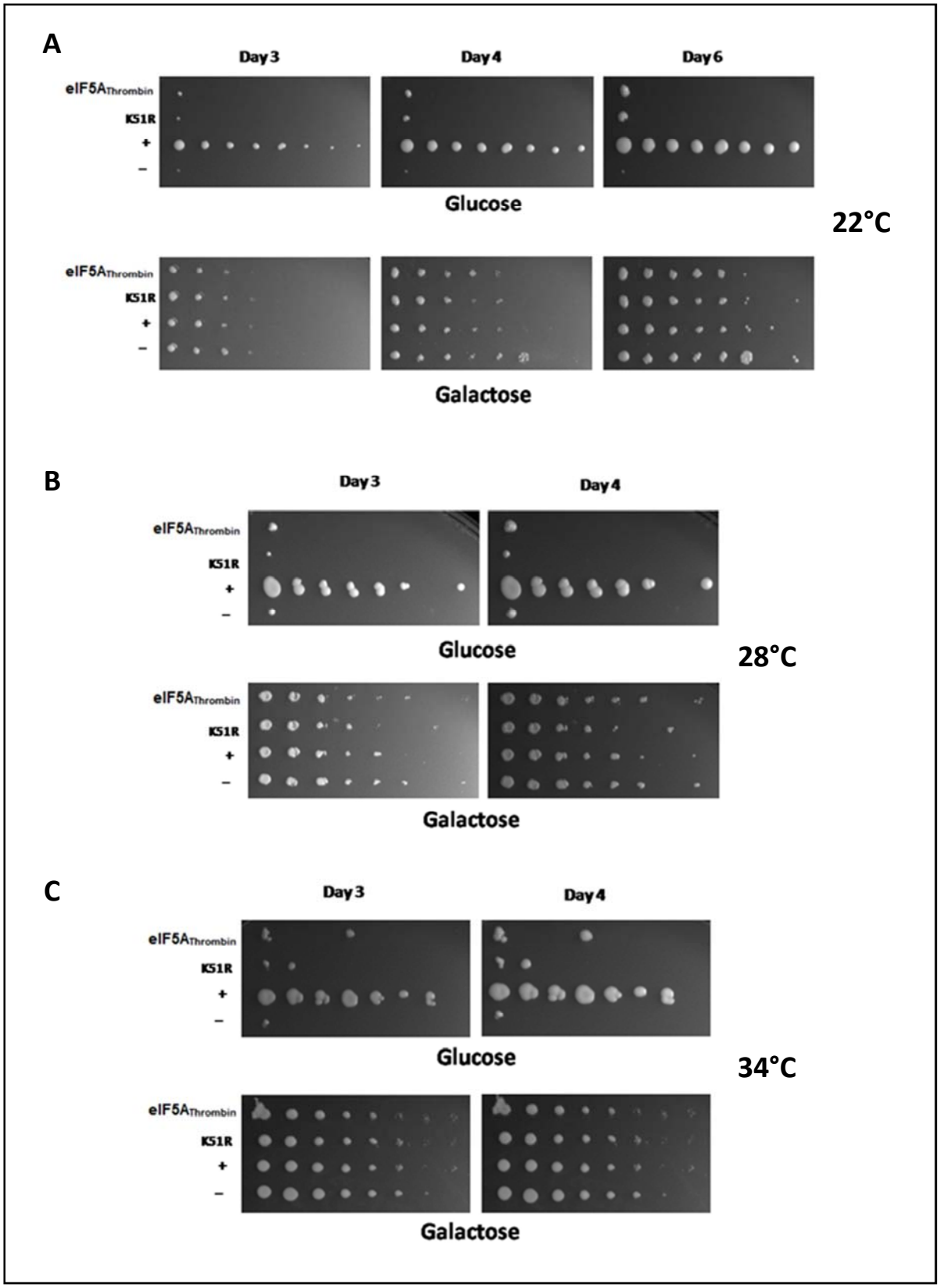

Figure 3.2: **Functional analysis and temperature sensitivity of strains harbouring eIF5A$_{Thrombin}$.** Yeast PGY10 cultures spotted on both glucose (above) and galactose (below) containing SMM plates and grown at (A) 22 ℃, (B) 2 8 ℃ and (C) 34 ℃. PGY10 competent cells were transformed with the following plasmid DNA: pYES-2 (-), pPG20 (+), pPG20 K51R (K51R) and pPG58 (eIF5A$_{Thrombin}$).

SDS-PAGE and western analysis confirmed the expression of recombinant proteins (figure 3.3). Although equivalent amounts of total protein were loaded on the SDS-acrylamide gels (figure 3.3A), western analysis depicts considerably lower levels of eIF5A$_{Thrombin}$ protein in comparison to wild-type eIF5A and K51R mutant proteins (figure 3.3B, lane 4 vs. lanes 2 and 3, respectively). Thus the eIF5A$_{Thrombin}$ mutant appears to be expressed at much lower levels than the wild-type protein. The most likely explanation is that the thrombin site in the linker region interferes with protein folding and thus function of eIF5A.

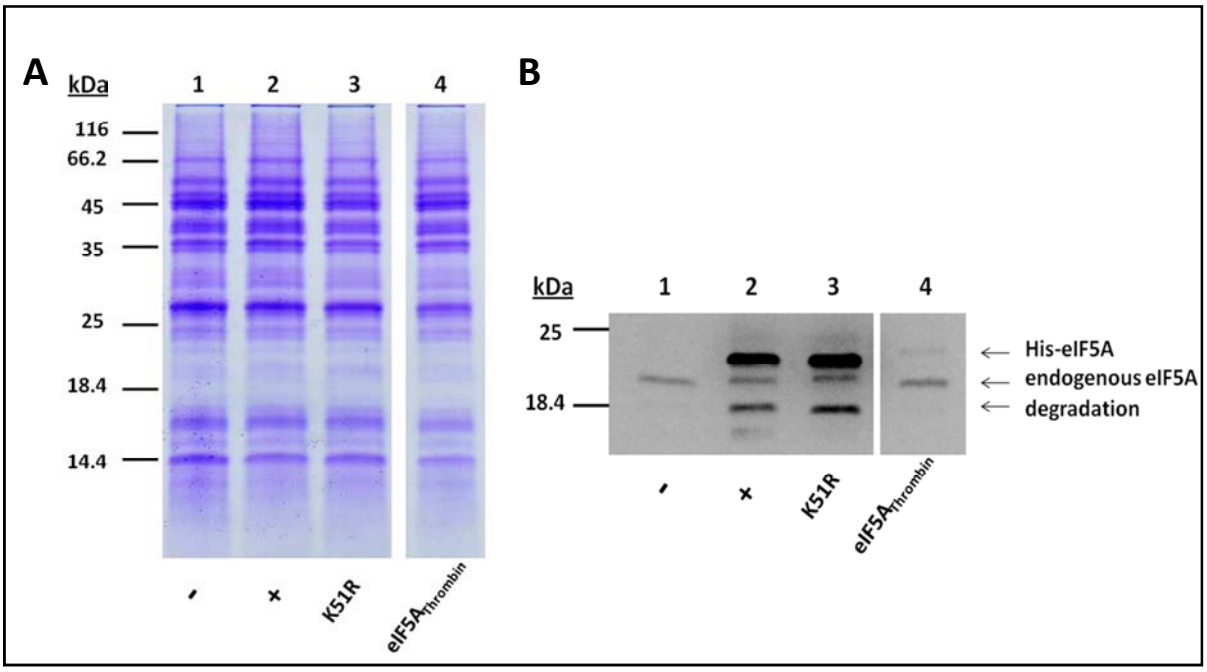

Figure 3.3: **Expression of eIF5A$_{Thrombin}$ protein in yeast PGY10 cells.** (A) SDS-PAGE analysis of yeast cell lysates showing total protein. (B) Western analysis using anti-eIF5A antibodies against a yeast cell lysate. PGY10 cells were transformed with the following plasmid DNA: lane 1: PYES2 (-), lane 2: pPG20 (+), lane 3: pPG20 K51R (K51R), lane 4: pPG58 (eIF5A$_{Thrombin}$).

3.3.2. Hypusination state of eIF5A$_{Thrombin}$

The next step was to determine whether the insertion of a thrombin site in the flexible linker region affected the hypusination of K51 in the N-terminal domain. Cells expressing wild-type eIF5A or eIF5A$_{Thrombin}$ were cultured in the presence of [C^{14}]-spermidine trihydrochloride and the presence of hypusine detected by autoradiography of protein extracts resolved by SDS-PAGE. As observed previously,

the eIF5A$_{Thrombin}$ mutant appeared to be expressed at lower levels than wild-type eIF5A (Figure 3.4B, lane 3 vs. lane 2). Since equivalent amounts of crude protein extracts were loaded on the gels (Figure 3.4A), it is reasonable to conclude that the differences in the expression of eIF5A relative to eIF5A$_{Thrombin}$ was significant.

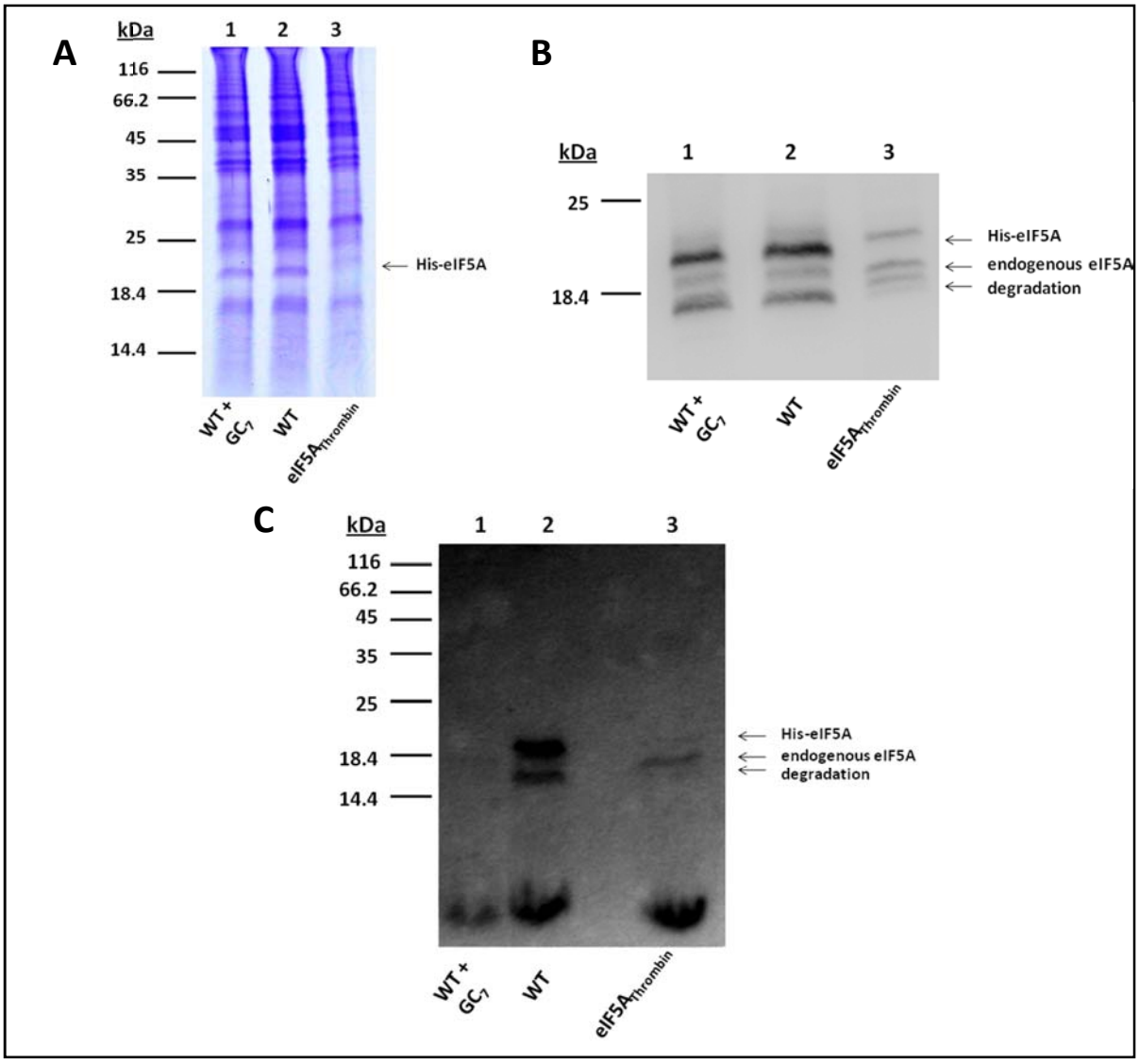

Figure 3.4: **eIF5A$_{Thrombin}$ expressed in *S. cerevisiae* INVSc1 cells is hypusinated *in vivo*.** (A) SDS-PAGE analysis of yeast cell lysates showing total protein. Protein bands were visualised by staining with Coomassie Brilliant blue. (B) Detection of recombinant eIF5A by western analysis using anti-eIF5A antibodies against a yeast cell lysate. (C) Autoradiograph of SDS-polyacrylamide gel containing radiolabeled eIF5A. INVSc1 cells were transformed with the following plasmid DNA: lane 1: pPG39 in the presence of 20 µg/mL GC$_7$ (WT + GC$_7$), lane 2: pPG39 (WT), lane 3: pPG57 (eIF5A$_{Thrombin}$). All cultures were grown in the presence of 0.1 µCi [C^{14}] spermidine trihydrochloride per mL of culture. eIF5A$_{Thrombin}$ expression was verified through SDS-PAGE and western analysis.

Autoradiography of the SDS-acrylamide gel showed that wild-type eIF5A was radiolabelled (Fig 3.4C, lane 2) and that the presence of the DOHH inhibitor, GC_7 resulted in inhibition of hypusination (Fig 3.4C, lane 1). A signal was detected for His-eIF5A$_{Thrombin}$ (figure 3.4B) indicating that the presence of the thrombin cleavage site in the linker region of the protein did not affect hypusination. The difference in the intensities of the signal obtained for wild-type eIF5A and eIF5A$_{Thrombin}$ was consistent with the lower levels of protein expression observed by western analysis and therefore it is reasonable to conclude that the mutant protein is efficiently hypusinated.

3.3.3 Purification of the N-terminal and C-terminal domains of eIF5A

3.3.3.1 Overexpression in *E. coli* and purification of eIF5A$_{Thrombin}$

In order to provide a comparison between hypusinated and unhypusinated eIF5A variants, eIF5A$_{Thrombin}$ was overexpressed in *E. coli*. The bacterial expression construct, pJC6 was transformed into *E. coli* BL21 (DE3) cells and transcription of the eIF5A$_{Thrombin}$ gene was induced for up to 3 hours. The presence of recombinant eIF5A$_{Thrombin}$ was first detected in cells after 1 hour and the amount of protein did not substantially increase after 2 or 3 hours (figure 3.5A, lane 4 vs. 6 and 8). This protein, represented by a band of approximately 20 kDa, was not present in cells transformed with the control vector, pT7-7 (figure 3.5A, lanes 1, 3, 5 and 7). The His-tagged eIF5A$_{Thrombin}$ was purified by nickel affinity chromatography (figure 3.5B) and concentrated down to a final volume of 2 mL (figure 3.5B, lane 6). Approximately 12 mg of eIF5A$_{Thrombin}$ protein (6 mg/mL) was routinely obtained from 200 mL of *E. coli* cells. Nickel affinity chromatography was run over a concentration gradient of 0 – 100 % buffer B instead of the optimised range of 8 – 100 % buffer B as described in section 2.2.6. This could be said to account for the low amounts of contaminating protein which have co-eluted with eIF5A$_{Thrombin}$ (Figure 3.5B, lane 6).

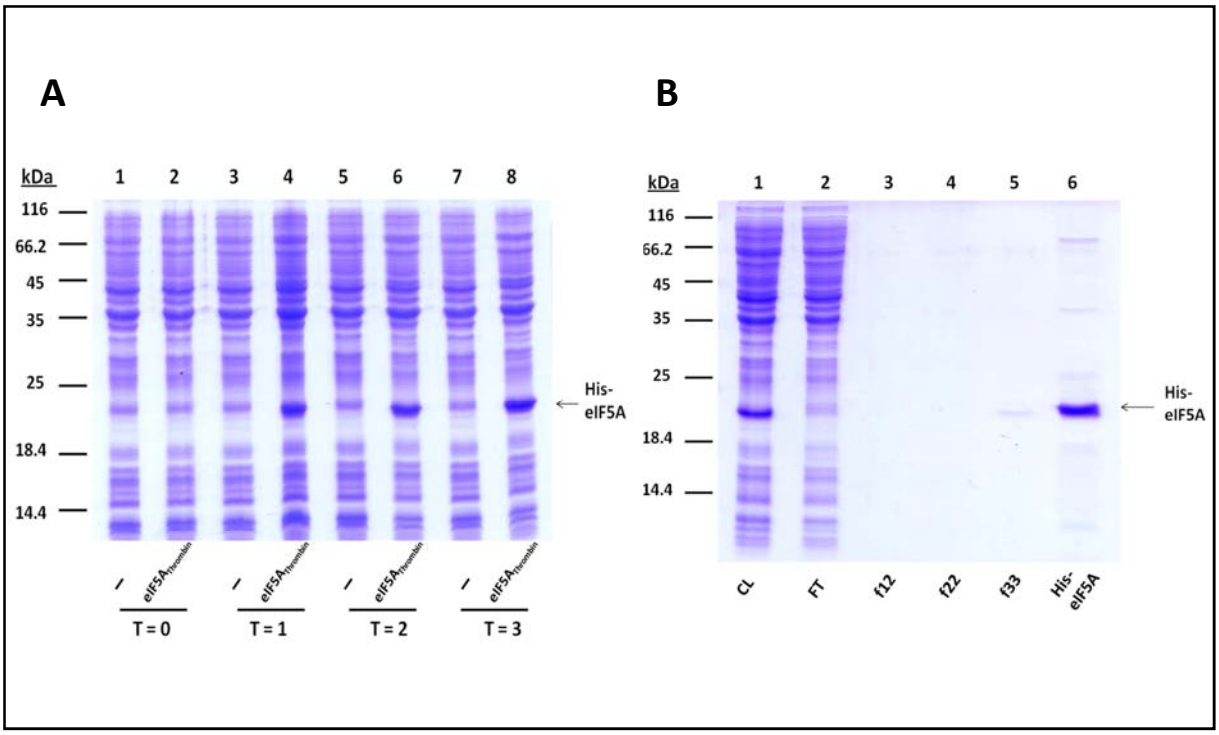

Figure 3.5: Over-expression and purification of His-eIF5A$_{Thrombin}$ from *E. coli* cells. (A) SDS-PAGE analysis of IPTG induced over-expression of His-eIF5A$_{Thrombin}$ in *E. coli* cells. Cells were transformed with pT7-7 (lanes 1, 3, 5 and 7) (-) or pJC6 (lanes 2, 4, 6, and 8) (TCS) and induced expression was monitored for 3 hours (T=0 – T=3). (B) SDS-PAGE analysis of the purification of His-eIF5A$_{Thrombin}$ from *E. coli* cells. Lane 1: clear lysate (CL), lane 2: flow through (FT), lanes 3-5: fractions 12, 22 and 33, lane 6: concentrated His-eIF5A$_{Thrombin}$ (His-eIF5A).

3.3.3.2 Overexpression and purification of eIF5A$_{Thrombin}$ produced in yeast

To purify native, hypusinated eIF5A, yeast INVSc1 cells were transformed with pPG57 plasmid DNA (table 3.1) and protein expression was induced via glucose starvation. As observed previously, the levels of eIF5A$_{Thrombin}$ as a function of the total cellular protein, were lower than that of wild-type eIF5A (figure 3.6A and B, lane 1 versus lane 2). In addition the eIF5A$_{Thrombin}$ protein migrated at a slightly higher molecular weight compared with the wild-type, which is expected due to the added amino acid residues. eIF5A$_{Thrombin}$ was then purified via nickel affinity chromatography (figure 3.6C). Since low levels of protein were obtained from 1 L of INVSc1 culture (figure 3.6C, lane 8), the total protein obtained from 4 L of cell culture was pooled and concentrated to approximately 2 mL (figure 3.6C, lane 9) giving a final concentration of 4 mg/mL.

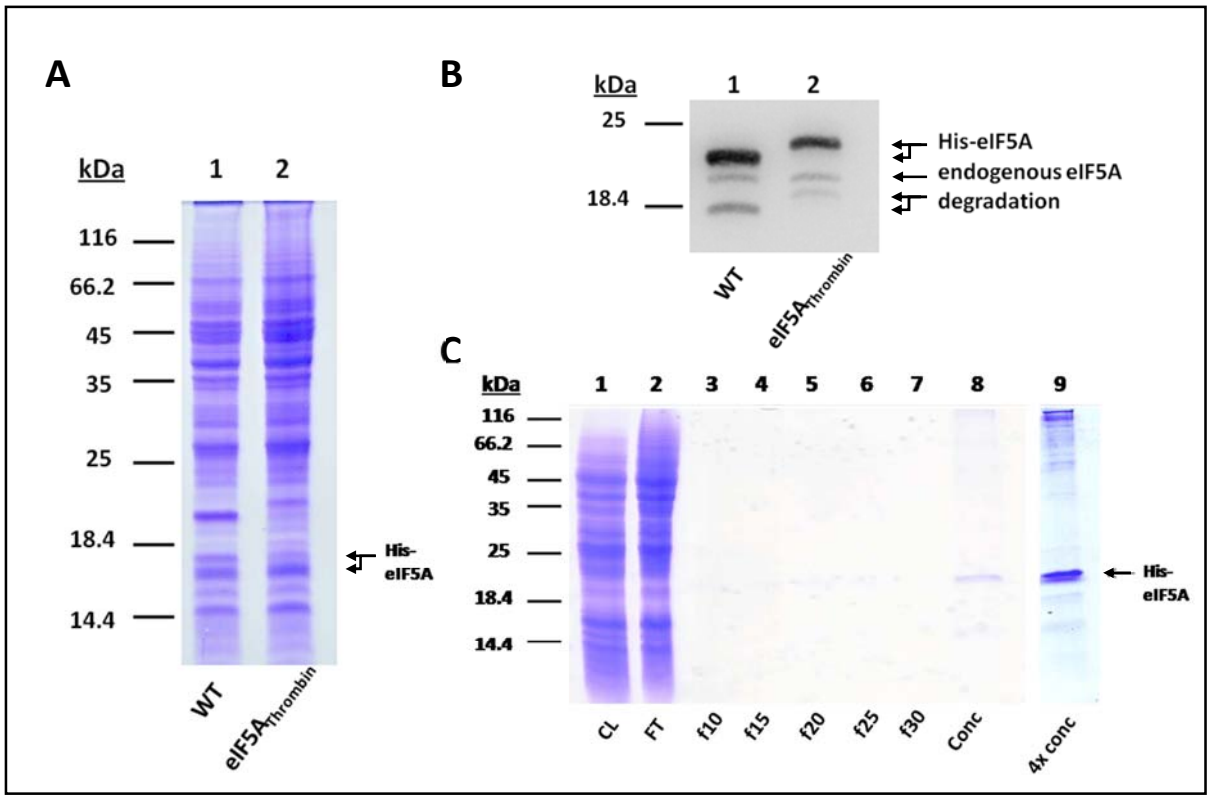

Figure 3.6: Purification of eIF5A$_{Thrombin}$ from yeast INVSc1 cells. (A) SDS-PAGE analysis of yeast cell lysates showing total protein. (B) Western analysis using anti-eIF5A antibodies against a yeast cell lysate. INVSc1 cells transformed with the following plasmid DNA: lane 1: pPG39 (WT), lane 2: pPG57 harbouring eIF5A with a thrombin cleavage site (TCS). (C) SDS-PAGE analysis of the purification of eIF5A$_{Thrombin}$ from INVSc1 cells. Lane 1: clear lysate (CL), lane 2: flow through (FT), lanes 3-7: fractions 10-30, lane 8: concentrated His-eIF5A$_{Thrombin}$ (Conc), lane 9: concentrated eIF5A$_{Thrombin}$ from 4 L of yeast INVSc1 culture (4x conc). (A, B) eIF5A$_{Thrombin}$ containing lysates were resolved alongside wild-type lysates for comparison.

3.3.3.3 Analysis of recombinant eIF5A$_{Thrombin}$ by size exclusion chromatography

eIF5A$_{Thrombin}$ purified by nickel affinity chromatography was subjected to gel filtration analysis to determine the native molecular weight of the purified protein. 1 mL of each sample was analysed via gel filtration (figure 3.7) and eIF5A containing fractions were collected and concentrated to a final volume of 300 µL. Protein concentrations subsequent to gel filtration for *E. coli* and yeast samples were calculated as approximately 3 and 2.5 mg/mL respectively. It was evident that both protein samples contained a large amount of contaminating, high molecular weight protein species (also seen in figure 3.5B: lane 6 and figure 3.6C: lane 9). This is likely to be due to the

fact that in these instances nickel affinity chromatography was run over a broader gradient of buffer B (see section 3.2.6) due to the unknown elution profile of eIF5A$_{Thrombin}$. Furthermore, very low amounts of His-eIF5A$_{Thrombin}$ were purified on each occasion from yeast INVSc1 cells allowing for a higher degree of non-specific binding to the nickel affinity column.

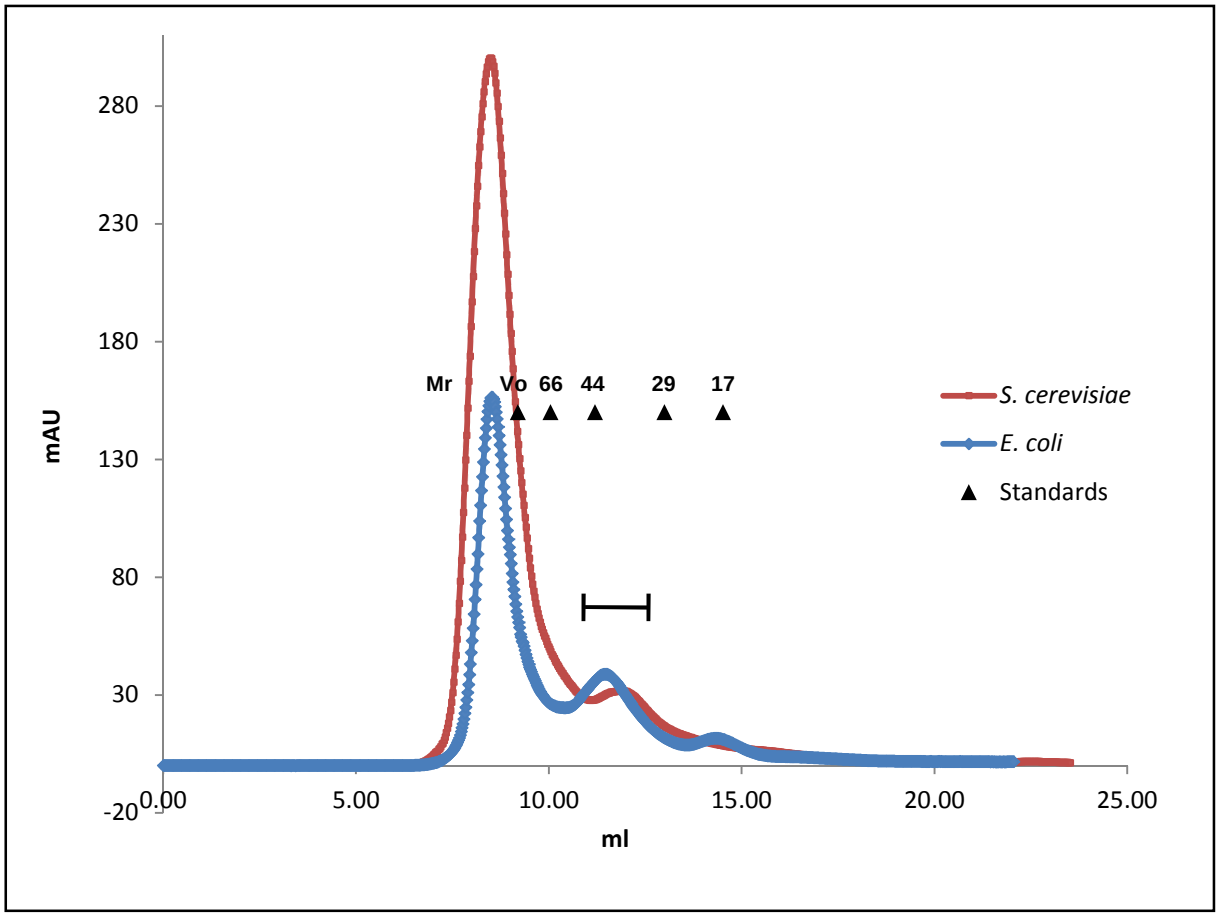

Figure 3.7: Gel filtration purification of eIF5A$_{Thrombin}$. Gel filtration elution profiles of both *E. coli* (blue) and *S. cerevisiae* (red) His-purified eIF5A$_{Thrombin}$. Fractions corresponding to the peaks highlighted on the chromatogram (⊢) were pooled and concentrated.

The theoretical molecular mass of His-tagged eIF5A is 17.9 kDa and that of His-tagged eIF5A$_{Thrombin}$ is 18.4 kDa. This small difference in molecular weight was evident in SDS-PAGE analysis of the proteins (figure 3.6A and B, lanes 1 and 2). During gel filtration analysis eIF5A$_{Thrombin}$ eluted at 37 and 42 kDa for protein purified from *S. cerevisiae* and *E. coli* cells respectively (figure 3.7). It therefore appeared that the protein is eluting as a dimer independent of its hypusination state. Gentz *et al.* (2009) have shown that eIF5A produced in *E. coli* has a high affinity to self-aggregate and

form dimers under certain conditions; however what these conditions are is unclear and will require further investigation.

3.3.3.4 Cleavage of eIF5A$_{Thrombin}$

eIF5A$_{Thrombin}$ purified from yeast and *E. coli* was incubated with thrombin, which theoretically should yield an N- and C-terminal domain of 10.35 and 8.03 kDa respectively. Since the molecular weight of thrombin is 37 kDa a combination of nickel affinity chromatography and gel filtration could be used to purify the N- and C-terminal eIF5A peptides. The purification and separation steps used here are depicted below (figure 3.8). Initial gel filtration of samples (section 3.3.3.3) removed a large proportion of contaminating proteins that were co-purified during nickel affinity chromatography (figure 3.8, lanes 2 vs. lanes 1). The cleaved protein (lanes 3) was separated using nickel affinity His-Spin columns (see methodology). The flow through therefore contained the C-terminal domain (lanes 4) and the elution fraction contained the N-terminal domain (lanes 6).

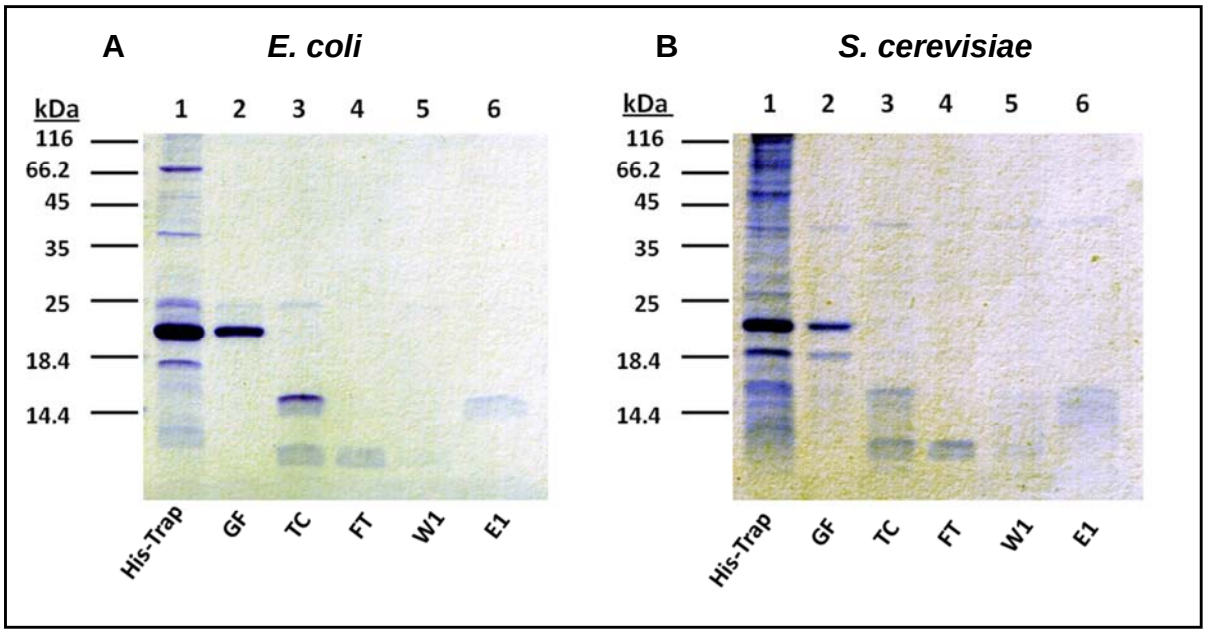

Figure 3.8: Thrombin cleavage of eIF5A$_{Thrombin}$. SDS-PAGE analysis depicting each purification step during thrombin cleavage of eIF5A. eIF5A$_{Thrombin}$ from both *E. coli* (A) and *S. cerevisiae* (B) were subjected to separate domain analysis. In each case lanes 4 and 6 show the C- and N-terminal domains of eIF5A respectively. Lane 1: nickel affinity-purified eIF5A$_{Thrombin}$, lane 2: eIF5A$_{Thrombin}$ purified by gel filtration (GF), lane 3: purified protein cleaved with thrombin (TC), lane 4: flow through subsequent to nickel affinity chromatography (FT), lane 5: wash 1 (W1) and lane 6: elution 1 (E1) of nickel affinity chromatography.

In total, approximately 80 µg of each domain was obtained from *E. coli* cells and 70 µg of each domain from yeast INVSc1 cells. However, taking into account a five-fold scaling down of protein during the gel filtration and thrombin cleavage steps (see methodology, section 3.2.6) one could assume that in total it is possible to obtain approximately 400 µg of each domain from 200 mL of *E. coli* BL21 (DE3) cells and 350 µg of each domain from 4 L of yeast INVSc1 cells. Since solution NMR spectroscopy requires at least 1 mM of protein (ideally 3-6 mM) (Wüthrich, 1995) that corresponds to 1 mg of a 10 kDa polypeptide, the volume of starting culture used in this study would therefore have to be scaled up considerably (at least 3-5 fold). Although this does not present a problem for bacterial protein expression as purifying protein from 1 L of cells is easily manageable, producing enough $eIF5A_{Thrombin}$ from yeast INVSc1 cells (12-20 L) may be challenging. However, the overexpression of $eIF5A_{Thrombin}$ in INVSc1 cells is a step that can still be optimised. This would involve determining the appropriate starting glucose concentration and time point at which maximum overexpression of $eIF5A_{Thrombin}$ is achieved.

3.4 Conclusions

The aim of this final experimental chapter was to determine the feasibility of producing sufficient amounts of both eIF5A variants (hypusinated and unhypusinated) for future analysis by solution NMR spectroscopy. Given the restrictions of a 600 *MHz* NMR spectrometer, it was decided to go about separating eIF5A into its two domains through the addition of a thrombin cleavage site for quicker and less complex analysis.

$eIF5A_{Thrombin}$ was unable to substitute for the wild-type eIF5A at both the permissive and non-permissive temperatures in PGY10 yeast cells suggesting that increasing the distance between the two eIF5A domains is detrimental to eIF5A function. Alternatively, the flexibility provided by the linker region may be essential to eIF5A function and the addition of a structurally rigid thrombin cleavage site may affect this flexibility. The observation that $eIF5A_{Thrombin}$ was hypusinated indicates that the addition of a thrombin cleavage site does not affect the overall folding of at least the N-terminal domain. Finally, gel filtration data suggests that both hypusinated and

unhypusinated eIF5A$_{Thrombin}$ elute as a dimer under native conditions. This suggests that eIF5A$_{Thrombin}$ may have a high affinity for self-association which is independent of hypusine (possibly involving only a single eIF5A domain such as indicative of the dimer crystallised by Kim *et al*., 1998).

The separation of both hypusinated and unhypusinated eIF5A into their domains through thrombin cleavage was achieved. However, these peptides would need to be generated in high quantity and quality in order for further analysis by solution NMR spectroscopy. This may present a problem when trying to achieve sufficient amounts of the hypusinated protein in yeast INVSc1 cells and is therefore a step which will require further optimisation. Nevertheless future structural studies on both hypusinated and unhypusinated eIF5A will provide valuable insights into eIF5As unique structure-function relationship as well as clarify whether hypusination induces conformational change within eIF5A.

Chapter 4: Is eIF5A required for eukaryotic IRES-driven translation initiation?

Chapter 4: Is eIF5A required for eukaryotic IRES-driven translation initiation?

4.1 Introduction

eIF5A (then eIF-4D) was first isolated from rabbit reticulytes in 1976 and so obtained its name because of its stimulation of methionyl-puromycin synthesis, an indication of the first peptide bond formation (Kemper *et al.*, 1976). However, despite three decades of research that followed, the fundamental function of eIF5A remains a mystery. The essential role of hypusine is still not clear and the plethora of downstream functions affected by eIF5A knockout or dysfunction has yet to be explained by a coherent mode of function for the protein in eukaryotic cells. Due to the apparent diversity of eIF5A functions, it seems unlikely that the protein is involved in a general cellular function. The popular assumption is that eIF5A is required for the translation of a select subset of mRNAs, thereby resulting in the proteins indirect effect on numerous cellular processes (Park *et al*., 1993; Shi *et al*., 1996). This chapter serves to provide a hypothesis as to the function of eIF5A and to present the substantiating evidence. The hypothesis proposes that eIF5A is not a canonical cap-dependent translation initiation factor as is currently held, but rather is required and is essential for, cap-independent, IRES-driven translation initiation.

4.2 A brief look at translation initiation

In prokaryotes initiation of mRNA translation requires the recognition of the Shine-Dalgarno (SD) sequence by the 16S rRNA of the 30S ribosomal subunit as well as three translation initiation factors (IF-1, IF-2 and IF-3). The formation of this preinitiation complex (figure 4.1A) results in the direct base pairing of the initiator tRNA (fMet-tRNA^{fMet}) anticodon with the mRNA start codon (AUG). This is followed by the recruitment of the 50S ribosomal subunit, the release of initiation factors and the

formation of the 70S initiation complex. Translation is initiated in this manner with ribosomes acting in tandem on polycistronic mRNA transcripts (Garrett *et al.*, 2000).

In contrast eukaryotic cap-dependent translation initiation is far more complex and requires numerous initiation factors (eIF4E, eIF4G, eIF4A, eIF4B, eIF3, eIF2, eIF1, eIF1A and poly (A) binding protein (PABP)) as well as capped, monocistronic mRNA transcripts. At first the 40S ribosome binds the ternary complex of eIF2-GTP-Met-$tRNA^{Met}$ to form the 43S preinitiation complex. Translation initiation is then reliant on the recognition of the cap structure by the cap-binding protein eIF4E and the subsequent formation of the cap complex called eIF4F (made up of eIF4E, eIF4G and eIF4A). After the formation of this the 48S preinitiation complex (figure 4.1B) the 40S ribosome scans along the mRNA for the first AUG codon. Once this association occurs the 60S ribosomal subunit is recruited forming the 80S complex and translation elongation commences (Nierhaus & Wilson, 2004).

In the archaea there are two alternate mechanisms of translation initiation prevalent which have been termed “leadered” and “leaderless” translation initiation (Benelli *et al.*, 2003). “Leadered” translation initiation resembles that of prokaryotes involving polycistronic mRNA transcripts containing SD sequences within their 5’ UTRs (Dalgaard & Garrett, 1993; Condo’ *et al*., 1999). “Leaderless” translation initiation involves mRNA molecules which completely lack a 5’ UTR and contain no SD sequence (Tolstrup *et al*., 2000; Slupska *et al*., 2001). Little is known about this mechanism of translation initiation however evolutionary history suggests that the last common universal ancestor (LUCA) utilised a leaderless mechanism (Londei, 2005; Allen & Frank, 2007) and is mostly supported by the fact that leaderless mRNAs are universally translatable across the three domains of life (Grill *et al*., 2000).

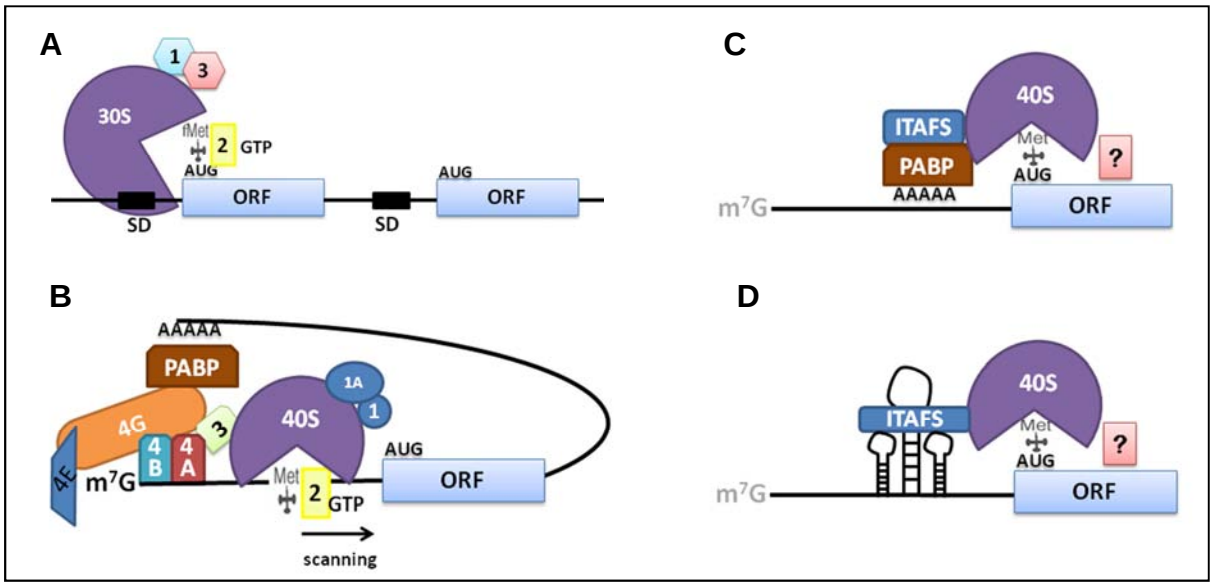

Figure 4.1: The alternate mechanisms of translation initiation. (A) Prokaryotic translation initiation requires interaction between the Shine-Dalgarno sequence (SD) and the 16S rRNA as well as three initiation factors (IF-1, IF-2 and IF-3). (B) Eukaryotic cap-dependent translation initiation requires numerous initiation factors (eIF4E, eIF4G, eIF4A, eIF4B, eIF3, eIF2, eIF1, eIF1A and PABP) as well as capped, monocistronic mRNA (m^7G). (C, D) IRES-dependent eukaryotic translation initiation is independent of capped mRNA. PABP and IRES transacting factors (ITAFs) are required in the case of adenine rich IRES-containing mRNAs (C) and ITAFs are required for IRESs with a high degree in secondary structure (D). The canonical initiation factors required in each case (C, D) remain unknown (?). In all four cases ORF denotes open reading frame.

4.3 Internal ribosome entry sites (IRESs)

In eukaryotes an internal ribosome entry site (IRES) is a nucleotide sequence that allows the ribosome to bind directly to mRNA and commence translation initiation independent of the presence of a 5' cap (Jang *et al.,* 1988; Pelletier & Sonenberg, 1988). IRESs are commonly found in the 5' UTR of RNA viruses thus providing the virus an effective means to shut down primary translation within the eukaryotic host cell whilst IRES-driven translation of viral transcripts continues (Hellen & Sarnow, 2001). The first viral IRES was discovered in the late 1980s when it was revealed that specific regions of picornavirus mRNA were able to attract and bind to the 40S ribosomal subunit and initiate translation in a cap-independent manner (Jang *et al.,* 1988; Pelletier & Sonenberg, 1988). In the early 1990s reports of the first cellular IRESs began to emerge after the observation that immunoglobulin heavy chain binding protein (BiP) was still being translated in cells infected with polio virus

(Macejak & Sarnow, 1991). According to IRESite (the database of experimentally verified IRES structures), there are now at least 68 viral and 115 eukaryotic cellular mRNAs containing IRESs (Mokrejš *et al.*, 2006, 2010). It is further estimated that 10-15 % of cellular mRNA has the ability to be translated in an IRES dependent manner (Spriggs *et al.*, 2008). Unfortunately identification of IRES-containing eukaryotic mRNAs has been difficult because cellular IRESs share no similarity in nucleotide sequence or secondary structure (Baird *et al.*, 2006, 2007). Cellular IRES sequences can however be classified into two groups (figure 4.1, C & D): one adenine rich in sequence and the other exhibiting a high degree of secondary structure (Martínez-Salas *et al*., 2002; Baird *et al*., 2006).

4.4 Activation and mechanism of cellular IRES-driven translation

During certain cellular events such as differentiation, mitosis and proliferation as well as adverse cellular conditions such as environmental stress, apoptosis and viral infection, cap-dependent translation is compromised. This is due to cleavage or changes in phosphorylation of certain initiation factors such as, for example, dephosphorylation of eIF4E (cap binding protein) or cleavage of eIF4G (cap scaffold protein) (reviewed in Spriggs *et al*., 2008). Under these conditions the cap-independent, IRES mechanism of translation initiation is favoured and ribosomes are reprogrammed to commence translation of IRES-containing mRNA (Yamasaki & Anderson, 2008). The IRES mechanism allows for a rapid turnover of proteins essential under conditions where cap-dependent translation is either reduced or suppressed, resulting in translation of proteins central to stress response and recovery, thus aiding in cell survival under adverse conditions (Spriggs *et al.*, 2008).

IRES-driven translation has been extensively studied in certain viruses and the mechanism of translation is well characterised for some RNA viruses. The IRES mechanism employed by different RNA viruses vary and so far three classes of viral IRESs have been described. The first is characterised by the 200 nt long discistrovirus IRES, which binds directly to the ribosome and initiates translation without the requirement of initiator tRNA and initiation factors (figure 4.2A) (Pestova & Hellen, 2003). IRES elements found in hepacivirus and pestivirus (HP) mRNA transcripts

make up the class of viral IRESs named HP IRESs which are approximately 300 nt long and require solely eIF3 for the formation of the 43S preinitiation complex (figure 4.2B) (Hellen & Breyne, 2007). The final class is made up of IRESs from a subset of *Picornaviruses* (*Aphthovirus* and *Cardiovirus*) and this mechanism requires the binding of eIF4G and eIF4A to the IRES element followed by their subsequent recruitment of the 43S preinitiation complex in an ATP-dependent manner (figure 4.2C) (Pestova *et al*., 2001).

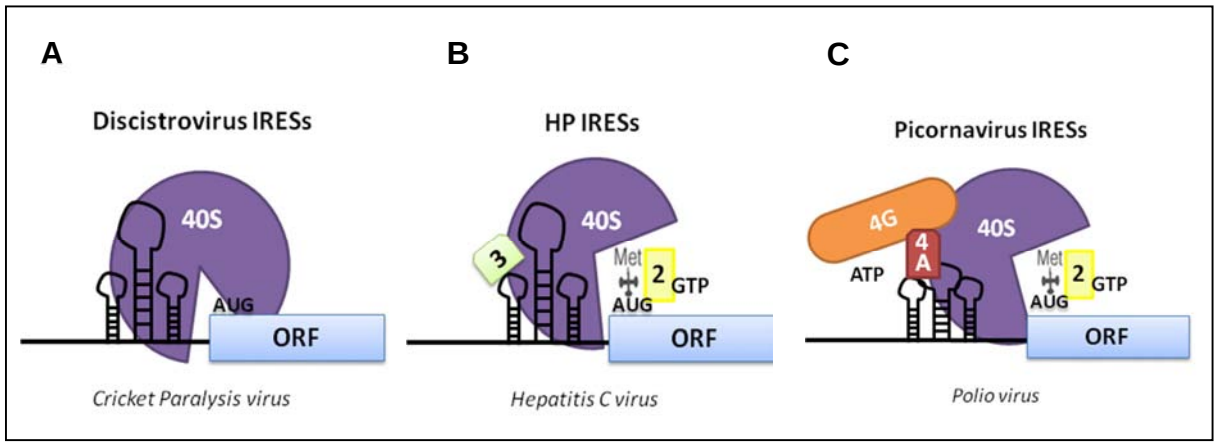

Figure 4.2: Different mechanisms of viral IRES-driven translation initiation. From left to right are the three current classes of viral IRES-driven translation initiation in increasing order of complexity. A) IRESs characterised by discistrovirus IRES require no initiation factors or initiator tRNA. B) Hepacivirus and pestivirus (HP) IRESs require eIF3 and the ternary complex and C) the class of IRESs characterised by a subset of picornaviruses require the initiation factors eIF4G and eIF4A, ATP as well as the ternary complex to initiate translation.

In contrast little is understood about cellular IRES-driven translation initiation. It seems that IRES trans-acting factors (ITAFs) are required in most cases for the proper functioning of initiation but only a few cellular ITAFs have been identified (Evans *et al*., 2003; Mitchell *et al*., 2003; Bonnal *et al*., 2005) and canonical factors are yet to be determined. Furthermore, not all IRES-containing mRNAs are translated in response to the switch to cap-independent translation initiation (Cornelis *et al.*, 2000; Qin & Sarnow, 2004; Lewis & Holcik, 2005). The response is seemingly condition-specific and it has therefore been suggested that activity is governed by cellular levels of various, specialised ITAFs (Spriggs *et al*., 2008), their subcellular localisation (Lewis *et al*., 2007) or phosphorylation state (Jo *et al*., 2008) as well as other factors such as ribosome stalling (Fernandez *et al.*, 2005) or ribosomal modification (Le Quesne *et al.*,

2010). It has been hypothesised that ITAFs may play one of two roles, acting as chaperones stabilising active form of IRES elements, or providing the connection between the IRES element and the ribosome (Spriggs *et al*., 2005). Future studies will undoubtedly reveal a deeper understanding of cellular IRESs, their mechanism of action as well as their regulation. In addition the identification of canonical initiation factors required for cellular IRES-driven translation initiation in comparison to the cap-dependent mechanism will be extremely interesting.

Since the discovery of cellular IRESs the assumption was that IRES-driven translation emerged later on in eukaryotic evolution as a means to cope with adverse environmental and physiological conditions (Stoneley & Willis, 2004; Komar & Hatzoglou, 2005). However, there is convincing evidence to support the theory that IRES-driven translation was the primary mechanism of translation initiation in early eukaryotes and that the more complex cap-dependant mechanism evolved later (Hernández, 2008). This hypothesis (as discussed by Hernández) is supported by the following: (1) the simplicity of IRES-driven translation; (2) the almost intrinsic ability of the ribosomes to bind IRES containing mRNA in a prokaryotic like manner, that is, without the presence of a cap, initiation factors and ATP; (3) the fact that eIF4E and eIF4G (initiation factors essential for cap-dependent translation) are the most recently evolved initiation factors and unique to eukaryotes and therefore cap-dependent translation could have only developed after the appearance of eIF4E, eIF4G and capped mRNAs (suggesting that there had to be a previously established mechanism of translation in early eukaryotes) and finally (4) cross-kingdom IRESs (suggesting a universal, simple, ancestral eukaryotic translation initiation mechanism). Furthermore, the increasing evolutionary complexity of the IRES mechanism is possible and is demonstrated by the three different classes of viral IRESs (Hernández, 2008). Hernández (2008) argues that the IRES mechanism was retained in eukaryotic cells to provide rapid responses in times of stress whereas the more complex cap-dependent mechanism became dominant for the degree of regulation it provided.

4.5 Is eIF5A involved in eukaryotic IRES-driven translation?

4.5.1 eIF5A is unlike most eukaryotic initiation factors

eIF5A is one of a few translation factors that are universally conserved throughout the taxa and considered to be common to some universal ancestor (the LUCA) (Kyrpides & Woese, 1998; Ganoza *et al.*, 2002). eIF5A has both archaeal and prokaryotic homologues, implying that an ancestral eIF5A homologue was present within cells at the onset of eukarygonesis. Cap-dependent translation initiation is unique to eukaryotes (Kyrpides & Woese, 1998; Aravind & Koonin, 2000) and therefore by inference eIF5A could have played a role in a cap-independent translation mechanism prior to the development of the fundaments to cap-dependent translation initiation (eIF3, eIF4E, eIF4G, and capped mRNAs).

Unlike most initiation factors, eIF5A is abundant in the cytoplasm of eukaryotic cells (Thomas *et al.,* 1979) and only a small fraction of the protein is found in the ribosomal high salt fraction (Kemper *et al.,* 1976). This suggests that eIF5A is largely present unbound to ribosomes and indeed in yeast eIF5A exists in several-fold excess over that necessary for normal cell growth (Chattopadhyay *et al*., 2008). In addition eIF5A and eIF4A (RNA helicase) are more abundant than ribosomes (3-5 times) whereas most other initiation factors are at 0.1-1 times the concentration of ribosomes (Hershey, 1994; Duncan & Hershey, 1983). Also significant is the fact that eIF5A expression is induced in early G1 phase and then the concentration of transcripts decreases steadily throughout the remainder of the cell cycle (Chan *et al*., 2002; Dresselhaus *et al*., 1999). Last but not least, eIF5A depletion only reduces protein synthesis by approximately 30 % (Kang & Hershey, 1994) and a recent report suggests that eIF5A is only suspected to be required for the synthesis of about 5 % of translated products (Li *et al.*, 2010).

4.5.2 Stress response and eIF5A

As discussed earlier, IRES-driven translation is predominant under various conditions of stress (reviewed in Spriggs *et al*., 2008). Under these conditions it would be expected that cells would induce expression of ITAFs required for this mechanism of translation (Spriggs *et al*., 2008). It is therefore curious that eIF5A expression is

induced under many of the same stress related conditions where cap-dependent translation is compromised. In rice cells abiotic stresses, salt and heavy metal induced the accumulation of OseIF5A-1 and OseIF5A-2 mRNAs suggesting that both OseIF5A genes might be regulated by plant development and environmental stresses (Chou *et al.,* 2004). Also it was found that eIF5A and DHS expression were induced with environmental stress and natural senescence in tomatoes suggesting the proteins involvement in programmed cell death (Wang *et al.,* 2001). Furthermore, eIF5A is up-regulated in cells subjected to apoptosis (Taylor *et al*., 2004), viral infection (Bevec *et al*., 1994; Shih *et al*., 2010), oxidative stress (Kim *et al*., 2007) and DNA damage (Decker *et al*., 2003), all of which result in a switch to IRES-driven translation (reviewed in Spriggs *et al*., 2008). Moreover, in *Rosa chinensis*, RceIF5A overexpressed plants developed an increased resistance to environmental stress whilst down-regulated RceIF5A plants were more susceptible to the same stress conditions confirming eIF5As involvement in stress response (Xu *et al.*, 2011). Finally eIF5A has been shown to be required for only approximately 5 % of translational products in unstressed cells, however a more striking effect was observed in cells subjected to oxidative stress (Li *et al.*, 2010). In the same study eIF5A was shown to be requisite for polysome disassembly and stress granule formation and this data resulted in the conclusion that “eIF5A may play an important role in reprogramming protein synthesis in stressed cells” (Li *et al.*, 2010).

4.5.3 Linking eIF5A with translation of IRES-containing mRNAs

Due to the variety of functions affected by eIF5A knockout/dysfunction, the prevailing hypothesis has been that eIF5A is required for the translation of a select subset of mRNA. As mentioned above eIF5A is up-regulated in times of stress (when cap-dependent translation is compromised), and therefore this select subset of mRNA may be defined by containing IRES elements within their 5’UTRs (see table 4.1 and Appendix G for further information). Thus it is proposed here that eIF5A function in numerous cellular processes is as an indirect result of the translation of an IRES-regulated set of proteins.

Supporting this hypothesis is the observation that eIF5A is a cellular regulator of p53 (Li *et al.*, 2004). Overexpression of hypusinated eIF5A resulted in the up-regulation of

p53 whilst silencing eIF5A reduced p53 protein levels (Li *et al.*, 2004). In fact, eIF5A is actually required for the expression of p53 subsequent to Actinomycin D-induced apoptosis (Taylor *et al.*, 2007). p53 is one of a few apoptosis-related proteins to be translated in an IRES-dependent manner (Candeias *et al*., 2006; Yang *et al.,* 2006). Further support for the hypothesis that eIF5A is involved in the translation of IRES-containing mRNAs is the observation by Zuk and Jacobson (1998) that uncapped mRNA accumulated at the non-permissive temperature using a yeast eIF5A temperature-sensitive mutant. One of the mRNA sequences identified (*PAB1*) is a known IRES-containing transcript (Gilbert *et al*., 2007). Zuk and Jacobson (1998) stated that their observations could be explained by an increase in the export of uncapped mRNAs from the nucleus after a temperature shift in ts1159 cells. This supports the hypothesis since the stress of a temperature shift would be expected to result in an increase in the export of IRES-containing (uncapped) mRNAs and their subsequent accumulation can be attributed to the inactivity of eIF5A at the non-permissive temperature.

Table 4.1: Summary of cellular proteins known to contain IRES elements in their mRNA (Mokrejš *et al.*, 2006, 2010). A more detailed list can be found in Appendix G.

Protein Group	**Proteins translated by IRESs**
Transcription factors	MYT-2, NF-κB repressing factor NRF, AML1/RUNX1, Gtx homeodomain transcription factor
Translation factors	eIF4G, elF4GI, eIF4GII, DAP5
Growth factors	VEGF, PDGF, FGF1, FGF2, IGF-II
Transcriptional regulators	YAP1, SMAD5, HIF-1α
Oncoproteins	c-Myc protein, L-myc-1 protein, Pim-1 protein
Apoptosis regulators	p58PITSLRE, p53, Apaf-1, XIAP, HIAP2, Bcl-xL, Bcl-2
Neuronal development	ARC, α-subunit of calcium calmodulin dependent kinase II dendrin, MAP2, RC3 and APP
Transporters	Notch2, CAT-1
Other	NDST1, Hsp70, Hsp90, PAB1, PKC, ODC, BiP, β-subunit of mitochondrial H+-ATP synthase, connexins 32 and 43, APC, cyclin D1, Boi1p

Further eIF5A studies can be linked to IRES-regulated translation. eIF5A-depleted cells arrest in G1/S phase (Park *et al*., 1993). Cyclin D1 and p53 are both critical regulators of the cell cycle at the G1/S transition and their translation is IRES-driven (Shi *et al*., 2005; Candeias *et al*., 2006). In 2002 eIF5A was implicated in angionesis (Clement *et al*., 2002) and later on in embryonic development (Parreiras-E-Silva *et al.*, 2010). The vascular endothelial and platelet-derived growth factors (VEGF and PDGF) are required for new blood vessel formation and embryonic development respectively and both are products of IRES-driven translation (Stein *et al.,* 1998; Bernstein *et al.,* 1997). Defects in cell polarity have been observed in a yeast eIF5A mutant (Zanelli & Valentini, 2005) and it is known that transcripts of the yeast Boi1 protein (required for polar growth) contain IRES elements (Gilbert *et al*., 2007).

eIF5A has been proposed to play a role in the nonsense-mediated decay (NMD) pathway (Schrader *et al.*, 2006). This was based on the observation that a yeast eIF5A temperature sensitive mutant (V81G) accumulated NMD transcripts (mRNA normally degraded by the NMD pathway) at the non-permissive temperature. In fact approximately 60 % of the up-regulated mRNA molecules in the V81G strain overlapped with those up-regulated in NMD-deficient yeast strains (Schrader *et al.*, 2006). Curiously IRES-mediated translation initiation activates NMD (Holbrook *et al*., 2006). Therefore the accumulation of NMD transcripts could be explained by the inactivity of IRES-driven translation due to the dysfunctional eIF5A at the restrictive temperature.

In 2008 Luchessi *et al.* concluded that eIF5A is involved in neuronal development in mammalian rat brains. An increase in eIF5A was found specifically within the neuronal dendrites (Luchessi *et al.*, 2008). The initiation of translation of numerous proteins localised within neuronal dendrites is IRES-dependent. These include proteins such as activity-regulated cytoskeletal protein (ARC), α-subunit of calcium calmodulin dependent kinase II dendrin, microtubule-associated protein 2 (MAP2), neurogranin (RC3) and amyloid precursor protein (APP) (Pinkstaff *et al.,* 2001). It has also been shown that overexpression of eIF5A in plants (no p53 homologue has been found in plants) caused programmed cell death (PCD) (Hopkins *et al.*, 2008) and moreover, it has been determined that overexpression of eIF5A can induce apoptosis in human

HT-29 cells independent of p53 (Taylor *et al.*, 2007). Death associated protein 5 (DAP5) signals cells for PCD and is also an IRES-regulated protein (Henis-Korenblit *et al*., 2000).

More recently eIF5A has been linked to diabetes where eIF5A mediates/induces inflammation in the pancreas under conditions of stress (Maier, Ogihara *et al.*, 2010). Therefore eIF5A might mediate the translation of proteins involved in the inflammatory response. Indeed bifunctional heparan sulfate N-deacetylase/N-sulfotransferase 1 (NDST1) transcripts contain IRES elements and is a critical inducer of the inflammatory response (Grobe & Esko, 2002). Also in 2010 it was demonstrated that eIF5A is required for the formation of stress granules (Li *et al.*, 2010). Stress granule assembly is known to require two IRES-regulated proteins, ornithine decarboxylase (ODC) (Pyronnet *et al.,* 2000) and PABP (Gilbert *et al*., 2007). Taken together, it can be argued that a large percentage of eIF5A associated functions can be correlated with either missing or upregulated IRES-translated proteins.

4.6 How is eIF5A involved in IRES-driven translation initiation?

4.6.1 The conserved evolutionary function of eIF5A

As discussed before (section 1.4.2) eIF5A has both archaeal (aIF5A) and prokaryotic (EF-P) homologues. The highest density of conservation between the homologues is found within the extended loop region, the site of hypusination in eukaryotic and archaeal cells. EF-P shares functional similarities with the IF5A family in that it is also essential for cell viability (Aoki *et al.*, 1997) and stimulates the first peptide bond formation (Glick & Ganoza, 1975). It is therefore reasonable to assume that eIF5A might carry out an evolved EF-P function hence the degree of conservation between the homologues. In prokaryotic translation initiation EF-P binds to and stabilises fMet-$tRNA_i^{fMet}$ for the first peptide bond formation (Blaha *et al*., 2009). Blaha *et al.* (2009) also showed when they reported the crystal structure of EF-P bound to the *Thermus thermophilus* 70S ribosome, that the extended loop region (the site of hypusination of eIF5A) reaches very near to the peptidyl transferase centre (PTC) and although not near enough for involvement in direct catalysis, the loop region and arginine 32 residue (*Thermus thermophilus* EF-P has arginine in place of the conserved lysine)

makes numerous interactions with the CCA end of the acceptor stem of fMet-tRNA$_i^{fMet}$ (figure 4.3). These interactions orientate and stabilise the initiator tRNA at the PTC interface promoting peptide bond formation. It was suggested by Blaha *et al*., (2009) that EF-P may play a further role in elongation by promoting peptide bond formation of less favourable aminoacyl-tRNA substrates (those bearing shorter amino acid side chains). In eukaryotes and archaea the initiator tRNA is not formylated and therefore it has been suggested that the hypusine residue extends into the PTC to replace the function of the formyl group (Hershey *et al.*, 1990; Blaha *et al.*, 2009). This suggestion is supported by the fact that fMet-tRNA$_i^{fMet}$ is almost 20-fold less dependent on the presence of eIF5A in the methionyl-puromycin assay when substituting for its eukaryotic counterpart, Met-tRNA$_i^{Met}$ (Hershey *et al.*, 1990).

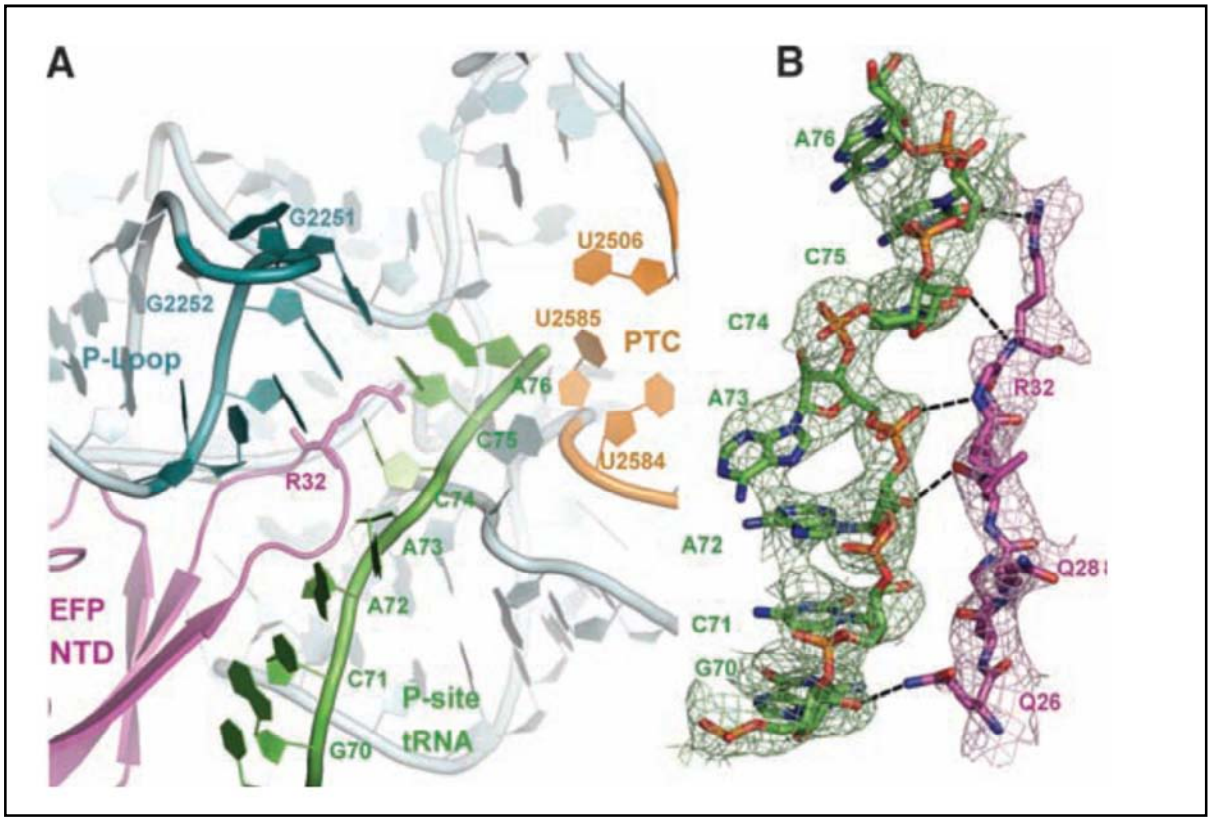

Figure 4.3: The conserved extended loop of domain I of EF-P makes numerous contacts with the CCA acceptor stem of the initiator tRNA. (A) The crystal structure of EF-P bound to the 80S ribosome showing the N-terminal domain of EF-P (EFP NTD) and the conserved lysine/arginine residue (R32) in purple; the CCA acceptor stem of the P-site tRNA in green; the P-Loop of the 23S rRNA in blue and the 23S rRNA nucleotides making up the PTC in yellow. (B) Hydrogen bonding between the extended loop of domain I of EF-P (purple) and the CCA acceptor stem of the P-site tRNA (green). Figure taken from Blaha *et al.* (2009).

As previously discussed, eIF5A is not a general translation factor. Therefore it could be possible that eIF5A was a canonical cap-independent translation initiation factor at the onset of eukarygonesis. However, as the cap-dependent mechanism evolved and became dominant, eIF5A might have become redundant due to changes in the spacial arrangement of the 80S ribosome and at the PTC or eIF5A function was promptly replaced by a more recently evolved initiation factor. Nevertheless, IRES-driven translation represents remnants of the translation mechanism present at the onset of eukarygonesis (Hernandez *et al*., 2008) and therefore it can be postulated that eIF5A remains a crucial factor for this early mechanism of translation initiation.

Finally, although it has been determined that eIF5A binds components of the translational machinery, no direct protein binding partner has as yet been established (Zanelli *et al.*, 2006). Therefore one can only assume that eIF5A binds to rRNA or tRNA at the ribosomal interface supporting an EF-P-similar function. Furthermore, eIF5A has yet to be found in complex with any exclusively cap-dependent translation initiation factors but has been found bound to known ITAFs such as ribosomal proteins L22 and S3 (Ma *et al*., 2010) and (Wood *et al*., 2001; Otto *et al*., 2002).

4.6.2 Nucleocytoplasmic shuttling of IRES containing mRNA

The attempt to identify eIF5A as a nucleocytoplasmic shuttling protein has presented contradictory and confusing results. Opposing data in the literature seems to suggest that eIF5A is localised within the nucleus in some cases (Rosorius *et al.,* 1999; Parreiras-e-Silva *et al.*, 2007; Taylor *et al.,* 2007; Lebska *et al.*, 2010) but not in others (Shi *et al.*, 1996; Lipowsky *et al*., 2000; Jao & Chen, 2002). Furthermore, it seems likely that localisation may be mediated by adverse cellular conditions as eIF5A is rapidly shuttled to the nucleus in response to apoptotic cell death or actinomycin D (Taylor *et al.,* 2007). In addition eIF5A is both upregulated and required for Rev export in HIV-1 infected human T-cells (Bevec *et al*., 1993, 1996) but is not essential for recombinant Rev export in yeast cells (Valentini *et al*., 2002). Therefore one could postulate that eIF5A is only shuttled to the nucleus under conditions where cap-dependent translation is compromised. eIF5A then acts as an adaptor molecule binding to the exportin 1 (CRM1/XPO1) receptor thereby allowing the translocation of uncapped or incompletely spliced mRNA by assisting them in overcoming their nuclear

retention signal (NRS). Further evidence in supporting this hypothesis is given by the disappearance of specific mRNAs from the polysomes with respect to inhibition of hypusination (Hanauske-Abel *et al.*, 1995), the abundance of eIF5A in the cytoplasm of eukaryotic cells (Thomas *et al.,* 1979), the ability of eIF5A to bind XPO1 (Rosorius *et al.*, 1999) and the requirement for eIF5A for translocation of Rev and Rex, which harbour incompletely spliced, IRES-containing viral transcripts (Bevec & Hauber, 1997; Katahira *et al.*, 1995). Finally it has been demonstrated that Nos2 mRNA requires eIF5A for cytoplasmic translocation via XPO1 (Maeir, Tersey *et al.*, 2010). Nos2 mRNA is upregulated in times of stress (Le Grevès *et al*., 1997; Sone *et al*., 2010) and is essential in producing nitric oxide during the innate immune response (Lowenstein & Padalko, 2004). However, it has yet to be determined whether Nos2 mRNA contains an IRES element. Future investigations will undoubtedly reveal a subset of mRNA molecules mediated by eIF5A for XPO1 translocation. What will be of great interest is if this subset of mRNA overlaps with those upregulated during IRES-driven translation initiation.

4.7 Concluding remarks

Several lines of evidence, as described above, support the involvement of eIF5A in IRES-driven translation. In summary this includes the relationship of eIF5A with stress responses in eukaryotic cells; the constant controversial data surrounding eIF5A function suggesting a context-dependent role of the protein; the phenotypes or secondary functions tied to eIF5A can be explained by a subset of IRES-regulated proteins and the evolution and conservation of eIF5A suggest the protein retained its “EF-P like” function from its prokaryotic ancestor.

In this novel hypothesis, based on the above evidence, it is inferred that eIF5A is required for eukaryotic IRES-driven translation. It is proposed that eIF5A carries out a fundamental role in initiation and possibly elongation of IRES-containing mRNA transcripts however is not essential in cap-dependent translation. The proposed function of eIF5A is similar to that of its prokaryotic predecessor, EF-P, where eIF5A is required for the correct positioning of initiator tRNA at the PTC for the formation of the

first peptide bond and possibly subsequent reactions thereafter (Blaha *et al*., 2009). Furthermore, eIF5A may play an additional role in eukaryotic cells by shuttling IRES-containing mRNA transcripts from the nucleus to the cytoplasm via XPO1. eIF5A may therefore permit specific mRNA to overcome their NRS, thereby bypassing certain RNA processing features, and mediating the speedy export of uncapped or even partially spliced mRNA. These mRNA molecules are then translated in an IRES-dependent manner in the cell's attempt to survive and recover from the imposed stress.

In conclusion, based on the variety of functions affected by eIF5A as well as the degree of controversy regarding eIF5A function, it is clear that eIF5A must exert a context-dependent role for a select subset of mRNA. It is even more apparent that highly proliferative cells as well as those under specific stress conditions require a more active eIF5A than others. Whether eIF5A is involved in eukaryotic IRES-driven translation remains to be determined; the consequence of which may finally elucidate the role of eIF5A and hypusine in eukaryotic translation initiation.

Chapter 5: General discussion and conclusions

At the onset, the aim of this study was to undertake a mutational analysis of the hypusine-containing loop region of yeast eIF5A to determine if conserved amino acid residues are involved in promoting dimerisation. The point mutations G50A, K48D, H52A and K56A were selected for this study because they had previously been identified as substitutions which resulted in a loss of eIF5A activity (Dias *et al*., 2008; Cano *et al*., 2008). A functional analysis, carried out using the yeast null mutant PGY10, revealed that mutant proteins were able to partially suppress the eIF5A$^-$ phenotype *in vivo* with G50A and K48D mutant proteins displaying the least complementation and mutant proteins did not exhibit temperature sensitivity. This suggests that the temperature sensitive phenotype observed by Dias *et al.* (2008) for the yeast K56A mutant protein may be related to the heat stress imposed at the high restrictive temperature of 37-38 ºC. Therefore it could be possible that the severity of the phenotype may be stress related and might account for the differences in complementation observed between this and other studies. This relationship is further supported by the results of Valentini *et al.* (2002) and Dias *et al.* (2008) where the addition of 1 M sorbitol (an osmotic stabiliser) partially suppressed the temperature sensitivity of all yeast *TIF51A* mutant strains at 37 ℃. The link between eIF5A and the stress response in eukaryotes has also been demonstrated in numerous studies (Li *et al*., 2010; Ma *et al*., 2010; Xu *et al*., 2011).

Hypusination assays showed that all mutant proteins were hypusinated *in vivo* however the extent to which could not be determined decisively as an overall weak signal was detected. The fact that all mutant proteins were able to complement growth to varying degrees *in vivo* suggested that a level of hypusine biosynthesis must have been present within the cells. In this, and other previous studies, the K51R mutant protein exhibits a non-viable phenotype while the other loop mutations generated in this study only resulted in an impaired growth phenotype. It could therefore be possible that the hypusine residue itself is critical in forming some interaction possibly

at the interface of a vital cellular process and substituting amino acid residues in the loop region only reduces the efficiency of this interaction.

The eIF5A loop residues were proposed to be involved in eIF5A dimerisation, mutant proteins were subjected to a biochemical analysis and their oligomeric state was investigated. Gel filtration profiles determined the molecular weight of eIF5A mutant and wild-type proteins to be 30 - 31 kDa. This is intermediate between those values obtained by Gentz *et al.* (2009) for both monomer (17 kDa) and dimer species (40 kDa). The apparent conflicting results produced in this study compared with that of Gentz *et al*. (2009) suggests that the eIF5A oligomeric state may be transitory and subject to certain conditions, which could not be duplicated in this study. In general gel filtration is not the most accurate method of determining the oligomeric state of native proteins and there is therefore a need to visit alternate methods for determining eIF5A tertiary structure. The ideal would be to obtain the crystal structure of the native, hypusinated eIF5A protein possibly through a technique such as solution NMR spectroscopy.

The aim of the final experimental chapter was therefore to determine the feasibility of producing sufficient amounts of native yeast (hypusinated) eIF5A protein for future analysis by solution NMR spectroscopy. Although $eIF5A_{Thrombin}$ appeared to be non-functional, the observation that $eIF5A_{Thrombin}$ was hypusinated indicates that the addition of a thrombin cleavage site did not affect the overall folding of at least the N-terminal domain. Finally, from the results of gel filtration, it appeared that both hypusinated and unhypusinated $eIF5A_{Thrombin}$ (expressed in yeast and *E. coli* respectively) eluted as a dimer under native conditions suggesting that a non-functional eIF5A has a high affinity for self-association which is independent of hypusine (possibly involving only a single eIF5A domain such as indicative of the dimer crystallised by Kim *et al*. (1998)).

The separation of both hypusinated and unhypusinated eIF5A into their domains through thrombin cleavage was achieved successfully. However, considerably more protein needs to be generated in order to consider further analysis by solution NMR spectroscopy. Recently active, recombinant eIF5A has been produced in *E. coli* by co-

expressing human eIF5A-1 with its modifying enzymes (Park *et al.*, 2011). This enables hypusinated eIF5A to be produced in high quantity and quality for structural studies. A hypusinated eIF5A structure will be valuable in providing insights into the unique structure-function relationship of eIF5A as well as the vital role of hypusine. Furthermore, crystallographic studies focusing on the formation of protein complexes will become possible as one requires active, hypusinated eIF5A for protein/RNA interactions to occur (Xu & Chen, 2001; Jao & Chen, 2006; Gentz *et al.*, 2009).

From the results generated in this study and the contradictory evidence surrounding eIF5A function in the literature (discussed in chapter 4); it is becoming apparent that eIF5A must exert a context-dependent role for a select subset of mRNA. Highly proliferative cells as well as those under specific stress conditions appear to require a more active eIF5A than others. The literature supports the hypothesis presented in this study for a role for eIF5A in eukaryotic IRES-driven translation initiation rather than its presumed role as a cap-dependent initiation factor. Evidence supporting this notion includes (1) the relationship of eIF5A with the stress response in eukaryotic cells; (2) the ability to link numerous eIF5A-associated functions with the translation of specific IRES-containing mRNAs; (3) the constant controversial data surrounding eIF5A function suggesting a context-dependent role of the protein and (4) the evolution and conservation of eIF5A which predicts that the protein has retained an “EF-P like” function from its evolutionary ancestor.

Whether eIF5A is involved in eukaryotic IRES-driven translation remains to be determined. Testing this hypothesis, when considering the systems already in place in this study, would be quite feasible. Various commercial vectors are currently available that place an IRES nucleotide sequence in front of a reporter gene such as the enhanced jellyfish green fluorescent protein (EGFP). Such a recombinant plasmid could be used within the yeast null mutant PGY10 and examined for EGFP expression thus providing a useful platform for determining eIF5A involvement in IRES-driven translation initiation. If eIF5A is deemed to be essential for IRES-driven translation initiation, the role of eIF5A and the hypusine residue may finally be elucidated.

Finally if one views the results of this study in light of an eIF5A-IRES hypothesis, the data could be explained as follows. The mutant proteins G50A, K48D, H52A and K56A are able to support growth to varying degrees in unstressed cells as an inefficient eIF5A protein is not crucial to growth and sustainability. However, under conditions of stress, resulting in an IRES-driven response, eIF5A functionality becomes critical as a direct relationship develops between protein synthesis and the growth defects observed. This relationship was determined by Dias *et al.* (2009) for the yeast K56A mutant at the high restrictive temperature of 38 ℃. Furthermore, if eIF5A did adopt an EF-P like function it would involve eIF5A binding to tRNA at the PTC when ribosomes are reprogrammed to translate IRES-containing mRNAs. There would therefore have to exist some regulatory mechanism by which hypusinated eIF5A is activated to bind tRNA under conditions of stress. If this were the case it would be plausible to suggest that eIF5A tertiary state may be governed by cellular conditions and activated by a post-translational regulatory mechanism such as acetylation. INVSc1 cells used in this study may have been subjected to stress, capturing a different tertiary structure than that observed in previous studies which also explains the lower protein yield initially obtained in this study. The relationship between eIF5A and stress in eukaryotic cells is evident (Li *et al*., 2010; Ma *et al*., 2010; Xu *et al*., 2011) however whether this stress relationship is due to eIF5A involvement in eukaryotic IRES-driven translation is yet to be determined.

References

Agarwal ML, Agarwal A, Taylor WR, Stark GR (1995) p53 controls both the G2/M and the G1 cell cycle checkpoints and mediates reversible growth arrest in human fibroblasts. *Proc Natl Acad Sci USA.* **92** (18): 8493-8497.

Allen GS and Frank J (2007) Structural insights on the translation initiation complex: ghosts of a universal initiation complex. *Mol Microbiol.* **63** (4): 941–950.

Aravind L and Koonin EV (2000) Eukaryote-specific domains in translation initiation factors: Implications for translation regulation and evolution of the translation system. *Genome Res*. **10** (8): 1172-84.

Ali MH and Imperiali B (2005) Protein oligomerization: How and why. *Bioorg Med Chem.* **13** (17): 5013–5020.

Aoki H, Dekany K, Adams S, Ganoza MC (1997) The gene encoding the elongation factor P protein is essential for viability and is required for protein synthesis. *J Biol Chem.* **272** (51): 32254–32259.

Aoki H, Xu J, Emili A, Chosay JG, Golshani A, Ganoza MC (2008) Interactions of elongation factor EF-P with the *Escherichia coli* ribosome. *FEBS J*. **275** (4): 671-681.

Baird SD, Turcotte M, Korneluk RG, Holcik M (2006) Searching for IRES. *RNA*. **12** (10): 1755-1785.

Baird SD, Lewis SM, Turcotte M, Holcik M (2007) A search for structurally similar cellular internal ribosome entry sites. *Nucleic Acids Res*. **35** (14): 4664-4677.

Bartig D, Schuêmann H, Klink F (1990) The unique posttranslational modification leading to deoxyhypusine or hypusine is a general feature of the archaebacterial Kingdom. *Syst appl microbiol*. **13** (2): 112-116.

Bartig D, Lemkemeier K, Frank J, Lottspeich F, Klink F (1992) The archaebacterial hypusine-containing protein. *Eur J Biochem*. **204** (2): 751-758.

Benelli D, Maone E, Londei P (2003) Two different mechanisms for ribosome/mRNA interaction in archaeal translation initiation. *Mol Microbiol.* **50** (2): 635-643.

Benne R, Brown-Luedi ML, Hershey JWB (1978) Purification and characterization of protein synthesis initiation factors eIF-1, eIF-4C, eIF-4D, and eIF-5 from rabbit reticulocytes. *J Biol Chem.* **253** (9): 3070-3077.

Berghammer H and Auer B (1993) "Easypreps": fast and easy plasmid minipreparation for analysis of recombinant clones in *E. coli*. *Biotechniques.* **14** (4): 524-528.

Bernstein J, Sella O, Le S, Elroy-Stein O (1997) PDGF2/c-sis mRNA leader contains a differentiation-linked internal ribosomal entry site (D-IRES). *J Biol Chem*. **272** (14): 9356-9362.

Bevec D, Klier H, Holters W, Tschachler E, Valent P, Lottspeich F, Baumruker T, Hauber J (1994) Induced gene expression of the hypusine-containing protein eukaryotic initiation factor 5A in activated human T lymphocytes. *Proc Natl Acad Sci USA.* **91** (23): 10829-10833.

Bevec D and Hauber J (1997) Eukaryotic initiation factor 5A activity and HIV-1 Rev function. *Biol Signals*. **6** (3): 124-133.

Blaha G, Stanley RE, Steitz TA (2009) Formation of the first peptide bond: The structure of EF-P bound to the 70S ribosome. *Science*. **325** (5943): 966-970.

Bonnal S, Pileur F, Orsini C, Parker F, Pujol F, Prats A, Vagner S (2005) Heterogeneous nuclear ribonucleoprotein A1 is a novel internal ribosome entry site trans-acting factor that modulates alternative initiation of translation of the fibroblast growth factor 2 mRNA. *J Biol Chem*. **280** (6): 4144-4153.

Bosch J and Hol WGJ (2004) Structural analysis of *Leishmania Mexicana* eukaryotic initiation factor 5A. *Structural genomics of pathogenic protozoa consortium (SGPP).*To be published.

Brochier C, López-García P, Moreira D (2004) Horizontal gene transfer and archaeal origin of deoxyhypusine synthase homologous genes in bacteria. *Gene*. **330** (1): 169-176.

Candeias MM, Powell DJ, Roubalova E, Apcher S, Bourougaa K, Vojtesek B, Bruzzoni-Giovanelli H, Fåhraeus R (2006) Expression of p53 and p53/47 are controlled by alternative mechanisms of messenger RNA translation initiation. *Oncogene.* **25** (52)**:** 6936-6947.

Cano VSP, Jeon GA, Johansson HE, Henderson CA, Park J, Valentini SR, Hershey JWB, Park MH (2008) Mutational analyses of human eIF5A-1 – Identification of amino acid residues critical for eIF5A activity and hypusine modification. *FEBS J.* **275** (1): 4-58.

Caraglia M, Marra M, Giuberti1 G, D'Alessandro AM, Budillon A, del Prete S, Lentini A, Beninati S, Abbruzzese A (2000) The role of eukaryotic initiation factor 5A in the control of cell proliferation and apoptosis. *Amino Acids.* **20** (2): 91–104.

Chan KL, New D, Ghandhi S, Wong F, Lam CMC, Wong JTY (2002) Transcript levels of the eukaryotic translation initiation factor 5A gene peak at early G1 phase of the cell cycle in the dinoflagellate *crypthecodinium cohnii*. *Appl Environ Microbiol*. **68** (5): 2278-2284.

Chattopadhyay MK, Park MH, Tabor H (2008) Hypusine modification for growth is the major function of spermidine in *Saccharomyces cerevisiae* polyamine auxotrophs grown in limiting spermidine. *Proc Natl Acad Sci USA.* **105** (18): 6554–6559.

Chenna R, Sugawara H, Koike T, Lopez R, Gibson TJ, Higgins TG, Thompson JD (2003) Multiple sequence alignment with the CLUSTAL series of programs. *Nucleic acids Res.* **31** (13): 3597-3599.

Chou W, Huang Y, Tsay W, Chiang T, Huang D, Huang H (2004) Expression of genes encoding the rice translation initiation factor, eIF5A, is involved in developmental and environmental responses. *Physiol Plant*. **121** (1): 50-57.

Chung SI, Park MH, Folk JE, Lewis MS (1991) Eukaryotic initiation factor 5A: the molecular form of the hypusine-containing protein from human erythrocytes. *Biochim Biophys Acta.* **1076** (3): 448-451.

Clement PMJ, Hanauske-Abel HM, Wolff EC, Kleinman HK, Park MH (2002) The antifungal drug ciclopirox inhibits deoxyhypusine and proline hydroxylation, endothelial cell growth and angiogenesis *in vitro. Int J Cancer.* **100** (4): 491–498.

Clement PMJ, Henderson CA, Jenkins ZA, Smit-McBride Z, Wolff EC, Hershey JWB, Park MH, Johansson HE (2003) Identification and characterization of eukaryotic initiation factor 5A-2. *Eur J Biochem*. **270** (21): 4254–4263.

Condò I, Ciammaruconi A, Benelli D, Ruggero D, Londei P (1999) Cis-acting signals controlling translational initiation in the thermophilic archaeon *Sulfolobus solfataricus. Mol Microbiol*. **34** (2): 377-384.

Cornelis S, Bruynooghe Y, Denecker G, Van Huffel S, Tinton S, Beyaert R (2000) Identification and characterization of a novel cell cycle–regulated internal ribosome entry site. *Mol Cell.* **5** (4): 597-605.

Cortay JC, Nègre D, Scarabel M, Ramseier TM, Vartak NB, Reizer J, Saier MH Jr, Cozzone AJ (1994) In vitro asymmetric binding of the pleiotropic regulatory protein, FruR, to the ace operator controlling glyoxylate shunt enzyme synthesis. *J Biol Chem*. **269** (21): 14885-14891.

Dagert M and Ehrlich SD (1979) Prolonged incubation in calcium chloride improves the competence of *E. coli* cells. *Gene.* **85** (6): 23.

Dalgaard JZ and Garret RA (1993) Archael hyperthermophile genes. *New Comprehensive Biochemistry.* **26** (1): 535-563.

Decker ED, Zhang Y, Cocklin RR, Witzmann FA, Wang M (2003) Proteomic analysis of differential protein expression induced by ultraviolet light radiation in HeLa cells. *Proteomics*. **3** (10): 2019-2027.

DeLano WL (2002) The PyMOL molecular graphics system. San Carlos, CA: DeLano Scientific.

Dias CAO, Cano VSP, Rangel SM, Apponi LH, Frigieri MC, Muniz JRC, Garcia W, Park MH, Garrat RC, Zanelli CF, Valentini SR (2008) Structural modeling and mutational analysis of yeast eukaryotic translation initiation factor 5A reveal new

critical residues and reinforce its involvement in protein synthesis. *FEBS J.* **275** (8): 1874-1888.

Dihazi H, Dihazi GH, Jahn O, Meyer S, Nolte J, Asif AR, Mueller GA, Engel W (2011) Multipotent adult germline stem cells and embryonic stem cells functional proteomics revealed an important role of eukaryotic initiation factor 5A (Eif5a) in stem cell differentiation. *J Proteome Res.* **10** (4): 1962-1973.

Dresselhaus T, Cordts S, Lörz H (1999) A transcript encoding translation initiation factor eIF-5A is stored in unfertilized egg cells of maize. *Plant Mol Biol*. **39** (5): 1063-1071.

Duncan R and Hershey JW (1983) Identification and quantitation of levels of protein synthesis initiation factors in crude HeLa cell lysates by two-dimensional polyacrylamide gel electrophoresis. *J Biol Chem*. **258** (11): 7228-7235.

Elfgang C, Rosorius O, Hofer L, Jaksche H, Hauber J, Bevec D (1999) Evidence for specific nucleocytoplasmic transport pathways used by leucine-rich nuclear export signals. *Proc Natl Acad Sci USA.* **96** (11): 6229–6234.

Evans JR, Mitchell SA, Spriggs KA, Ostrowski J, Bomsztyk K, Ostarek D, Willis AE (2003) Members of the poly (rC) binding protein family stimulate the activity of the c-*myc* internal ribosome entry segment *in vitro* and *in vivo. Oncogene.* **22** (39): 8012–8020.

Fernandez J, Yaman I, Huang C, Liu H, Lopez AB, Komar AA, Caprara MG, Merrick WC, Snider MD, Kaufman RJ, Lamers WH, Hatzoglou M (2005) Ribosome stalling regulates IRES-mediated translation in eukaryotes, a parallel to prokaryotic attenuation. *Mol Cell.* **17** (3): 405-416.

Frydman L, Rossomando PC, Frydman V, Fernandez CO, Frydman B, Samejima (1992) Interactions between natural polyamines and tRNA: An ^{15}N NMR analysis. *Proc Natl Acad Sci USA*. **89** (19): 9186-9190.

Futterer E (1988) Antidandruff hair tonic containing piroctone olamine. *Cosmetics and toiletries.* **103** (2): 49-52.

Ganoza MC, Kiel MC, Aoki H (2002) Evolutionary conservation of reactions in translation. *Microbiol Mol Biol Rev.* **66** (3): 460-485.

Garrett RA, Douthwate SR, Matheson AT, Moore PB, Noller HF (2000) The ribosome: structure, function, antibiotics, and cellular interaction. ASM Press: Washington DC. pp 85-91, 477.

Gasteiger E, Hoogland C, Gattiker A, Duvaud S, Wilkins MR, Appel RD, Bairoch A (2005) Protein identification and analysis tools on the ExPASy server. In *The proteomics protocols handbook.* Walker JM (ed.) Humana Press Inc: New Jersey. pp 571-607.

Gentz PM, Blatch GL, Dorrington RA (2009) Dimerisation of the yeast eukaryotic translation initiation factor 5A requires hypusine and is RNA dependent. *FEBS J*. **276** (3): 695-706.

Gentz P (2008) Towards understanding the mechanism of dimerisation of *Saccharomyces cerevisiae* eukaryotic translation initiation factor 5A. PhD Thesis, Rhodes University.

Gilbert WV, Zhou K, Butler TK, Doudna JA (2007) Cap-independent translation is required for starvation-induced differentiation in yeast. *Science*. **317** (5842): 1224-1227.

Glick BR and Ganoza MC (1975) Identification of a soluble protein that stimulates peptide bond synthesis. *Proc Natl Acad Sci USA.* **72** (11): 4257-4260.

Goodsell DS and Olson AJ (2000) Structural symmetry and protein function. *Annu Rev Biophys Biomol Struct*. **29** (1):105–153.

Gordon ED, Mora R, Meredith SC, Lee C, Lindquist SL (1987) Eukaryotic initiation factor 4D, the hypusine-containing protein, is conserved among eukaryotes. *J Biol Chem.* **262** (34): 16585-16589.

Gray D and Subramaniam S (2001) Choice of cellular protein expression system. *Curr Protoc in Protein Sci*. 5.16.1-5.16.34.

Le Grevès P, Sharma HS, Westman J, Alm P, Nyberg F (1997) Acute heat stress induces edema and nitric oxide synthase upregulation and down-regulates mRNA levels of the NMDAR1, NMDAR2A and NMDAR2B subunits in the rat hippocampus. *Acta Neurochir Suppl.* **70** (1): 275-278.

Grill S, Gualerzi CO, Londei P, Bläsi U (2000) Selective stimulation of translation of leaderless mRNA by initiation factor 2: evolutionary implications for translation. *EMBO J*. **19** (15): 4101-4110.

Grobe K and Esko JD (2002) Regulated translation of heparan sulfate N-Acetylglucosamine N-Deacetylase/N-Sulfotransferase isozymes by structured 5′-untranslated regions and internal ribosome entry sites. *J Biol Chem*. **277** (34): 30699-30706.

Hanahan D (1983) Studies on transformation of *Escherichia coli* with plasmids. *J Mol Biol.* **166** (4): 557-580.

Hanauske-Abel HM, Slowinska B, Zagulska S, Wilson RC, Staiano-Coico L, Hanauske AR, Mccaffrey T, Szabo P (1995) Detection of a sub-set of polysomal mRNAs associated with modulation of hypusine formation at the G1-S boundary. Proposal of a role for eIF-5A in onset of DNA replication. *FEBS Lett.* **366** (2-3): 92-98.

Handa P, Thanedar S, Varshney U (2002) Rapid and reliable site-directed mutagenesis. In *In vitro mutagenesis protocols.* Humana Press Inc: New Jersey. Chapter 1: pp 1-7.

Hauber I, Bevec D, Heukeshoven J, Krätzer F, Horn F, Choidas A, Harrer T, Hauber J (2005) Identification of cellular deoxyhypusine synthase as a novel target for antiretroviral therapy. *J Clin Invest*. **115** (1): 76-85.

He L, Zhao H, Li B, Liu Y, Liu M, Guan X (2011) Overexpression of eIF5A-2 is an adverse prognostic marker of survival in stage I non-small-cell lung cancer patients. *Int J Cancer.* **129** (1): 143-150.

Hellen CU and de Breyne S (2007) A distinct group of hepacivirus/pestivirus-like internal ribosomal entry sites in members of diverse picornavirus genera: evidence for modular exchange of functional noncoding RNA elements by recombination. *J Virol*. **81** (11): 5850-5863.

Hellen CUT and Sarnow P (2001). Internal ribosome entry sites in eukaryotic mRNA molecules. *Genes Dev.* **15** (13): 1593-1612.

Henis-Korenblit S, Strumpf NL, Goldstaub D, Kimchi A (2000) A novel form of DAP5 protein accumulates in apoptotic cells as a result of caspase cleavage and internal ribosome entry site-mediated translation. *Mol Cell Biol*. **20** (2): 496-506.

Hernández G (2008) Was the initiation of translation in early eukaryotes IRES-driven? *Trends Biochem Sci*. **33** (2): 58-64.

Hershey JWB, Smit-McBride Z, Schnier J (1990) The role of mammalian initiation factor eIF-4D and its hypusine modification in translation. *Biochim Biophys Acta.* **1050** (1): 160-162.

Hershey JWB (1994) Expression of initiation factor genes in mammalian cells. *Biochimie*. **76** (9): 847-852.

Holbrook JA, Neu-Yilik G, Gehring NH, Kulozik AE, Hentze MW (2006) Internal ribosome entry sequence-mediated translation initiation triggers nonsense-mediated decay. *EMBO Rep.* **7** (7): 722-726.

Hommes D, Van Den Blink B, Plasse T, Bartelsman J, Xu C, Macpherson B, Tytgat G, Peppelenbosch M, Van Deventer S (2002) Inhibition of stress-activated MAP kinases induces clinical improvement in moderate to severe Crohn's disease. *Gastroenterol*. **122** (1): 7-14.

Hopkins MT, Lampi Y, Wang T, Liu Z, Thompson JE (2008) Eukaryotic translation initiation factor 5A is involved in pathogen-induced cell death and development of disease symptoms in arabidopsis. *Plant Physiol*. **148** (1): 479-489.

Hoque M, Hanauske-Abel HM, Palumbo P, Saxena D, Gandolf DD, Park MH, Pe'ery T, Mathews MB (2009) Inhibition of HIV-1 gene expression by Ciclopirox and

Deferiprone, drugs that prevent hypusination of eukaryotic initiation factor 5A. *Retrovirology.* **6** (1): 90.

Humphrey W, Dalke A, Schulten K (1996) VMD - Visual Molecular Dynamics. *J Molec Graphics.* **14** (1): 33-38.

Jang SK, Krausslich HG, Nicklin MJ, Duke GM, Palmenberg AC, Wimmer E (1988) A segment of the 5' nontranslated region of encephalomyocarditis virus RNA directs internal entry of ribosomes during in vitro translation. *J Virol*. **62** (8): 2636-2643.

Jansson BP, Malandrin L, Johansson HE (2000) Cell cycle arrest in archaea by the hypusination inhibitor *N*-guanyl-1,7-diaminoheptane. *J Bacteriol*. **182** (4): 1158-1161.

Jao DL and Chen KY (2002) Subcellular localization of the hypusine-containing eukaryotic initiation factor 5A by Immunofluorescent staining and green fluorescent protein tagging. *J Cell Biochem.* **86** (3): 590–600.

Jao DL and Chen KY (2006) Tandem affinity purification revealed the hypusine-dependent binding of eukaryotic initiation factor 5A to the translating 80S ribosomal complex. *J Cell Biochem.* **97** (3): 583–598.

Jenkins GM, **Richards A, Wahl T, Mao C, Lina Obeid L, Yusuf Hannun Y** (1997) Involvement of yeast sphingolipids in the heat stress response of *Saccharomyces cerevisiae*. *J Biol Chem.* **272** (51): 32566-32572.

Jenkins ZA, Hååg PG, Johansson HE (2001) Human EIF5A2 on chromosome 3q25–q27 is a phylogenetically conserved vertebrate variant of eukaryotic translation initiation factor 5A with tissue-specific expression. *Genomics.* **71** (1): 101–109.

Jo OD, Martin J, Bernath A, Masri J, Lichtenstein A, Gera J (2008) Heterogeneous nuclear ribonucleoprotein A1 regulates cyclin D1 and c-myc internal ribosome entry site function through akt signalling. *J Biol Chem*. **283** (34): 23274- 23287.

Kang H and Hershey J (1994) Effect of initiation factor eIF-5A depletion on protein synthesis and proliferation of *Saccharomyces cerevisiae*. *J Biol Chem.* **269** (6): 3934-3940.

Kang KR, Kim YS, Wolff EC, Park MH (2007) Specificity of the deoxyhypusine hydroxylase-eukaryotic translation initiation Factor (eIF5A) interaction: Identification of amino acid residues of the enzyme required for binding of its substrate, deoxyhypusine-containing eIF5A. *J Biol Chem.* **282** (11): 8300–8308.

Katahira J, Ishizaki T, Sakai H, Adachi A, Yamamoto K, Shida H (1995) Effects of translation initiation factor eIF-5a on the functioning of Human T-Cell Leukemia Virus Type I Rex and Human Immunodeficiency Virus Rev inhibited *trans* dominantly by a Rex mutant deficient in RNA binding. *J Virol.* **69** (5): 3125–3133.

Kellner HM, Arnold C, Christ OE, Eckert HG, Herok J, Hornke I, Rupp W (1982) Pharmacokinetics and biotransformation of the antimycotic drug ciclopiroxolamine in

animals and man after topical and systemic administration. *Arzneimittelforschung*. **31** (8): 1337-1353.

Kemper WM, Berry KW, Merrick WC (1976) Purification and properties of rabbit reticulocyte protein synthesis initiation factors M2Bα and M2Bβ. *J Biol Chem.* **251** (18): 5551-5557.

Kim IS, Yun HS, Kwak SH, Jin IN (2007) The physiological role of CPR1 in *Saccharomyces cerevisiae* KNU5377 against menadione stress by proteomics. *J Microbiol*. **45** (4): 326-332.

Kim KK, Hung LW, Yokota H, Kim R, Kim SH (1998) Crystal structures of eukaryotic translation initiation factor 5A from *Methanococcus jannaschii* at 1.8 Å resolution. *Biochemistry.* **95** (18): 10419–10424.

Kim YS, Kang KR, Wolff EC, Bell JK, McPhie P, Park MH (2006) Deoxyhypusine hydroxylase is an Fe(II)-dependent, heat-repeat enzyme. *J Biol Chem.* **281** (19): 13217–13225.

Klier H, Csonga R, Joäo HC, Eckerskorn C, Auer M, Lottspeich F, Eder J (1995) Isolation and structural characterization of different isoforms of the hypusine-containing protein eIF-5A from HeLa cells. *Biochemistry.* **34** (45): 14693-14702.

Komar AA, Hatzoglou M (2005) Internal ribosome entry sites in cellular mRNAs: Mystery of their existence. *J Biol Chem*. **280** (25): 23425-23428.

Kouzarides T (2000) Acetylation: A regulatory modification to rival phosphorylation? *EMBO J.* **19** (6): 1176–1179.

Kyrpides NC and Woese CR (1998) Universally conserved translation initiation factors. *Proc Natl Acad Sci USA.* **95** (1): 224-228.

Laemmli UK (1970) Cleavage of structural proteins during the assembly of the head of bacteriophage T4. *Nature*. **227**(5259): 680-685.

Le Quesne JP, Spriggs KA, Bushell M, Willis AE (2010) Dysregulation of protein synthesis and disease. *J Pathol*. **220** (2): 140-151.

Lebska M, Ciesielski A, Szymona L, Godecka L, Lewandowska-Gnatowska E, Szczegielniak J, Muszynska G (2010) Phosphorylation of maize eIF5A by CK2: Identification of phosphorylated residue and influence on intracellular localization of eIF5A. *J Biol Chem*. **285** (9): 6217-6226.

Lee YB, Joe YA, Wolff EC, Dimitriadis EK, Park MH (1999) Complex formation between deoxyhypusine synthase and its protein substrate, the eukaryotic translation initiation factor 5A (eIF5A) precursor. *Biochem J*. **340** (1): 273-281.

Lee SB, **Park JH**, **Kaevel J**, **Sramkova M**, **Weigert R**, **Park MH** (2010) The effect of hypusine modification on the intracellular localization of eIF5A. *Biochem Biophys Res Commun*. **383**(4): 497–502.

Lewis SM and Holcik M (2005) IRES in distress: Translational regulation of the inhibitor of apoptosis proteins XIAP and HIAP2 during cell stress. *Cell Death Differ.* **12** (6): 547–553.

Lewis SM, Veyrier A, Hosszu Ungureanu N, Bonnal S, Vagner S, Holcik M (2007) Subcellular relocalization of a trans-acting factor regulates XIAP IRES-dependent translation. *Mol Biol Cell*. **18** (4): 1302-1311.

Li A, Li H, Jin B, Ye Q, Zhou T, Yu X, Pan X, Man J, He K, Yu M, Hu M, Wang J, Yang S, Shen B, Zhang Z (2004) A novel eIF5A complex functions as a regulator of p53 and p53-dependent apoptosis. *J Biol Chem.* **279** (47): 49251-49258.

Li CH, Ohn T, Ivanov P, Tisdale S, Anderson P (2010) eIF5A promotes translation elongation, polysome disassembly and stress granule assembly. *PLoS One*. **5** (4): e9942.

Lipowsky G, Bischoff FR, Schwarzmaier R, Kraft R, Kostka S (2000) Exportin 4: a mediator of a novel nuclear export pathway in higher eukaryotes. *EMBO J*. **19** (16): 4362-4371.

Liu YP, Nemeroff M, Yan YP, Chen KY (1997) Interaction of eukaryotic initiation factor 5A with the human immunodeficiency virus type 1 Rev response element RNA and U6 snRNA requires deoxyhypusine or hypusine modification. *Biol Signals.* **6** (3):166-174.

Londei P (2005) Evolution of translational initiation: new insights from the archaea. *FEMS Microbiology Reviews.* **29** (2): 185-200.

Lowenstein CJ and Padalko E (2004) iNOS (NOS2) at a glance. *J Cell Sci*. **117** (14): 2865-2867.

Luchessi AD, Cambiaghi TD, Alves AS, Parreiras-E-Silva LT, Britto LRG, Costa-Neto CM, Curi R (2008) Insights on eukaryotic translation initiation factor 5A (eIF5A) in the brain and aging. *Brain Res.* **1228** (1): 6–13.

Luchessi AD, Cambiaghi TD, Hirabara SM, Lambertucci RH, Silveira LR, Baptista IL, Moriscot AS, Costa-Neto CM, Curi R (2009) Involvement of eukaryotic translation initiation factor 5A (eIF5A) in skeletal muscle stem cell differentiation. *J Cell Physiol.* **218** (3): 480-489.

Ma Y, Miura E, Ham B, Cheng H, Lee Y, Lucas WJ (2010) Pumpkin eIF5A isoforms interact with components of the translational machinery in the cucurbit sieve tube system. *Plant J*. **64** (3): 536-550.

Macejak DG and Sarnow P (1991) Internal initiation of translation mediated by the 5' leader of a cellular mRNA. *Nature.* **353** (6339): 90-94.

Magdolen V, Klier H, Wöhl T, Klink F, Hirt H, Hauber J, Lottspeich F (1994) The function of the hypusine-containing proteins of yeast and other eukaryotes is well conserved. *Mol Gen Genet*. **244** (6): 646-652.

Maier B, Ogihara T, Trace AP, Sarah AT, Robbins RD, Chakrabarti SK, Nunemaker CS, Stull ND, Taylor CA, Thompson JE, Dondero RS, Lewis EC, Dinarello CA, Nadler JL, Mirmira RG (2010) The unique hypusine modification of eIF5A promotes islet β cell inflammation and dysfunction in mice. *J Clin Invest*. **120** (6): 2156–2170.

Maier B, Tersey SA, Mirmira RG (2010) Hypusine: A new target for therapeutic intervention in diabetic inflammation. *Discov Med*. **10** (50): 18-23.

Martínez-Salas E, Quinto SL, Ramos R, Fernández-Miragall O (2002) IRES elements: Features of the RNA structure contributing to their activity. *Biochimie*. **84** (8): 755-763.

Miller MJ, Xuong N, Geiduschek EP (1979) A response of protein synthesis to temperature shift in the yeast *Saccharomyces cerevisiae*. *Proc Natl Acad Sci USA*. **76** (10): 5222-5225.

Mitchell SA, Spriggs KA, Coldwell MJ, Jackson RJ, Willis AE (2003) The Apaf-1 internal ribosome entry segment attains the correct structural conformation for function via interactions with PTB and unr. *Mol Cell*. **11** (3): 757-771.

Mokrejš M, Vopálenský V, Kolenatý O, Mašek T, Feketová Z, Sekyrová P, Škaloudová B, Kříž V, Pospíšek M (2006) IRESite: The database of experimentally verified IRES structures (www.iresite.org). *Nucleic Acid Res*. **34**: D125-D130.

Mokrejš M, Mašek T, Vopálenský V, Pospíšek M (2010) IRESite - a tool for the examination of viral and cellular internal ribosome entry sites. *Nucleic Acid Res*. **38**: D131–D136.

Murphey R and Gerner E (1987) Hypusine formation in protein by a two-step process in cell lysates. *J Biol Chem.* **262** (31): 15033-15036.

Nierhaus KH and Wilson DN (2004) Protein synthesis and ribosome structure: Translating the genome. John Wiley & Sons, Germany. Pp 107 - 108.

Nishimura K, Murozumi K, Shirahata A, Park MH, Kashiwagi K, Igarashi K (2005) Independent roles of eIF5A and polyamines in cell proliferation. *Biochem J.* **385** (3): 779-785.

Nishimura K, Lee SB, Park JH, Park MH (2011) Essential role of eIF5A-1 and deoxyhypusine synthase in mouse embryonic development. *Amino Acids.* Epub ahead of print.

Otto GA, Lukavsky PJ, Lancaster AM, Sarnow P, Puglisi JD (2002) Ribosomal proteins mediate the hepatitis C virus IRES–HeLa 40S interaction. *RNA*. **8** (7): 913–923.

Park JH, Aravind L, Wolff EC, Kaevel J, Kim YS, Park MH (2006) Molecular cloning, expression, and structural prediction of deoxyhypusine hydroxylase: A HEAT-repeat-containing metalloenzyme. *Proc Natl Acad Sci USA.* **103** (1): 51-56.

Park JH, Dias CA, Lee SB, Valentini SR, Sokabe M, Fraser CS, Park MH (2011) Production of active recombinant eIF5A: reconstitution in *E.coli* of eukaryotic hypusine modification of eIF5A by its coexpression with modifying enzymes. *Protein Eng Des Sel*. **24** (3): 301-309.

Park MH, Cooper HL, Folk JE (1982) The biosynthesis of protein-bound hypusine (N^{ϵ} (4-amino-2-hydroxybutyl) lysine). *J Biol Chem.* **257** (12): 7217-7222.

Park MH (1989) The essential role of hypusine in eukaryotic translation initiation factor 4D (eIF-4D). Purification of eIF-4D and its precursors and comparison of their activities. *J Biol Chem.* **264** (31): 18531-18535.

Park MH, Wolff E, Smit-Mcbride Z, Hershey J, Folk J (1991) Comparison of the activities of variant forms of eIF-4D. The requirement for hypusine or deoxyhypusine. *J Biol Chem.* **266** (13): 7988-7994.

Park MH, Wolff EC, Folk JE (1993) Hypusine: Its post-translational formation in eukaryotic initiation factor 5A and its potential role in cellular regulation. *Biofactors.* **4** (2): 95-104.

Park MH, Young BL, Young AJ (1997) Hypusine is essential for eukaryotic cell proliferation. *Biol Signals.* **6** (3): 115-123.

Park MH (2006) The post-translational synthesis of a polyamine-derived amino acid, hypusine, in the eukaryotic translation initiation factor 5A (eIF5A). *J Biochem*. **139** (2): 161–169.

Parreiras-e-Silva LT, Gomes MD, Oliveira EB, Costa-Neto CM (2007) The N-terminal region of eukaryotic translation initiation factor 5A signals to nuclear localization of the protein. *Biochem Biophys Res Commun*. **362** (2): 393-398.

Parreiras-e-Silva LT, Luchessi AD, Reis RI, Oliver C, Jamur MC, Ramos RGP, Oliveira EB, Curi R, Costa-Neto CM (2010) Evidences of a role for eukaryotic translation initiation factor 5A (eIF5A) in mouse embryogenesis and cell differentiation. *J Cell Physiol*. **225** (2): 500-505.

Pay A, Heberle-Bors E, Hirt H (1991) Isolation and sequence determination of the plant homologue of the eukaryotic initiation factor 4D cDNA from alfalfa, *Medicago sativa. Plant Mol Biol.* **17** (4): 927-929.

Peat TS, Newman J, Waldo GS, Berendzen J, Terwilliger TC (1998) Structure of translation initiation factor 5A from *Pyrobaculum aerophilum* at 1.75 Å resolution. *Structure.* **6** (9): 1207-1214.

Pelletier J and Sonenberg N (1988) Internal initiation of translation of eukaryotic mRNA directed by a sequence derived from poliovirus RNA. *Nature*. **334** (6180): 320-325.

Pestova TV and Hellen CUT (2003) Translation elongation after assembly of ribosomes on the cricket paralysis virus internal ribosomal entry site without initiation factors or initiator tRNA. *Genes Dev*. **17** (2): 181-186.

Pestova TV, de Breyne S, Pisarev AV, Abaeva IS, Hellen CUT (2008) eIF2-dependent and eIF2-independent modes of initiation on the CSFV IRES: A common role of domain II. *EMBO J.* **27** (7): 1060-1072.

Pinkstaff JK, Chappell SA, Mauro VP, Edelman GM, Krushel LA (2001) Internal initiation of translation of five dendritically localized neuronal mRNAs. *Proc Natl Acad Sci USA*. **98** (5): 2770-2775.

Prinz H, Furgac N, Cramer F (1976) Spermine stabilizes the conformation of tRNAPhe in crystals. *Biochem Biophys Acta*. **447** (1): 110-115.

Pyronnet S, Pradayrol L, Sonenberg N (2000) A cell cycle–dependent internal ribosome entry site. *Mol Cell*. **5** (4): 607-616.

Qin X and Sarnow P (2004) Preferential translation of internal ribosome entry site-containing mRNAs during the mitotic cycle in mammalian cells. *J Biol Chem*. **279** (14): 13721-1378.

Reis PJ, Tunks DA, Chapman RE (1975) Effects of mimosine, a potential chemical defleecing agent, on wool growth and the skin of sheep. *Aust J Biol Sci*. **28** (1): 69-84.

Rosorius O, Reichart B, Krätzer F, Heger P, Dabauvalle MC, Hauber J (1999) Nuclear pore localization and nucleocytoplasmic transport of eIF-5A: Evidence for direct interaction with the export receptor CRM1. *J Cell Sci*. **112** (14): 2369-2380.

Ruhl M, Himmelspach M, Bahr G, Hammerschmid F, Jaksche H, Wolff B, Aschauer H, Farrington G, Probst H, Bevec D (1993) Eukaryotic initiation factor 5A is a cellular target of the human immunodeficiency virus type 1 Rev activation domain mediating trans- activation. *J Biol Chem.* **123** (6): 1309-1320.

Sakai TT and Cohen S (1975) The binding of polyamines and of ethidium bromide to tRNA**.** *Nucleic Acid Res.* **2** (7):1005-1022.

Sambrook J, Fritsch ED, Maniatis T (1989) Molecular cloning: a laboratory manual 2 Ed. Cold Spring Harbor: New York. pp 49-55.

Schnier J, Schwelberger HG, Smit-Mcbride Z, Kang HA, Hershey JW (1991) Translation initiation factor 5A and its hypusine modification are essential for cell viability in the yeast *Saccharomyces cerevisiae*. *Mol Cell Biol.* **11**(6): 3105-3114.

Schwelberger H, Kang H, Hershey J (1993) Translation initiation factor eIF-5A expressed from either of two yeast genes or from human cDNA. Functional identity under aerobic and anaerobic conditions. *J Biol Chem.* **268**(19): 14018-14025.

Schrader R, Young C, Kozian D, Hoffmann R, Lottspeich F (2006) Temperature-sensitive eIF5A mutant accumulates transcripts targeted to the nonsense-mediated decay pathway. *Biol Chem.* **281**(46): 35336-35346.

Shi X, Yin K, Zimolo ZA, Stern AM, Waxman L (1996) The subcellular distribution of eukaryotic translation initiation factor, eIF-5A, in cultured cells. *Exp Cell Res.* **225** (2): 348-356.

Shi Y, Sharma A, Wu H, Lichtenstein A, Gera J (2005) Cyclin D1 and c-*myc* internal ribosome entry site (IRES)-dependent translation is regulated by AKT activity and enhanced by rapamycin through a p38 MAPK- and ERK-dependent pathway. *J Biol Chem.* **280** (12): 10964–10973.

Shih YT, Yang CF, Chen WJ (2010) Upregulation of a novel eukaryotic translation initiation factor 5A (eIF5A) in dengue 2 virus-infected mosquito cells. *Virol J.* **7**: 214.

Slupska MM, King AG, Fitz-Gibbon S, Besemer J, Borodovsky M, Miller JH (2001) Leaderless transcripts of the crenarchaeal hyperthermophile *Pyrobaculum aerophilum*. *J Mol Biol.* **309** (2): 347-360.

Smith BJ (1996) Drying polyacrylamide gels. In *The protein protocols handbook*. Walker JM (Ed.) Humana Press Inc: New Jersey. pp 223-227.

Sommer MN, Bevec D, Klebl B, Flicke B, Hölscher K, Freudenreich T, Hauber I, Hauber J, Mett H (2004) Screening assay for the identification of deoxyhypusine synthase inhibitors. *J Biomol Screen.* **9** (5): 434-438.

Sone H, Akanuma H, Fukuda T (2010) Oxygenomics in environmental stress. *Redox Rep*. **15** (3): 98-114.

Spriggs KA, Bushell M, Mitchell SA, Willis AE (2005) Internal ribosome entry segment-mediated translation during apoptosis: The role of IRES-*trans*-acting factors. *Cell Death Differ*. **12** (6): 585–591.

Spriggs KA, Stoneley M, Bushell M, Willis AE (2008) Re-programming of translation following cell stress allows IRES-mediated translation to predominate. *Biol Cell.* **100** (1): 27-38.

Stage-Zimmermann T, Schmidt U, Silver PA (2000) Factors affecting nuclear export of the 60S ribosomal subunit in vivo. *Mol Biol Cell.* **11** (11): 3777–3789.

Stein I, Itin A, Einat P, Skaliter R, Grossman Z, Keshet E (1998) Translation of vascular endothelial growth factor mRNA by internal ribosome entry: Implications for translation under hypoxia. *Mol Cell Biol*. **18** (6): 3112-3119.

Stoneley M and Willis AE (2004) Cellular internal ribosome entry segments: Structures, *trans*-acting factors and regulation of gene expression. *Oncogene.* **23** (18): 3200–3207.

Studier FW, Moffatt BA (1986) Use of bacteriophage T7 RNA polymerase to direct selective high-level expression of cloned genes. *J Mol Biol*. **189** (1): 113-130.

Studier FW, Rosenberg AH, Dunn JJ, Dubendorff JW (1990) Use of T7 RNA polymerase to direct expression of cloned genes. *Methods Enzymol.* **185** (1): 60-89.

Tabor CW and Tabor H (1985) Polyamines in microorganisms. *Microbiol Rev.* **49** (1): 81-99.

Tomasicchio M (2007) The biology of Omegatetravirus capsid assembly in yeast. PhD Thesis, Rhodes University.

Tan X, Wang D, Lu X, Wei H, Zhu R, Zhu S, Jiang H, Yang Z (2010) Doxorubicin induces apoptosis in H9c2 cardiomyocytes: Role of overexpressed eukaryotic translation initiation factor 5A. *Biol Pharm Bull.* **33** (10): 1666-1672.

Taylor CA, Senchyna M, Flanagan J, Joyce EM, Cliche DO, Boone AN, Culp-Stewart S, Thompson JE (2004) Role of eIF5A in TNF-α-mediated apoptosis of lamina cribrosa cells. *Invest Ophthalmol Vis Sci.* **45** (10): 3568 – 3576.

Taylor CA, Sun Z, Cliche DO, Ming H, Eshaque B, Jin S, Hopkins MT, Thai B, Thompson JE (2007) Eukaryotic translation initiation factor 5A induces apoptosis in colon cancer cells and associates with the nucleus in response to tumour necrosis factor α signalling. *Exp Cell Res.* **313** (3): 437 – 449.

Thomas A, Goumans H, Amesz H, Benne R, Voorma HO (1979) A comparison of the initiation factors of eukaryotic protein synthesis from ribosomes and from the postribosomal supernatant. *Eur J Biochem*. **98** (2): 329-337.

Thompson GM, Cano VSP, Valentini SR (2003) Mapping eIF5A binding sites for Dys1 and Lia1: in vivo evidence for regulation of eIF5A hypusination. *FEBS Lett*. **555** (3): 464-468.

Tolstrup N, Sensen CW, Garrett RA, Clausen IG (2000) Two different and highly organized mechanisms of translation initiation in the archaeon *Sulfolobus solfataricu. Extremophiles.* **4** (3): 175-179.

Tong Y, Park I, Hong BS, Nedyalkova L, Tempel W, Park HW (2009) Crystal structure of human eIF5A1: Insight into functional similarity of human eIF5A1 and eIF5A2. *Proteins.* **75** (4): 1040-1045.

Towbin H, Staehelin J, Gordon J (1979) Electrophoretic transfer of proteins from polyacrylamide gels to nitrocellulose sheets; Procedure and some applications. *Proc Natl Acad Sci USA.* **76** (9): 4350-4354.

Tropp JS and Redfield AG (1983) Proton exchange rates in transfer RNA as a function of spermidine and magnesium. *Nucleic Acids Res.* **11** (7): 2121-2134.

Umland TC, Wolff EC, Park MH, Davies DR (2004) A new crystal structure of deoxyhypusine synthase reveals the configuration of the active enzyme and of an enzyme·NAD·inhibitor ternary complex. *J Biol Chem.* **279** (27): 28697–28705.

Valentini SR, Casolari JM, Oliveira CC, Silver PA, McBride AE (2002) Genetic interactions of yeast eukaryotic translation initiation factor 5A (eIF5A) reveal connections to poly(A)-binding protein and protein kinase C signaling. *Genetics*. **160** (2): 393-405.

Wagner S and Klug G (2007) An archaeal protein with homology to the eukaryotic translation initiation factor 5A shows ribonucleolytic activity. *J Biol Chem.* **282** (19): 13966 - 13976.

Wang T, Lu L, Wang D, Thompson JE (2001) Isolation and characterization of senescence-induced cDNAs encoding deoxyhypusine synthase and eukaryotic translation initiation factor 5A from tomato. *J Biol Chem*. **276** (20): 17541-17541.

Wolff EC, Kang KR, Kim YS, Park MH (2007) Posttranslational synthesis of hypusine: evolutionary progression and specificity of the hypusine modification *Amino Acids*. **33** (2): 341–350.

Wood J, Frederickson RM, Fields S, Patel AH (2001) Hepatitis C virus 39X region interacts with human ribosomal proteins. *J Virol*. **75** (3): 1348–1358.

Wüthrich K (1995) Protein structure determination in solution by NMR spectroscopy. In *NMR in structural biology: A collection of papers by Kurt Wüthrich*. Wüthrich K (Ed.) World Scientific: New Jersey. **5**: 11-14.

Xu A and Chen KY (2001) Hypusine is required for a sequence-specific interaction of eukaryotic initiation factor 5A with postsystematic evolution of ligands by exponential enrichment RNA. *J Biol Chem.* **276** (4): 2555-2561.

Xu A, Jao DL, Chen KY (2004) Identification of mRNA that binds to eukaryotic initiation factor 5A by affinity co-purification and differential display. *Biochem J.* **384** (3): 585–559.

Xu J, Zhang B, Jiang C, Ming F (2010) RceIF5A, encoding an eukaryotic translation initiation factor 5A in *Rosa chinensis*, can enhance thermotolerance, oxidative and osmotic stress resistance of *Arabidopsis thaliana*. *Plant Mol Biol.* **75** (1-2): 167-178.

Yamasaki S and Anderson P (2008) Reprogramming mRNA translation during stress. *Curr Opin Cell Biol*. **20** (2): 222-226.

Yang DQ, Halaby MJ, Zhang Y (2006) The identification of an internal ribosomal entry site in the 5′-untranslated region of p53 mRNA provides a novel mechanism for the regulation of its translation following DNA damagep53 protein synthesis and DNA damage. *Oncogene.* **25** (33): 4613-4619.

Yao M, Ohsawa A, Kikukawa S, Tanaka I, Kimura M (2003) Crystal structure of hyperthermophilic archaeal initiation factor 5A: A homologue of eukaryotic initiation factor 5A (eIF-5A). *J Biochem.* **133** (1): 75–81.

Yuan P, Jedd G, Kumaran D, Swaminathan S, Shio H, Hewitt D, Chua, N, Swaminathan K (2003) A HEX-1 crystal lattice required for Woronin body function in *Neurospora crassa. Nat Struct Biol.* **10** (4): 264-270.

Zanelli CF and Valentini SR (2005) Pkc1 acts through Zds1 and Gic1 to suppress growth and cell polarity defects of a yeast eIF5A mutant. *Genetics.* **171**: 1571-1581.

Zanelli CF, Maragno ALC, Gregio APB, Komili S, Pandolfi JR, Mestriner CA, Lustri WR, Valentini SR (2006) eIF5A binds to translational machinery components and affects translation in yeast. *Biochem Biophys Res Commun.* **348** (4): 1358-1366.

Zanelli CF and Valentini SR (2007) Is there a role for eIF5A in translation? *Amino Acids.* **33** (2): 351-358.

Zuk D and Jacobson A (1998) A single amino acid substitution in yeast eIF-5A results in mRNA stabilization. *EMBO J*. **17** (10): 2914-2925.

Appendices

Appendix A. Plasmid maps

A.1 Recombinant plasmids used in this study

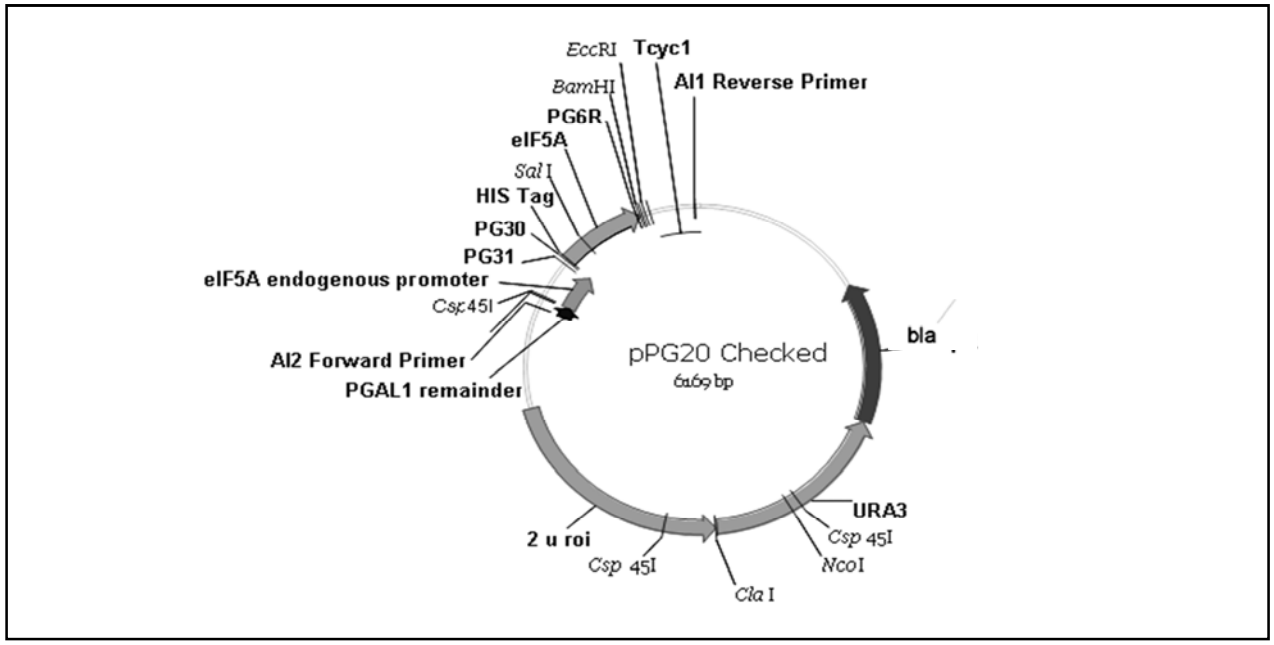

Figure A.1: Plasmid map of the pPG20 complementation vector. pPG20 contains the yeast 6x His-*TIF51A* gene under control of its endogenous promoter. bla: β-lactamase.

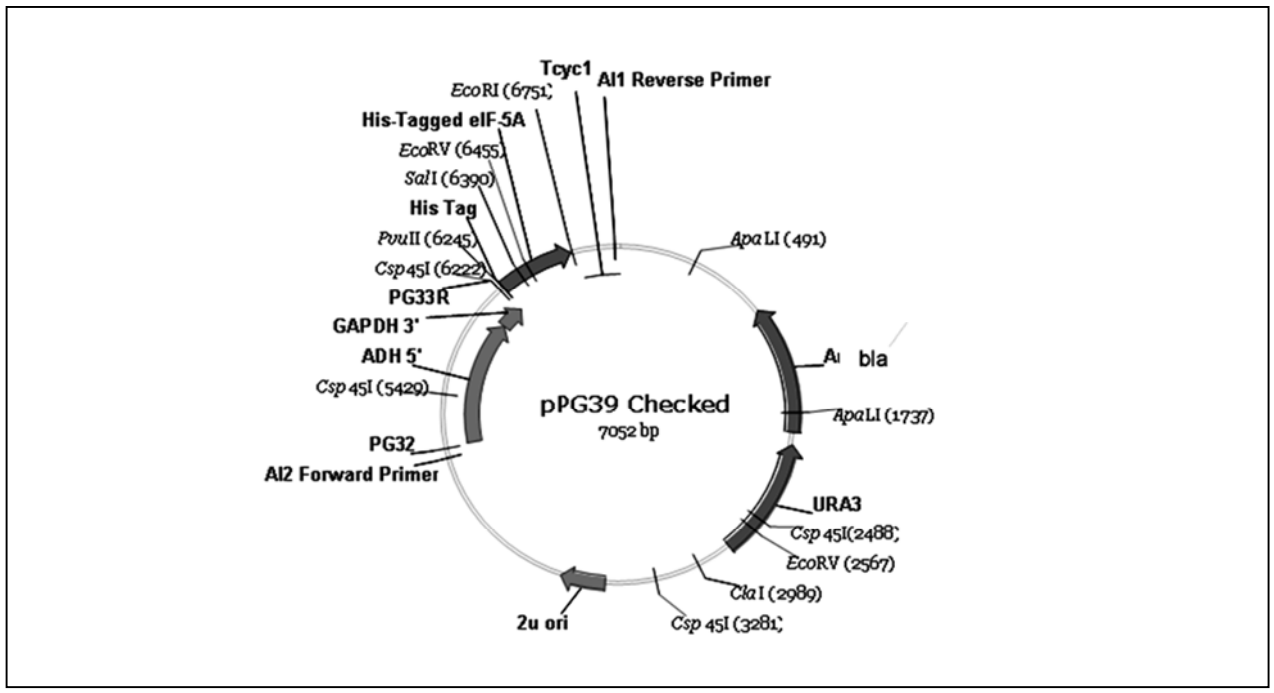

Figure A. 2: **Plasmid map of the pPG39 expression vector.** pPG39 contains the yeast 6x His-*TIF51A* gene under control of the *ADH-GAPDH* promoter. bla: β-lactamase.

A.2 Construction of the recombinant plasmid pJC6

The *TIF51A*$_{Thrombin}$ containing bacterial expression vector pJC6 was constructed by subcloning the yeast *TIF51A* gene, with inserted thrombin cleavage site (*TIF51A*$_{Thrombin}$), from the pPG57 vector (Gentz, unpublished) into the backbone of the pT7-7 6xHis bacterial expression vector (Cortay *et al*., 1994) in a two-step process (figure A.3). Restriction of plasmid DNA was carried out using the appropriate restriction endonucleases (Promega) as instructed by the manufacturer and all ligations were performed as per the manufacturer's instructions of T4 DNA ligase (Promega). A portion of the *TIF51A*$_{Thrombin}$ gene was subcloned from the pPG57 vector by restriction with *Eco* RV and *Bam* HI and ligated into pPG36 (Gentz, unpublished) restricted with *Eco* RV and *Bam* HI. As the pPG36 vector contained a dysfunctional promoter region, the *TIF51A*$_{Thrombin}$ gene was further subcloned into pT7-7 6xHis by restricting the newly formed clone with *Pst* I and *Nde* I and ligating the resulting fragment into pT7-7 6xHis restricted with *Pst* I and *Nde* I. The final construct was named pJC6 and the sequence was confirmed by restriction analysis and DNA sequencing.

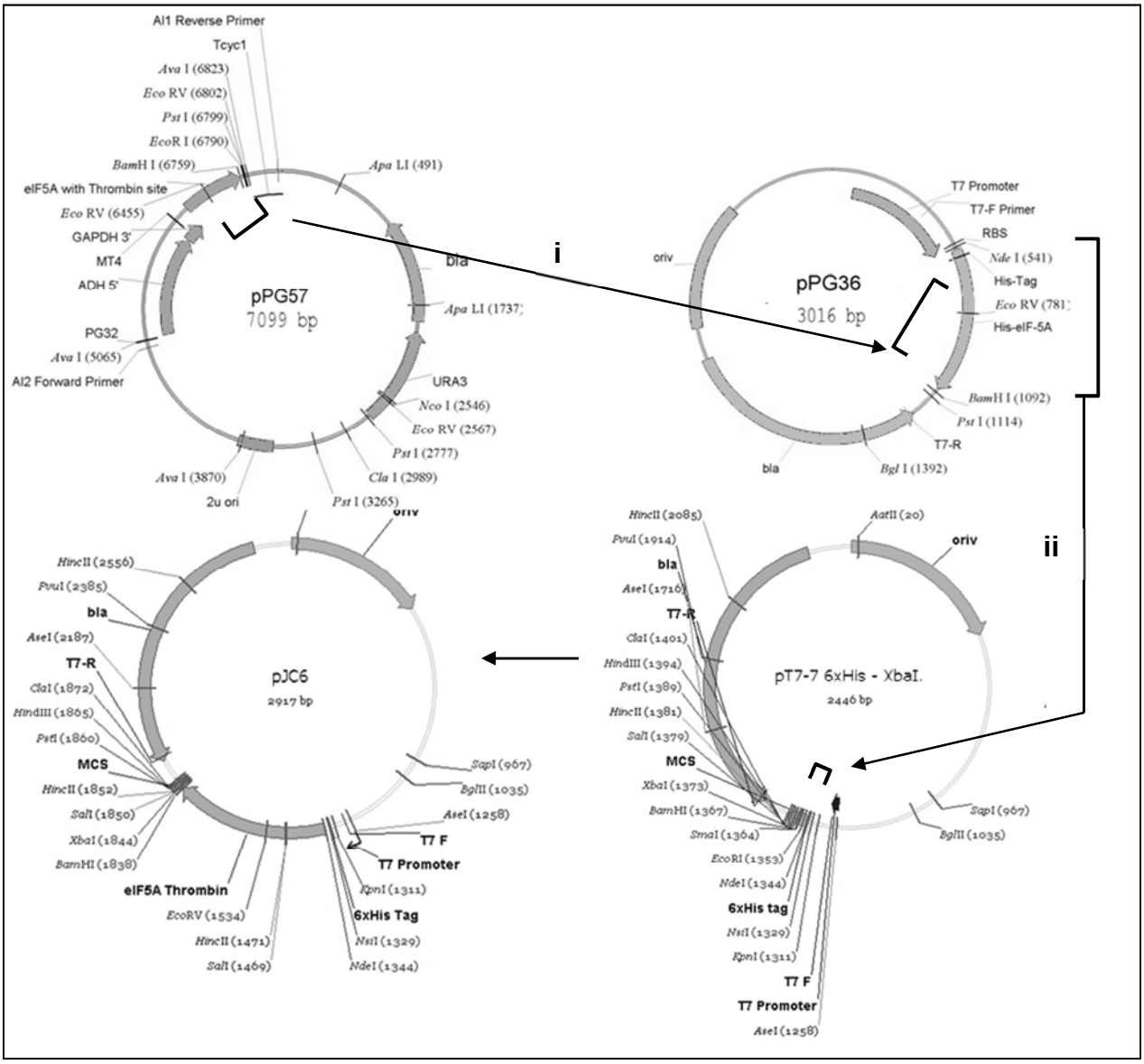

Figure A.3: Schematic representation of the construction of plasmid pJC6. (i) A fragment of the *TIF51A*$_{\text{Thrombin}}$ gene was subcloned from the pPG57 vector by restriction with *Eco* RV and *Bam* HI and ligated into pPG36 restricted with *Eco* RV and *Bam* HI. (ii) The *TIF51A*$_{\text{Thrombin}}$ gene was then restricted with *Pst* I and *Nde* I and ligated into pT7-7 6xHis restricted with *Pst* I and *Nde* I to form pJC6 (below, left). bla: β-lactamase, T7 promoter: T7 bacteriophage RNA polymerase promoter, MCS: multiple cloning site.

Appendix B. Primers

Primers used in this study:

Table A.1: A list of mutagenic oligonucleotides used in this study. The primer names, nucleotide sequences, direction as well as the mutations and introduced or removed restriction sites, are summarised below. The codon encoding the mutated residue is highlighted in bold and the introduced or removed restriction sites are underlined.

Primer name	**Sequence**	**Sense / antisense**	*Binds*, introduced / removed restriction site, **mutation**
JC3	GTAAGATTGTCGATATGTCCACTTCA**GAC**ACTGGTAAGCACGG	**Sense**	*TIF51A*, *Sal* I, **K48D**
JC4	CCGTGCTTACCAGT**GTC**TGAAGTGGACATATCGACAATCTTAC	**Antisense**	*TIF51A*, *Sal* I, **K48D**
JC5	CATGTCCACTTCGAAGACT**GCT**AAGCACGGTCACGC	**Sense**	*TIF51A*, *Csp* 45I, **G50A**
JC6	GCGTGACCGTGCTT**AGC**AGTCTTCGAAGTGGACATGTCG	**Antisense**	*TIF51A*, *Csp* 45I, **G50A**
JC9	GGTAAGCACGGTCACGCT**GCA**GTCCATTTGGTTGCC	**Sense**	*TIF51A*, *Pst* I, **K56A**
JC10	GGCAACCAAATGGAC**TGC**AGCGTGACCGTGCTTACC	**Antisense**	*TIF51A*, *Pst* I, **K56A**
JC11	CTTCTAAGACTGGTAAG**GCC**GGCCACGCTAAAGTCCATTTGG	**Sense**	*TIF51A*, *Ngo* MIV, **H52A**
JC12	CCAAATGGACTTTAGCGTGGCC**GGC**CTTACCAGTCTTAGAAG	**Antisense**	*TIF51A*, *Ngo* MIV, **H52A**

Table A.2: Characteristics of primers used in SDM. The primer names, nucleotide length, percent GC content (% GC) and melting point (T_m) values are summarised below.

Primer names	Length	%GC	T_m (℃)
JC1 & JC2	36	55.6	79.99
JC3 & JC4	43	46.5	77.89
JC9 & JC10	36	58.3	94.2
JC11 & JC12	42	52.4	93.5

Table A.3: List of primers used in DNA sequencing. The primer names, nucleotide sequence, direction and region to which the primers bind are summarised below.

Primer name	Sequence	Sense / antisense	Binds
PG8F	ACCGGTGTTTCGAAGGTGAAGGAAC	**Sense**	5'-P_{TIF51A} (yeast constructs)
PG6R	GGGATCCTTAATCGGTTCTAGCAG	**Antisense**	3'-*TIF51A* (yeast constructs)
T7-F	TAATACGACTCACTATAGGG	**Sense**	5'-P_{T7} (bacterial constructs)
T7-R	GCTAGTTATTGCTCAGCGG	**Antisense**	3'-*TIF51A* (bacterial constructs)

Appendix C. Thermal cycling programmes

Table A.4: Temperature cycling programme adapted from the QuickChange™ Site-Directed Mutagenesis Kit. The stage, number of cycles, temperature and time of each cycle are summarised below.

Stage	Cycles	Temperature	Time
1	1	95 ℃	30 seconds
2	20	95 ℃ 55 ℃ 68 ℃	30 seconds 1 minute 14 minutes

Table A.5: Temperature cycling programme for DNA sequencing. The stage, number of cycles, temperature and time of each cycle are summarised below.

Stage	Cycles	Temperature	Time
1	1	94 ℃	1 minute
2	25	94 ℃ 50 ℃ 60 ℃	10 seconds 10 seconds 4 minutes
3	1	4 ℃	∞

Appendix D. Growth media

Luria agar (Sambrook *et al*., 1989)

Per 1 L: 5 g NaCl
5 g yeast extract
10 g tryptone
[15 g agar]
1 L ddH_2O

autoclaved

[..] omit for broth

Selective minimal medium (SMM)

Per 1 L: 1.7 g yeast nitrogen base (YNB) without amino acids and ammonium sulphate (Difco)
5 g ammonium sulphate
[20 g agar]
796 mL dddH_2O
After autoclaving add appropriate amino acids and carbon source:
{10 mL 1 % leucine}
2 mL 1 % tryptophan
2 mL 1 % histidine
200 mL of 0.1-10 % galactose or glucose as required

[..] omit for broth

{..} omit for PGY10 SMM, include for INVSc1 SMM

Yeast extract, peptone, dextrose (YPD) or galactose (YPG) medium

Per 1 L: 20 g yeast extract
10 g peptone
[20 g agar]
20 g glucose or galactose
1L dddH_2O

[..] omit for broth

Appendix E. General methods

E.1 Site directed mutagenesis (SDM) (QuikChange^{TM} Site-Directed Mutagenesis Kit, Stratagene)

SDM reaction mix

Per 25 µL: 2.5 µL *Pfu* 10x buffer
2.5 µL 2mM dNTP mix
2.5 µL DMSO
1.25 µL 10 µM forward primer
1.25 µL 10 µM reverse primer
1 µL DNA (50 ng)
14 µL dddH_2O

Add 1 µL *Pfu* Turbo (Promega)

2 mM dNTP mix

Per 125 µL: 2.5 µL dATP (100 mM)
2.5 µL dCTP (100 mM)
2.5 µL dGTP (100 mM)
2.5 µL dTTP (100 mM)
115 µL dddH_2O

E.2 SDS and native PAGE (Laemmli, 1970)

Table A.6: Preparation of 15 % SDS and 10 % native PAGE gels

Reagents	SDS resolving gel (15 %)	SDS stacking gel (4 %)	Native resolving gel (10 %)	Native stacking gel (4 %)
30 % acrylamide/bisacrylamide (29:1)	5 mL	0.66 mL	3.3 mL	0.66 mL
ddd H_2O	1.1 mL	3.58 mL	2.9 mL	4.08 mL
1 M Tris-HCl pH 8.8	3.75 mL	-	3.75 mL	-
1 M Tris-HCl pH 6.8	-	0.625 mL	-	0.625 mL
10 % SDS	100 µL	50 µL	-	-
10 % APS	37.5 µL	71.25 µL	37.5 µL	71.25 µL
TEMED	8.25 µL	8.25 µL	8.25 µL	8.25 µL

2x SDS-PAGE sample buffer

Per 10 mL: 1.25 mL 1 M Tris-HCl, pH 6.8
4 mL 10 % SDS
1 mL β-mercaptoethanol
1 mL glycerol
0.001 g bromophenol blue
2.75 mL ddH_2O

2x SDS-PAGE running buffer

Per 1 L: 57.6 g glycine
12 g Tris-HCl
4 g SDS
1 L ddH_2O

2x native PAGE sample buffer

Per 10 mL: 1.25 mL 1 M Tris-HCl, pH 8.8
1 mL glycerol
0.001 g bromophenol blue
7.75 mL ddH_2O

2x native PAGE running buffer

Per 1 L: 12 g Tris-HCl
57.6 g glycine
1 L ddH_2O

	Destain I	**Destain II**	**Destain III**
Per 1 L:	500 mL methanol	80 mL methanol	50 mL methanol
	100 mL glacial acetic acid	70 mL glacial acetic acid	70 mL acetic acid
	400 mL ddH_2O	880 mL ddH_2O	30 mL glycerol
			850 mL ddH_2O

Coomassie stain

Per 500 mL: 1.25 g Coomassie R125
500 mL Destain I

Filtered through a Buchner funnel and stored at room temperature.

E.3 Western analysis (Towbin *et al.,* 1979)

Transfer buffer

Per 1 L: 3.03 g Tris-HCl
14.4 g glycine
1 L 20% methanol

Made fresh and chilled

TBS-Tween

Per 1 L: 100 mL 1 M Tris-HCl pH7.5
30 mL 5 M NaCl
1 mL Tween-20

Made up to 1 L with ddH2O

10x Ponceau stain

Per 100 mL: 2 g Ponceau 5
30 g TCA
30g sulfosalicylic acid
100 mL ddH_2O

1 % BSA

Per 100 mL: 1 g BSA (Fraction V)
100mL TBS-Tween

5 % Milk powder

Per 100 mL: 5 g of fat free milk powder
100 mL TBS-Tween

Appendix F. Column efficiency and calibration

Superdex 75 preparation grade resin (GE Healthcare) was chosen as the column packing material for this study as it has a fractionation range of 3-70 kDa. The column was packed according to the manufacturer's instructions and was then subjected to an efficiency test (figure A.4) by resolving a 2 % (v/v) acetone tracer solution and calculating the number of theoretical plates per meter (N/m) and peak asymmetry values (A_s). According to the manufacturers of Superdex 75 prep grade (GE Healthcare) a well packed column should have an N/m of approximately 10 000 (but no less than 5000) and an A_s value between 0.8 and 1.3.

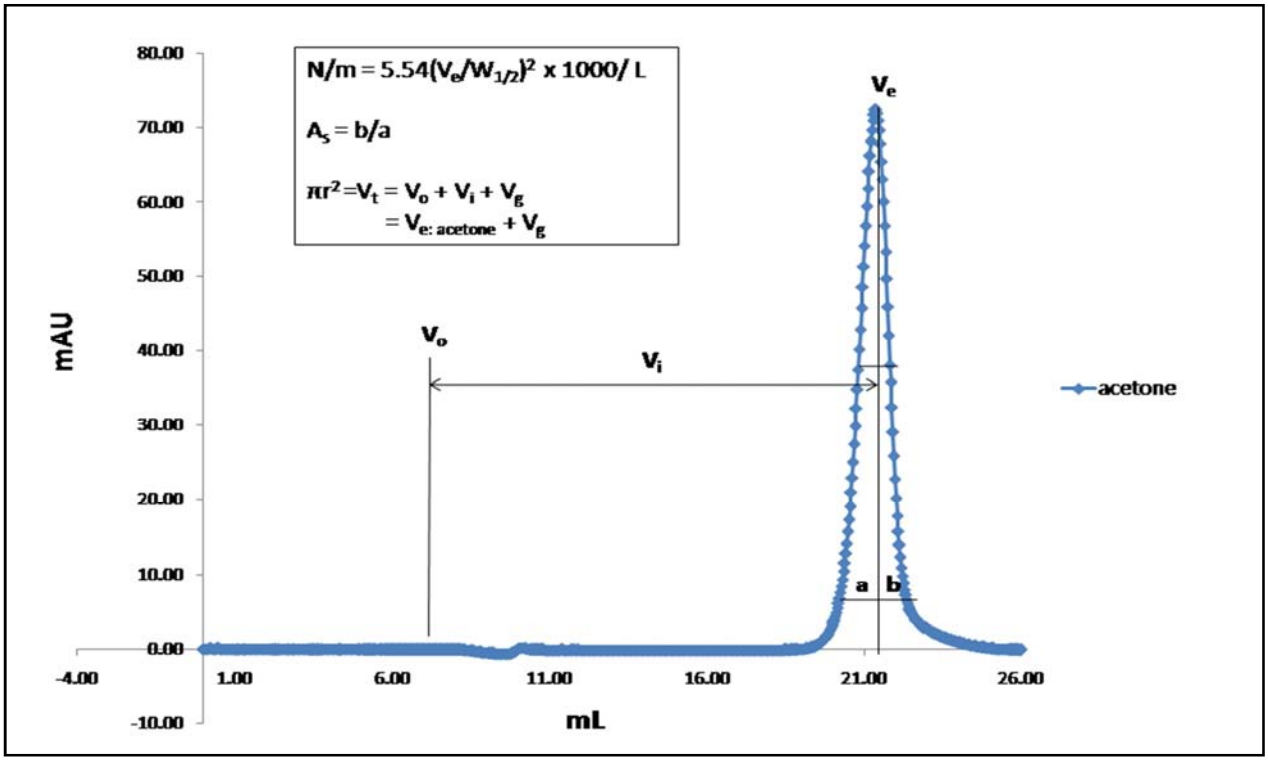

Figure A.4: Calculation of column efficiency. The column efficiency was tested by resolving 100 µL 2 % (v/v) acetone at 280 nm and calculating the number of theoretical plates per meter (N/m) and peak asymmetry (A_s) values. V_o represents the void volume, V_i the interstitial volume and V_e the elution volume of the acetone solution. The relative equations are given above where $W_{1/2}$ represents the volume of eluent measured across the peak at half the peak height (in mL), L represents the height of the column (in mm), a and b represent the first and second halves of the peak width (in mm) at 10 % of the peak height and V_g represents the volume taken up by the packing matrix itself.

The elution volume (V_e) of the acetone solution was found to be 22.64 mL with a theoretical plate number of 9 736.6 per metre (N/m) and a peak asymmetry of 1.03 (A_s). As these values fell well within the range specified by the manufacturers, it was concluded that the column was of a sufficient quality to be calibrated.

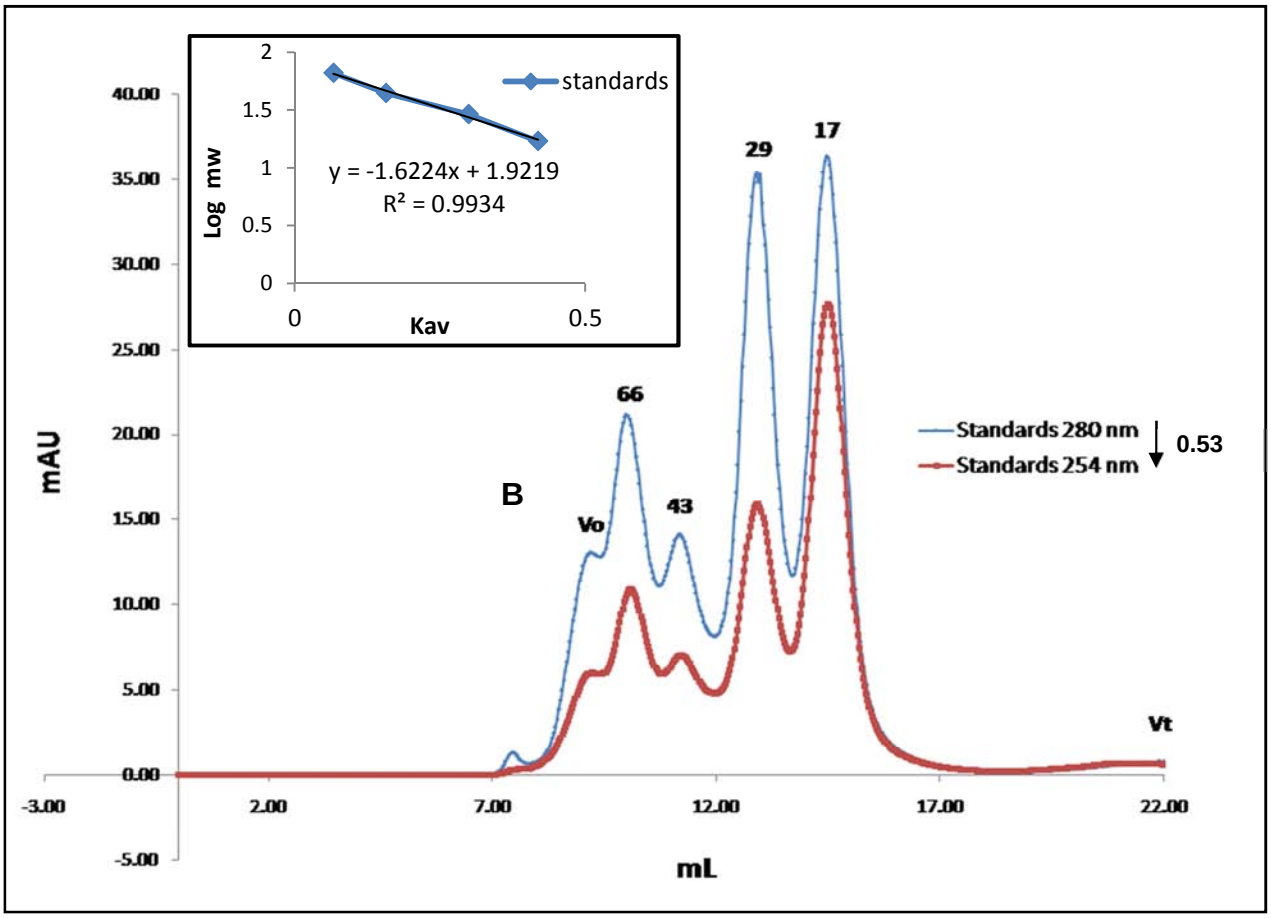

Figure A.5: Calibration of the GF column used in this study. The column was calibrated with a mix of 80 µg of each of the following globular proteins: myoglobin (17 kDa), carbonic anhydrase (29 kDa), ovalbumin (44 kDa) and β-galactosidase (116 kDa). β-galactosidase was used to indicate the void volume (V_o).The Kav values (V_e-V_o / V_t-V_o) were calculated and plotted against the log of molecular weight for each standard to give the linear equation y=-1.6224x+1.9219 with a correlation of 0.9934 (inset above left). The proteins standards were resolved at both 280 nm and 254 nm to give a normal correlation between the two wavelengths of 0.53.

The newly packed column was calibrated with a suitable range of globular proteins (figure A.5). The void volume represented by the elution volume of β-galactosidase was found to be 9.19 mL. The linear standard curve was calculated to be y= -1.6224x + 1.9219. The average difference in absorbance between standards at 280 nm versus

that at 254 nm was calculated as 53 %. The column was calibrated by resolving standards in triplicate to obtain averaged elution volumes for increased accuracy and was re-calibrated throughout the course of the columns use to ensure that the packing material had not shifted. In addition standards were analysed individually to ensure there were no interfering interactions between proteins.

Appendix G. Viral and cellular IRESs

Table A.7: A detailed list of viral and cellular IRESs. A complete list can be found at IRESite -the database of experimentally verified IRES structures (Mokrejs *et al.*, 2006, 2010).

Cellular	
Protein Group	**Proteins (whose mRNA contain IRESs)**
Transcription factors	Myelin transcription factor 2 (MYT-2), NF-κB repressing factor (NRF), runt-related transcription factor 1 (RUNX1), Gtx homeodomain transcription factor
Translation factors	Eukaryotic translation initiation factor 4G (eIF4G), eukaryotic translation initiation factor 4GI (eIF4GI), eukaryotic translation initiation factor 4GII (eIF4GII), death associated protein 5 (DAP5)
Growth factors	Fibroblast growth factor (FGF-1 and FGF-2), platelet-derived growth factor B (PDGF), vascular endothelial growth factor (VEGF), insulin-like growth factor 2 (IGF-II)
Transcriptional regulators	Yes-associated protein 1 (YAP1), SMAD family member 5 (SMAD5), hypoxia-inducible factor 1-alpha (HIF-1α)
Oncoproteins	c-Myc protein, L-myc-1 protein, Pim-1 protein
Apoptosis regulators	Apoptotic protease activating factor (Apaf-1), X-linked inhibitor of apoptosis (XIAP), human inhibitor of apoptosis protein-2 (HIAP2), B-cell lymphoma-2 and extra large proteins (Bcl-2 and Bcl-xL), p58PITSLRE, p53
Proteins localized in neuronal dendrites	Activity-regulated cytoskeletal protein (ARC), α-subunit of calcium calmodulin dependent kinase II dendrin, microtubule-associated protein 2 (MAP2), neurogranin (RC3), amyloid precursor protein
Transporters	Cationic amino acid transporter-1 (CAT-1), Nuclear form of Notch 2
Other	Heat shock proteins 70 and 90 (Hsp70 and Hsp90), poly(A) binding protein (PAB1), protein kinase C (PKC), ornithine decarboxylase (ODC), immunoglobulin heavy chain binding protein (BiP), β-subunit of mitochondrial H+-ATP synthase, connexins 32 and 43, adenomatous polyposis coli (APC), cyclin D1, Bem1 interacting protein (Boi1p), bifunctional heparan sulfate N-deacetylase/N-sulfotransferase 1 (NDST1)

Viral	
IRES group	**Viruses**
Picornavirus (Aphthovirus and Cardiovirus) IRESs	Poliovirus, foot-and-mouth disease virus (FMDV), encephalomyocarditis virus (EMCV), Theiler's murine enceaphalomyelitis virus (TMEV), Saffold virus (SAFV)
Hepacivirus and Pestivirus (HP) IRESs	Hepatitis C virus (HCV), classical swine fever virus (CSFV), bovine viral diarrhea virus (BVDV), avian encephalomyelitis virus (AEV)
Discistrovirus IRESs	Cricket paralysis virus (CPV), Plautia stali intestine virus (PSIV), Rhopalosiphum padi virus (RhPV), Triatoma virus (TrV), aphid lethal paralysis virus (ALPV), Drosophila C virus (DCV)
Other	Human immunodeficiency virus (HIV), Marek's disease virus (MDV), Rous sarcoma virus (RSV), murine leukemia virus (MLV), hepatitis A virus (HAV), rhinovirus (RV), Kaposi's sarcoma-associated herpesvirus (KSHV), tobacco mosaic virus (TMV)